Spring 2019

Performance of one-part and two-part class C fly ash-based alkali activated mortars

Cedric Chani Kashosi

PERFORMANCE OF ONE-PART AND TWO-PART CLASS C FLY ASH-BASED ALKALI ACTIVATED MORTARS

by

CEDRIC CHANI KASHOSI

A THESIS

Presented to the Faculty of the Graduate School of the

MISSOURI UNIVERSITY OF SCIENCE AND TECHNOLOGY

In Partial Fulfillment of the Requirements for the Degree

MASTER OF SCIENCE IN CIVIL ENGINEERING

2019

Approved by:

Dr. Mohamed ElGawady, Advisor
Dr. John J. Myers
Dr. Aditya Kumar

PUBLICATION THESIS OPTION

The present thesis comprises two research articles which have been submitted for publication, or are intended to be submitted for publication as described below:

Paper I: Pages 5 – 45 are intended to be submitted to the Journal of Construction and Building Materials.

Paper II: Pages 46 – 87 are intended to be submitted to the Journal of Construction and Building Materials.

ABSTRACT

Seeking an eco-friendly concrete, researchers have conducted studies to fully replace ordinary Portland cement (OPC) with fly ash (FA) producing alkali-activated concrete (AAC). Results showed better performance of AAC in terms of high early compressive strength, and durability compared to conventional concrete. However, much is still unknown about the behavior of AAC. From the type of materials used, the curing procedure, and long-term strength development of these binders; a thorough investigation is needed in order to fill the existing gap from previous studies and thus make a step forward to the safely use of AAC in the construction industry. The present thesis reports results of studies conducted on class C fly ash-based alkali-activated mortars (AACFA). A study was conducted on two-part AACFA mortars subjected to a rest time of 2, 6, 12, 24, 30, or 36 hours; then, cured under ambient curing, and heat curing regimes (oven, and steam) for 9 hours at two different temperatures of 55℃ and 80℃. The temporal evolution of the compressive strength at ages of 1, 7, 28, 56, and 90 days was also determined. In addition, in an attempt to produce a user-friendly material similar to OPC, one-part AACFA mortars were synthesized and their behaviors were compared to those of the two-part mortars. It was observed that two-part mortars exhibited better fresh and hardened properties than one-part mortars. For two-part AACFA mortars, a rest time of 12 hours increased the short term strength by approximately 45%, while a considerable change in the long term strength occurred up to 56 days and 90 days depending on the chemical composition of the FA.

ACKNOWLEDGMENTS

I am extremely grateful to my advisor Dr. Mohamed ElGawady, for the opportunity given to me to conduct my research under his supervision. He is an outstanding professor and excellent researcher. I highly appreciate his mentorship, assistance and encouragement throughout my research and completion of my master's degree.

Special thanks to my advisory committee members, Dr. John J. Myers, and Dr. Aditya Kumar for their time to review this manuscript.

I would like to thank all my family members, my dad Desmond Kashosi, my brothers Wany, Daniel, Israel and Daddy Kashosi; my sister Nakinja Thelemuka and my love Sandra Bahati Ujeneza for their unconditional love and supports.

I am dedicating this thesis to the living memory of my beloved mother Jeannette Kwali Thelemuka who always believed in me and inspired my decision to pursue my master's degree. May her soul rest in eternal peace.

My great thanks to my wonderful team members, Dr. Ahmed Gheni and Eslam Gomaa for their time and efforts.

My sincere appreciation to the technical staff, Dr. Michael Lusher, John Bullock, Greg Leckrone, Brian Swift, Jason Cox, and Gary Abbott their indispensable technical assistance.

TABLE OF CONTENTS

Page

PUBLICATION THESIS OPTION iii

ABSTRACT iv

ACKNOWLEDGMENTS v

LIST OF ILLUSTRATIONS x

LIST OF TABLES xiii

NOMENCLATURE xiv

SECTION

1. INTRODUCTION 1

1.1. BACKGROUND 1

1.2. RESEARCH SIGNIFICANCE 4

1.3. THESIS OUTLINE 4

PAPER

I. EFFECTS OF REST TIME AND CURING REGIME ON SHORT AND LONG-TERM STRENGTH OF CLASS C FLY ASH-BASED ALKALI ACTIVATED MORTAR 5

ABSTRACT 6

1. INTRODUCTION 6

2. RESEARCH SIGNIFICANCE 8

3. EXPERIMENTAL PROGRAM 9

3.1. MATERIAL CHARACTERISTICS 9

3.2. MIXTURES PROPORTIONS AND PREPARATION 10

3.3. FRESH PROPERTIES OF THE AACFA MORTARS 12

3.4. CURING REGIMES AND REST TIME 12

3.5. COMPRESSIVE STRENGTH TESTING 14

3.6. MICROSTRUCTURE ANALYSIS 14

3.6.1. X-Ray Diffraction (XRD). 14

3.6.2. Scanning Electron Microscopy (SEM) and Energy Dispersive X-Ray Spectroscopy (EDS). 15

4. RESULTS AND DISCUSSIONS 15

4.1. FLOW AND SETTING PROPERTIES OF AACFA MORTARS 15

4.2. EFFECTS OF REST TIME ON THE SHORT TERM STRENGTH OF AACFA MORTARS 16

4.3. LONG TERM STRENGTH DEVELOPMENT OF AACFA MORTARS 22

4.3.1. Ambient-cured Specimens. 22

4.3.2. Thermally-cured Specimens. 24

4.3.2.1. Oven-cured strength development. 25

4.3.2.2. Steam-cured strength development. 26

4.3.3. Strength of Ambient vs. Thermally-cured Specimens. 27

4.4. MICROSTRUCTURE AND NANOSTRUCTURE ANALYSIS 31

4.4.1. X-Ray Diffraction Analysis. 31

4.4.2. SEM and EDS Analysis. 36

5. CONCLUSIONS 41

REFERENCES 43

II. A COMPARISON BETWEEN ONE-PART AND TWO-PART MIXING OF CLASS C FLY ASH-BASED ALKALI-ACTIVATED MORTARS 46

ABSTRACT 47

1. INTRODUCTION 48

2. MATERIALS PROPERTIES 51

2.1. FLY ASH 51

2.2. ACTIVATORS 52

2.3. SAND 52

3. EXPERIMENTAL PROCEDURE 52

3.1. MIX DESIGN 52

3.2. MIXING PROCEDURE 53

3.3. CURING PROCESS 55

3.4. FRESH AND HARDENED PROPERTIES TESTS 55

3.5. MICRO STRUCTURE ANALYSIS 56

4. RESULTS AND DISCUSSION 57

4.1. FRESH PROPERTIES 57

4.2. COMPRESSIVE STRENGTH DEVELOPMENT OF ZERO-CEMENT MORTAR 60

4.2.1. Compressive Strength of Zero-cement Mortars Cured at Ambient Temperatures. 60

4.2.2. Compressive Strength of Zero-Cement Mortars Cured at Elevated Temperatures. 63

4.3. MICRO STRUCTURE ANALYSIS 70

4.3.1. XRD Results of M29 AA Paste Mixtures. 71

4.3.2. XRD Results of M21 AA Paste Mixtures. 75

4.3.3. XRD Results of M37 AA Paste Mixtures. 79

4.3.4. XRD Summary. 81

5. CONCLUSIONS 83

REFERENCES 85

SECTION

2. SUMMARY, CONCLUSIONS AND RECOMMENDATIONS 88

2.1. COMPREHENSIVE SUMMARY 88

2.2. CONCLUSIONS 89

2.3. RECOMMENDATIONS 91

2.3.1. Recommendations for Current Study. 91

2.3.2. Recommendations for Future Work. 92

BIBLIOGRAPHY 93

VITA 98

LIST OF ILLUSTRATIONS

PAPER I Page

Figure 1. Particles size distribution of cement and FA using Microtrac S3500 laser particle size analyzer 11

Figure 2. Steam chamber system. 13

Figure 3. Fresh properties of AACFA mortars. 16

Figure 4. Effect of rest time on the compressive strength of ambient-cured AACFA mortars. 18

Figure 5. Effect of rest time on the compressive strength of steam-cured: a) M21, and b) M37. 19

Figure 6. Percentage strength increase of AACFA mortar relative to the 2 hours of rest time compressive strength of: a) Steam-cured M21 mixes. b) Oven-cured M21 mixes. c) Steam-cured M37 mixes. d) Oven-cured M37 mixes. 20

Figure 7. Effect of rest time on the compressive strength of oven-cured: a) M21, and b) M37. 21

Figure 8. Ambient compressive strength development of AACFA mortars: (a) absolute value, and (b) normalized $f'_{m.}$ 23

Figure 9. Compressive strength evolution of oven-cured specimens cured at: a) 55℃ (131℉), and b) 80℃ (176℉). 28

Figure 10. Compressive strength evolution of steam cured specimens cured at: a) 55℃ (131℉), and b) 80℃ (176℉). 29

Figure 11. Comparison between ambient curing, oven, and steam curing for: a) M21-HA at 55ºC (131ºF), b) M21-HA at 80ºC (176ºF), c) M21-HS at 55ºC (131ºF), and d) M21-HS at 80ºC (176ºF). 30

Figure 12. Comparison between ambient curing, oven, and steam curing for: a) M37-HA at 55ºC (131ºF), b) M37-HA at 80ºC (176ºF), c) M37-HS at 55ºC (131ºF), and d) M37-HS at 80ºC (176ºF). 31

Figure 13. XRD patterns of unreacted FAs and AACFA pastes ambient-cured for one day: a) M21 mixes, and b) M37 mixes. 35

Figure 14. XRD patterns of unreacted FAs and AACFA pastes oven-cured at 55ºC or 80ºC for: a) M21 mixes, and b) M37 mixes. 36

Figure 15. XRD patterns of unreacted FAs and AACFA pastes steam-cured at 55ºC or 80ºC for 9 hours. a) M21 mixes. b) M37 mixes. 37

Figure 16. XRD patterns of AACFA pastes ambient-cured, stored and tested after 1, 7, 56, and 90 days. a) M21 mixes. b) M37 mixes. 38

Figure 17. SEM images of FA and geopolymer pastes: a) Unreacted FA C21-2.20, and b) P21 paste. 39

Figure 18. EDS results of FA C21.20 and geopolymer pastes. a) Unreacted FA C21-2.20. b) Reacted M21 FA particle "A" and c) Reacted M21 FA particle "B". 40

PAPER II

Figure 1. Tests on fresh properties of zero-cement mortars. a) Flow test. b) Setting time test. 56

Figure 2. Setting time results of AAM. 57

Figure 3. Correlation between Si/Al and setting time of AAM: a) One-part mortar mixtures. b) Two-part mortar mixtures. 58

Figure 4. Workability of AAM. 59

Figure 5. Compressive strength of AAM cured at 30° C for 24 hours and 7 days: a) M29 mixtures. b) M21 mixtures. c) M37 mixtures. 61

Figure 6. Compressive strength of M21 mortar specimen's oven cured at: a) 55° C (131° F), b) 70° C (158° F) 65

Figure 7. Compressive strength of M29 mortar specimen's oven cured at: a) 55° C (131° F), or b) 70° C (158° F). 66

Figure 8. Compressive strength of M37 mortar specimens oven cured at: a) 55° C (131° F), b) 70° C (158° F) 69

Figure 9. XRD Results of M29 mixes ambient-cured. a) One-part mixes. b) two-part mixes. 72

Figure 10. XRD Results of M29 mixes oven-cured at 55º C (131º F). a) One-part mixes. b) two-part mixes. 73

Figure 11. XRD Results of M29 mixes oven-cured at 55º C (131º F). a) One-part mixes. b) two-part mixes..... 76

Figure 12. XRD Results of M21 mixes ambient-cured. a) One-part mixes. b) Two-part mixes..... 77

Figure 13. XRD Results of M21 mixes oven-cured at 55º C (131º F). a) One-part mixes. b) Two-part mixes. 78

Figure 14. XRD Results of M21 mixes oven-cured at 70º C (158º F). a) One-part mixes. b) Two-part mixes. 79

Figure 15. XRD Results of M37 mixes ambient-cured. a) One-part mixes. b) two-part mixes..... 81

Figure 16. XRD Results of M37 mixes oven-cured at 55º C (131º F). a) One-part mixes. b) Two-part mixes. 82

Figure 17. XRD Results of M37 mixes oven-cured at 70º C (158º F). a) One-part mixes. b) Two-part mixes. 83

LIST OF TABLES

PAPER I Page

Table 1. X-Ray Fluorescence of Fly Ashes 11

Table 2. Mix Design Ratio and Quantities..... 12

Table 3. Summary of short-term compressive strength development 22

Table 4. Summary of Long-Term compressive strength development..... 26

Table 5. Measured crystalline content (%) 34

PAPER II

Table 1. Characteristics of Fly ashes 51

Table 2. Mix design ratio 53

Table 3. Unit quantities of mix design..... 54

NOMENCLATURE

Symbol	Description
Θ	Diffraction angle location

1. INTRODUCTION

1.1. BACKGROUND

The use of concrete in the construction industry has increased so much to a level of making it the most used man made material, and second used material on earth after water. Approximately 8% of global CO_2 emission is due to the global production of cement which is mainly used in concrete construction [1], [2]. To reduce the usage of Portland cement (OPC), by-products such as fly ash (FA) have been used as a partial Portland cement replacement. Using FA, the waste from coal power plants, into concrete increases concrete sustainability while reducing the amount of FA that goes to landfills. The disposal of FA is becoming detrimental to environment since the majority of it is disposed off into landfills and ponds [3]. For example, 180 million ton of FA was generated in the US during 2017, and expected to reach 221 million ton for 2018, but its re-utilization rate remains very low at approximately 50% [4], [5]. One approach to reuse FA in large volumes is to use it as the main binder in concrete producing alkali activated concrete (AAC) [6].

Alkali activated binder included an aluminosilicate precursors that is activated using alkaline solution[10]. This chemical reaction, geopolymerization, consists of the dissolution of solid reactants in the alkaline solution, hydrolysis of the dissolved species followed by gel formation[11]. The most used precursors are ground granulated blast furnace slag(GGBFS), FA, and metakaolin (MK); while sodium silicate (Na_2SiO_3), sodium hydroxide (NaOH), potassium silicate (K_2SiO_3), and potassium hydroxide (KOH) are the commonly used activators. AA binders are normally produced either through a two-part mix [6], [9]–[11] where a solid source material is mixed with an alkaline liquid activator,

or through a one-part mix where both the source material and activators are solids which are mixed together before adding water, similar to OPC [13]–[16]. Most of AA binders are two-part mixed. In the present thesis, FA was used as a precursor in order to synthesize both one-part and two-part alkali-activated mortars (AAM).

FA is classified per ASTM C618 as class C or class F based on the chemical composition[12]. Due to the low CaO content of class F FA, binders generated using this type of FA do require elevated temperature for high strength development while binders activated using class C FA with relatively higher calcium content, had the potential of developing higher compressive strength when cured either under ambient conditions or at elevated temperatures.

In the case of two-part mixed AA binders, several researchers used class F FA to produce AA binders (AAFFA) and obtained compressive strengths up to 60 MPa (8700 psi) when the investigated concrete, mortar, and/or paste specimens were cured at elevated temperatures ranging from 60˚C (140˚F) to 80˚C (176˚F) for different durations ranging from six to 24 hours[9], [17], [18]. Both the short-term and long-term behavior of these binders have been investigated, for a time period ranging from 1-day up to 540-days after their initial curing. Investigated parameters included engineering properties and durability properties of concrete, mortar and paste specimens oven-cured [19]–[23]. It was observed that 70% - 90% of strength development of these binders occurred within 3 - 28 days followed by a very small continuous increase for the remaining time up to 540 days.

The rest time, time between the end of mixing process and the beginning of the heat curing, is an important parameter that affects the strength and durability of AAC and CC. In the case of CC, different rest times ranging from two to 6 hours increased the

compressive strength by up to 40% compared to 30- 60 minutes [13], [14]. In the case of AAFFA, a rest time of one hour before curing in the oven at 60°C (140℉) increased the strength by 16% compared to no rest time[15]. However, increasing the rest time beyond that, the strength decreased by 8%. Other researchers [16][17], reported that a rest time of 24 hours before curing at 80℃ (176℉) for two days, resulted in a 50% increase in the compressive strength compared to curing for three days.

In the case of one-part mixed AAC, over tdifferent combinations of materials have been proposed by researchers over the years in order to synthesize these binders. Proposed precursor materials consisted of complex mixing such as a combination of metakaolin with amorphous silica and slag [13], or a mix of metakaolin and slag [14]. More recently, much less complex mixing have been proposed by different authors. Using precursors such as class F FA activated with solid sodium silicate and sodium hydroxide pellets to synthesize AAM, resulting in a compressive strength of 65 MPa (9430 psi) after three weeks of continuous heat curing at 40°C (104°F) which is hard to implement in industry [15], or substituting class F FA with slag and obtaining a compressive strength of 50 MPa (7250 psi) after 28 days of ambient curing [29].

Despite the high availability of literature on AA binders, most of these studies developed binders synthesized using either class F FA, MK, or GGBFS. But only a few studies are available on alkali-activated class C fly ash (AACFA) binders[31]–[35]. Since the majority of the produced FA in the United States are class C, it is important to develop AA binders that utilize this fly ash as the precursor.

1.2. RESEARCH SIGNIFICANCE

Most of available studies on AACFA focused on the short-term behavior of these binders. Therefore, less information is known about the long-term strength development. Furthermore, steam curing is a common practice in the precast industry for CC as it yields early high strength [25]; however, the authors are not aware of any research on the performance of steam-cured AACFA binder.

In addition, most of AACFA are two-part mixed. However, the use of the liquid activators which are very corrosive materials requires handling extreme precautions and thus restricts its applicability to laboratory and pre-cast industries with available facilities, and well-trained personnel required to accommodate for storage, and handling and production of this type of binders. All of which put extra limit on using it; therefore the importance of using one-part mixing.

1.3. THESIS OUTLINE

The present thesis is divided into three sections, the first section is a brief introduction about AA binders and the importance of the present research. The next section will include two research articles on AAM; the first paper investigated the long-term and short-term strength evolution of AAM cured under different curing regimes, and the second paper establishes a parallelism between the fresh and hardened properties of one-part and two-part mixed AAM. The third section comprises a comprehensive summary, conclusions and future work recommendations.

PAPER

I. EFFECTS OF REST TIME AND CURING REGIME ON SHORT AND LONG-TERM STRENGTH OF CLASS C FLY ASH-BASED ALKALI ACTIVATED MORTAR

Cedric Chani Kashosi[1], and Mohamed A. ElGawady[2]

[1]Graduate Research Assistant; Civil, Architectural and Environmental Engineering, Missouri University of Science and Technology.

[2]Professor and Benavides Faculty Scholar; Civil, Architectural and Environmental Engineering, Missouri University of Science and Technology, senior author.

EMPHASIZE

- The resting time period between mixing and curing of mortar samples was investigated by subjecting them to six different rest time of 2, 6, 12, 24, 30, and 36 hours prior the curing process, testing cured specimens for compressive strength, and selecting the optimum resting time as the one resulting in higher compressive strength.
- The long-term strength development of mortar specimens was investigated by testing all specimens for compressive strength at a specific time interval ranging between 1 and 90 days of storage under laboratory conditions, after the initial curing process.

ABSTRACT

This paper investigated the temporal evolution of compressive strength of class C fly ash-based alkali activated mortar (AACFA). Fly ash (FA) sourced from two different power plants having different chemical compositions were used to synthesize four different mixes with different mix proportions obtained by varying ratios of sodium silicate to sodium hydroxide. The effects of different rest times ranging from 2 to 36 hours on the compressive strength of AACFA was investigated. The specimens were also subjected to ambient, oven, or steam-curing. The oven and steam-curing were at either 55℃ (131℉) or 80℃ (176℉). The compressive strengths of the investigated specimens were examined at different ages up to 90 days. Results demonstrated that a rest time of 12 hours resulted in an approximately 45% increase in the compressive strength compared to two hours rest time. Furthermore, in average 15 - 25%, and 125% increase in the compressive strength of the thermally-cured and ambient-cured specimens synthesized using relatively higher calcium content FA occurred up to 56 days, respectively. Beyond that, insignificant increase was observed. For specimens synthesized using relatively low calcium content, 30 – 50%, and 295% increase in the compressive strength was observed up to 90 days for heat and ambient curing regimes, respectively.

1. INTRODUCTION

Approximately 8% of global CO_2 emission is due to the production of cement which is mainly used in concrete construction. To reduce this usage of cement, by-products such as fly ash (FA) have been used as a partial Portland cement replacement. Using FA, the waste from coal power plants, into concrete increases concrete sustainability while

reducing the amount of FA that goes to landfills. The disposal of FA is becoming detrimental to environment since the majority of it is disposed off into landfills and ponds. One approach to reuse FA in large volumes is to use it as the main binder in concrete producing alkali activated concrete (AAC) [1].

Alkali activated binder includes an aluminosilicate precursors such as FA activated using alkaline solution such as a solution of sodium silicate (Na_2SiO_3) and sodium hydroxide (NaOH) [2]. This chemical reaction, geopolymerization, consists of the dissolution of solid reactants in the alkaline solution, hydrolysis of the dissolved species followed by gel formation [3].

FA is classified as class C or class F based on the chemical composition. Due to the low CaO content of class F FA, binders alkali-activated with class F fly ash (AAFFA) require heat-curing for high strength development. Researchers developed AAFFA having compressive strengths up to 60 MPa (8700 psi) when the investigated specimens were heat-cured at 60˚C (140℉) to 80˚C (176℉) for durations from six to 24 hours [4]–[6].

The rest time, time between the end of mixing process and the beginning of the heat curing, is an important parameter that affects the strength and durability of AAC. In the case of AAFFA, a rest time of one hour before curing in the oven at 60°C (140°F) increased the strength by 16% compared to no rest time [7]. However, increasing the rest time beyond that, the strength decreased by 8%. Other researchers [8,9], reported that a rest time of 24 hours before curing at 80℃ (176℉) for two days, resulted in a 50% increase in the compressive strength compared to curing for three days.

The development of the properties of AAFFA have been investigated up to an age of 540-days [10,11]. It was observed that about 80% of strength development of AAFFA

occurred within 3 - 28 days followed by a small increase in the strength up to 540 days. This is different from that of ground granulated blast furnace slag (GGBFS) where the strength of GGBFS binders increased up to 90 days, after which a strength degradation was observed due to the combined effect of disjoining pressure and self-desiccation, resulting in a less dense CSH gel [12].

The literature focused on AAC synthesized using either class F FA, metakaolin, or GGBFS [13]. Few studies focused on alkali-activated class C fly ash (AACFA) binders [14,15] yet with different applications potential such as repair properties [16]. The behavior of AACFA binders differs from AAFFA binders as the two precursors have different chemical compositions. Unlike AAFFA which requires heat for reaction activation, AACFA binders do not require that and can be cured at ambient or heat. This is due to the relatively higher calcium content in the precursor in the case of AACFA binders. For example, Gomaa et al. [15,17], reported that the 7-day ambient-cured compressive strength of AACFA mortars reached up to 15 MPa (2180 psi) while those oven-cured at 70ºC for 24 hours displayed compressive strength up to 40 MPa (5800 psi). The strength of oven-cured specimens continued to increase beyond the oven-curing period reaching , Guo et al. [18] reported also a compressive strength up to 30.6 MPa (4440 psi) after oven curing for 8h at 75°C and then the strength reached 63.4 (9200 psi) MPa after 28 days of ambient curing.

2. RESEARCH SIGNIFICANCE

Most of the literature focused on AAFFA binders and much less research was carried out on AACFA. Those available studies focused on the short-term behavior of

AACFA binders. Therefore, less information is known about the long-term strength development. Furthermore, steam curing is a common practice in the precast industry for CC as it yields early high strength [19]; however, the authors are not aware of any research on the performance of steam-cured AACFA binder. Furthermore, a common rest time of two hours is used in the literature; however, unlike AAFFA there has been no detailed investigation of the effect of rest time on the strength of AACFA. The present manuscript reports the effect of rest time and curing regimes on the strength of AACFA mortar. Furthermore, the strength development of AACFA up to age of 90-days was investigated.

3. EXPERIMENTAL PROGRAM

This study investigated the long-term strength temporal evolvement of AACFA mortar cured under different regimes. The specimens were subjected to rest times ranging from 2 hours to 36 hours prior to being cured to determine the optimum rest time. Once the optimum rest time was determined, the specimens were cured under ambient, oven, or steam conditions. The steam and oven curing were carried out for nine hours at two different temperatures of 55ºC (131ºF) or 80ºC (176ºF). The mortar samples were then tested for compressive strength at different ages up to 90 days. Also, the micro structure of alkali activated paste (AAP) mixes were conducted in order to better understand the performance of the different mixture.

3.1. MATERIAL CHARACTERISTICS

A saturated surface dry (SSD) Missouri river sand was used in this study with a specific gravity of 2.6. Fly ashes, classified as class C per ASTM 618-17, were sourced

from Labadie and Sikeston power plants located in Missouri (US) and were used as precursors (Table 1, Figure 1).

A solution consisting of sodium hydroxide (SH) and sodium silicate (SS) was used as an activator. Solid pellets of SH were mixed with water using a concentration of 10M. Type D SS solution had 55.9% water, 14.7% SiO_2, and 29.4% Na_2O. This solution was used in an earlier study and produced a good combination of strength and workability [15]. Extra water was added to the mix for workability purposes. The nomenclature of each FA consisted the letter "C" representing the classification of the FA (i.e. class C FA), followed by a two-digit integer representing the first two digit of the calcium oxide (CaO) content of the FA. For example, FA from Labadie power plant, is called C37 since it had a CaO content of ~37%. Mortar and paste made out of Labadie FA will be called M37 and P37, respectively.

3.2. MIXTURES PROPORTIONS AND PREPARATION

Two different mixes using SS/SH of one and two were synthesized for each FA (Table 2) [20]. Hereinafter the former is called high alkaline (HA) mix and the latter is called high silicates (HS) mix. It was anticipated that increasing the SS/SH would trigger more geopolymerization reaction to occur [21].

To prepare a mixture, sand and FA were homogeneously mixed together for about 1.5 minutes in a Hobart mixer at speed of 136 rpm. Water was gradually added to the mix over 1.5 minutes. These steps preceded the addition of the activator to prevent agglomeration of the FA particles. The mixing was stopped, and the mixture was scraped for 30 seconds to prevent the mixture from sticking into the bottom of the mixer bowl. The

activator chemicals were mixed together few minutes before adding them to the mixture to ensure a proper and homogenous mix of the two solutions.

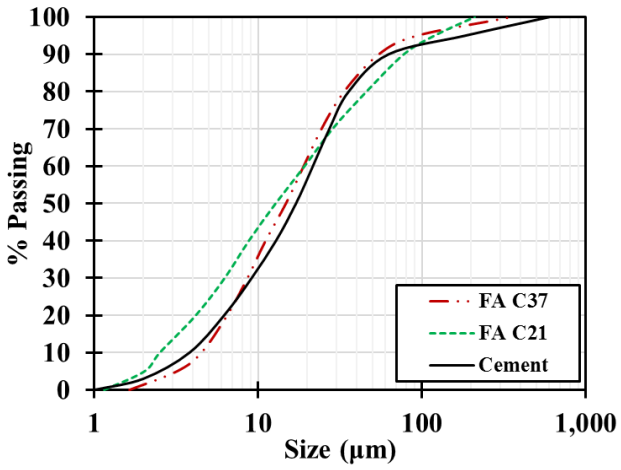

Figure 1. Particles size distribution of cement and FA using Microtrac S3500 laser particle size analyzer

Table 1. X-Ray Fluorescence of Fly Ashes

Fly ash	CaO	Al_2O_3	SiO_2	MgO	Fe_2O_3	Na_2O	TiO_2	P_2O_5	K_2O	LOI
Labadie C37	36.9	13.99	36.89	4.80	3.52	1.62	0.87	0.70	0.62	0.50
Sikeston C21	21.1	20.12	43.91	4.29	4.96	2.87	1.36	0.51	0.70	0.40

Then, the activator was gradually added to the mixture over five minutes to prevent flash setting. The mixing was stopped, and the mixture was scraped for about one minute. Then, mixing the overall mixture at speed of 281 rpm for another five minutes. The mixing speed was increased in order to increase the rate of dissolution of the alumina and silica species in the solution [15,22], . The mixture was then removed from the bowl and placed in 50 mm (2 in.) brass mold.

Table 2. Mix Design Ratio and Quantities

Mix Name	**HA**	**HS**
Ratio		
AC/FA	0.30	0.275
W/FA	0.38	0.40
SS/SH	1.00	2.00
Quantities (Kg/m^3 (lb/ft^3))		
SH	82 (5.12)	49 (3.06)
SS	82 (5.06)	98 (6.12)
Water	113 (7.05)	132 (8.24)
Sand	1500 (93.6)	1470 (91.7)
Fly ash	545 (34.0)	535 (33.4)

W/FA: water-to- fly ash, AC/FA: activator-to-fly ash

3.3. FRESH PROPERTIES OF THE AACFA MORTARS

The flow and final setting time properties of each AACFA mortar mixture were evaluated per ASTM C143/C143M [23] and Vicat needle (ASTM C807-13)[24].

3.4. CURING REGIMES AND REST TIME

The mortar mixtures were cured using either ambient, steam, or heat regimes. For ambient curing, the mortar samples were kept in their respective molds and covered with an impermeable sheet to minimize moisture loss. Then, the samples were placed in the laboratory in ambient conditions at a controlled temperature of 22°C, ±2 (72°F) until the required testing age.

For the steam and heat curing, the specimens had rest time periods of either 2 hours, 6 hours, 12 hours, 24 hours, 30 hours, or 36 hours before starting the curing process. During the rest time the specimens were cured at ambient temperature, as explained before, when

the specimens were let to set and develop initial strength that minimize micro cracks during elevated-temperature curing. For the steam-curing, the specimens were subjected to a combined heat and humid environment created inside a steam chamber at two different temperatures of either 55℃ (131℉) or 80℃ (176℉) for 9 hours (Figure 2). The 9 hours was found to result in the highest strength (Kashosi 2019). For heat curing, the mortar samples, while placed in their respective molds, were encased in thermal bags and placed in an oven at two different temperatures of either 55℃ (131℉) or 80℃ (176℉) for 9 hours. Thermal bags were used to avoid loss of moisture which resulted in surface cracking of the test specimens.

At the end of the required heat and steam-curing time, the cured samples were removed from their respective molds and put in the moisture room until either the test day or seven days whichever occurred first; then, the specimen were kept in a closed container stored in the laboratory under ambient conditions until the test day.

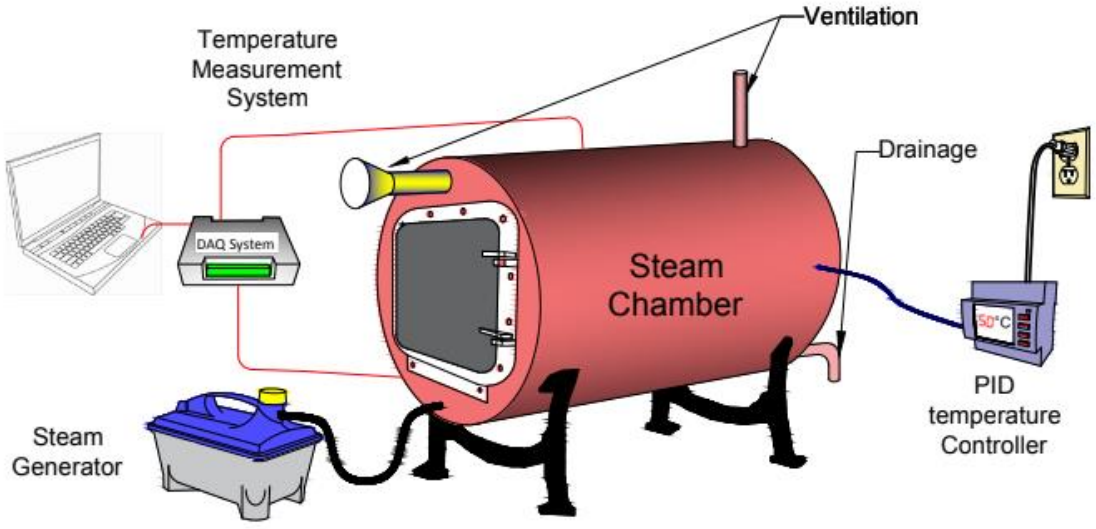

Figure 2. Steam chamber system.

3.5. COMPRESSIVE STRENGTH TESTING

Three sets of compressive strength testing were carried out (Tables 3-4). The first set was carried out after rest times of 2 hours, 6 hours, 12 hours, 24 hours, 30 hours, and 36 hours to determine evolution of early age strength of the different mixtures. For the second set, the compressive strengths of the specimens were determined after being left to rest for the required time and then steam or oven-cured. The third set of specimens was tested to determine the long-term temporal evolution of compressive strength at the ages of 1 day, 7 days, 28 days, 56 days, and 90 days of ambient, steam, and oven-cured specimens. The compressive strength was determined by testing three replicate specimens for each condition in a Tinius Olsen machine at a loading rate of 0.34 MPa/sec (50 psi/ sec) and the average strength value of the three replicate cubes were reported in the results section.

3.6. MICROSTRUCTURE ANALYSIS

3.6.1. X-Ray Diffraction (XRD). AACFA pastes were casted using the same proportions of mortar mixes and cured under the same conditions. Then, the paste samples were crushed into powder and X-Ray diffraction (XRD) test were conducted, using An X'Pert Pro Diffractometer, on each sample as well as the corresponding raw FA to determine the presence and evolution of crystal phases. Pastes samples were used instead of mortars to exclude the participation of quartz crystal present in sand particles, and thus having relatively accurate results. In order to quantify the amorphous and crystalline phases, Anatase Titanium Oxide (TiO2) was added to each sample powder in 10 percent mass proportion.

3.6.2. Scanning Electron Microscopy (SEM) and Energy Dispersive X-Ray Spectroscopy (EDS). FA is a material predominantly composed of amorphous particles, the formed geopolymeric gel resulting from the reaction of the FA, is mainly in an amorphous state. Thus, to complement the XRD data, SEM and EDS analyses were also conducted using a Hitachi S-4700 SEM, to observe the microstructure development and determine the elements composition of the formed products.

4. RESULTS AND DISCUSSIONS

4.1. FLOW AND SETTING PROPERTIES OF AACFA MORTARS

All mixtures had good workability that ranged from 50 to 95% . All setting times were within the specified limits values of the ASTM C807-13 for hydraulic cement of 45 minutes and 375 minutes corresponding to $ASTM_{min}$ and $ASTM_{max}$ in Figure 3, respectively. The flow and setting times of AACFA mortars depended on the chemical composition of precursor such as the Si/Al ratio and Ca content as well as that of the activator. Due to the high calcium content of FA C37 compared to FA C21, M37 mixtures set faster than M21 with an average of 225 minutes for M37 and 325 minutes for M21. In addition, increasing the SS in mixtures HS compared to mixtures HA led to poorer workability due to the high viscosity of the SS [2]; however, increasing the SS did not affect the setting time.

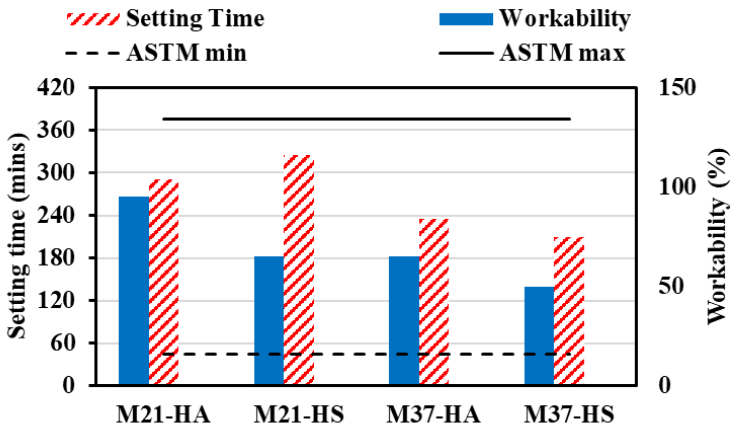

Figure 3. Fresh properties of AACFA mortars.

4.2. EFFECTS OF REST TIME ON THE SHORT TERM STRENGTH OF AACFA MORTARS

The attempts to measure the compressive strengths at early ages of up to 6 hours were not successful as the mortar samples had not set yet or were not hard enough to be safely removed from their respective molds. Beyond that, for ambient curing specimens (Table 3 and Figure 4), after 12 hours of rest time and with FA C37 having nearly twice as much calcium content as FA C21 (Table 1), mixes M37 developed an average compressive strength of 9.8 MPa (1425 psi) compared to mixes M21 which developed an average compressive strength of 0.5 MPa (78 psi). When the calcium oxide present in the FA gets in contact with water, it dissolves, precipitates, nucleates, and grows into calcium silicate hydrate (C-S-H) which is responsible for strength development. Therefore, the higher the calcium content is the higher C-S-H and higher strength. Increasing the rest time to 36 hours, significantly increased the compressive strength by 203% for mixtures M37 as well as 1173% and 205% for M21-HA and M21-HS, respectively (Figure 4). The observed difference in the compressive strength of mixtures HA and HS was essentially due to the

Si/Al content. Mixture HS contained a relatively higher Si/Al or lower concentration of Al compared to mixture HA which reduced the strength gain at early ages [3].

Specimens oven or steam-cured at 80℃ (176℉) displayed higher strength in comparison to those cured at 55℃ (131℉). Increasing the temperature increased the energy available to break the Si-O covalent bond of oligomers and thus allowing a fusion between two oligomers during the polycondensation phase of the geopolymerization. The strengths of the steam-cured mixtures ranged from 18.3 MPa (2660 psi) to 63.6 MPa (5810 psi) for M21 and from 26.2 MPa (5520 psi) to 59.6 MPa (8650 psi) for M37 (Figure 5) depending on the rest time, curing temperature, activator constituents.

For M21, increasing the rest time from 2 hours to 12 hours, increased the compressive strengths by 40% to 86% (Figure 6a). Beyond that the compressive strengths either remained constant in the case of M21-HA cured at 55 ºC (131 ºF) or increased by 94% to 136% of the corresponding 12 hours rest time compressive strength. Furthermore, M21-HS specimens displayed relatively higher increases in strengths with increasing the rest time. This can be linked to the evolvement of strength under ambient conditions. M21-HS and M21-HA reached approximately 100 psi (0.7 MPa) at 30 hours and 12 hours, respectively, which is the minimum recommended compressive strength before starting steam curing for Portland cement-based concrete [25].

For M37, increasing the rest time to 12 hours, increased the compressive strengths by 28% to 56% (Figures 6c). Beyond that the strength remained either constant or decreased except for M37-HA cured at 55℃ (131℉) where the compressive strength slightly increased with increasing the rest time. M37 mixtures gained significant strengths

of more than 1200 psi by 12 hours rest time beyond that less benefits from heat curing occurred at this point.

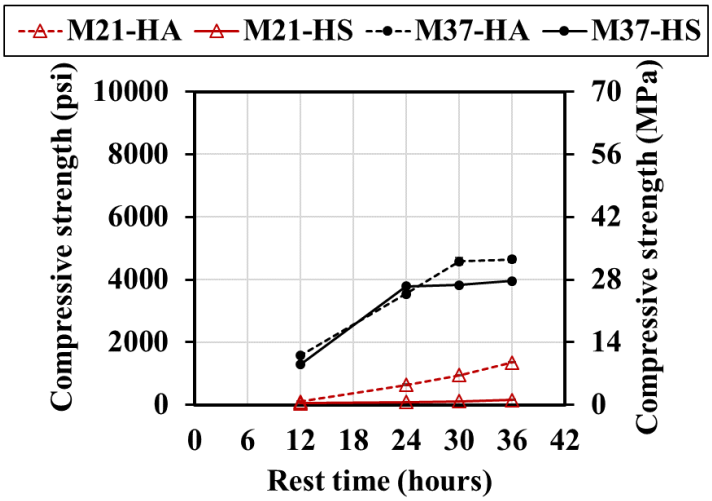

Figure 4. Effect of rest time on the compressive strength of ambient-cured AACFA mortars.

The strengths of the oven-cured specimens ranged from 13 MPa (1888 psi) to 58.6 MPa (8493 psi) for M21and from 25.7 MPa (3732 psi) to 50.7 MPa (73547 psi) for M37 (Figure 7) depending on the rest time, curing temperature, activator constituents. For M21, increasing the rest time from 2 hours to 12 hours, increased the compressive strengths by 27% to 106% (Figure 6b).

Beyond that and at rest times of 24 hours – 30 hours, the mixes reached their peak strengths reaching 49% to 136% of the corresponding 2 hours rest time compressive strength. That was followed by a slight reduction in the compressive strength except M21-HS cured at 80ºC (176ºF). For M21-HS cured at 80 ºC (176 ºF), the compressive strength continuously increased reaching 90% of the corresponding 2 hours rest time compressive strength at 36 hours rest time.

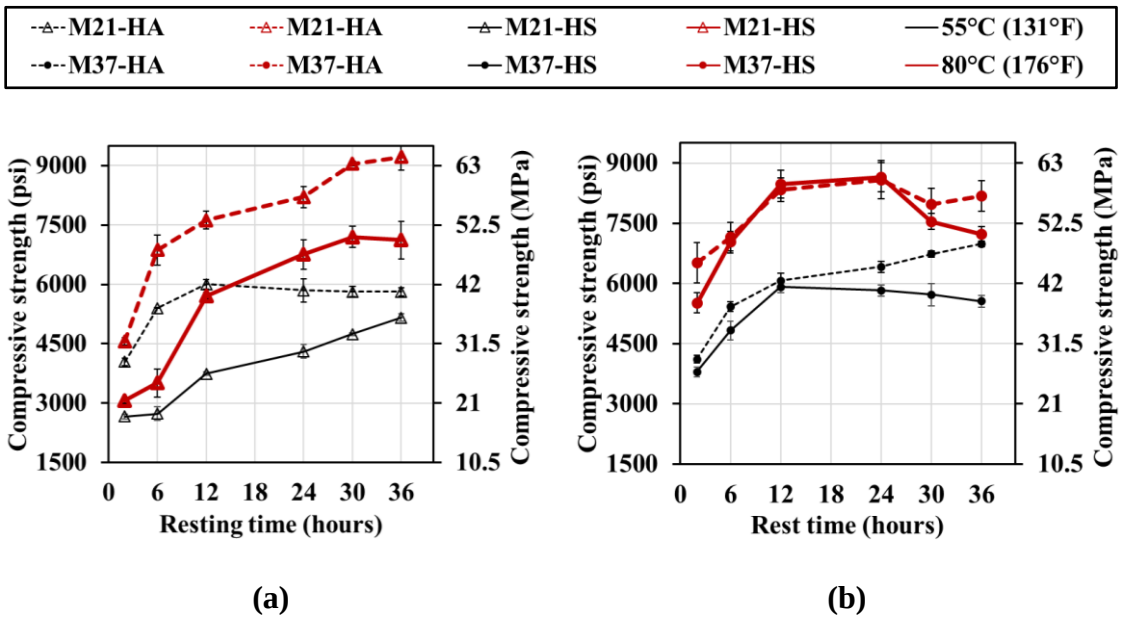

Figure 5. Effect of rest time on the compressive strength of steam-cured: a) M21, and b) M37.

The strengths of the oven-cured specimens ranged from 13 MPa (1888 psi) to 58.6 MPa (8493 psi) for M21and from 25.7 MPa (3732 psi) to 50.7 MPa (73547 psi) for M37 (Figure 7) depending on the rest time, curing temperature, activator constituents. For M21, increasing the rest time from 2 hours to 12 hours, increased the compressive strengths by 27% to 106% (Figure 6b).

Beyond that and at rest times of 24 hours – 30 hours, the mixes reached their peak strengths reaching 49% to 136% of the corresponding 2 hours rest time compressive strength. That was followed by a slight reduction in the compressive strength except M21-HS cured at 80ºC (176ºF). For M21-HS cured at 80 ºC (176 ºF), the compressive strength continuously increased reaching 90% of the corresponding 2 hours rest time compressive strength at 36 hours rest time.

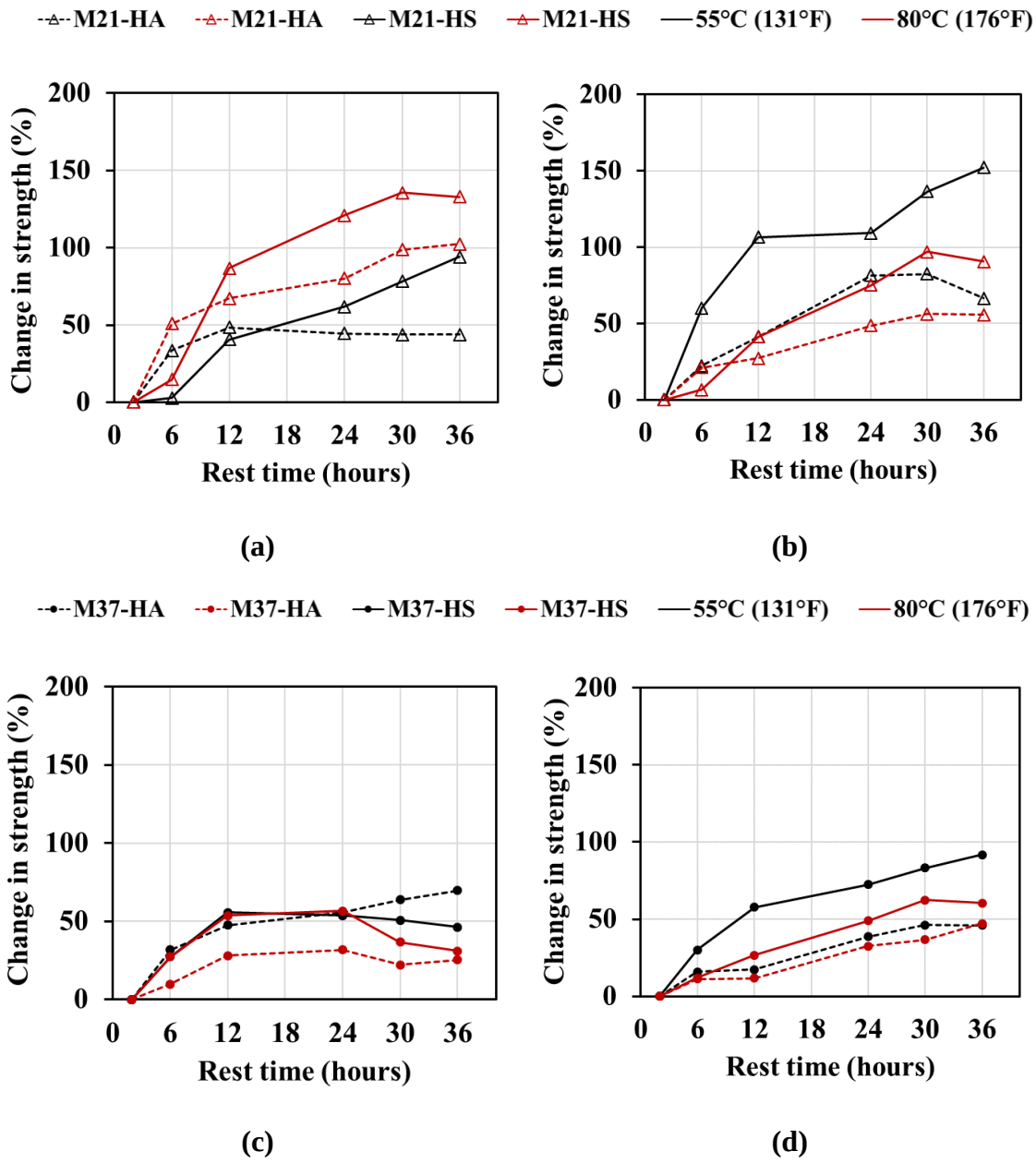

Figure 6. Percentage strength increase of AACFA mortar relative to the 2 hours of rest time compressive strength of: a) Steam-cured M21 mixes. b) Oven-cured M21 mixes. c) Steam-cured M37 mixes. d) Oven-cured M37 mixes.

Increasing the rest time for M37 from 2 hours to 12 hours, increased the compressive strengths by 11% to 84% depending on the curing temperature and activator constituents. Beyond that and at rest time of 30 – 36 hours, the mixes reached 37% to 63%

of the corresponding 12 hours rest time compressive strength (Figure 6d). That was followed by insignificant reduction or increase in the compressive strength.

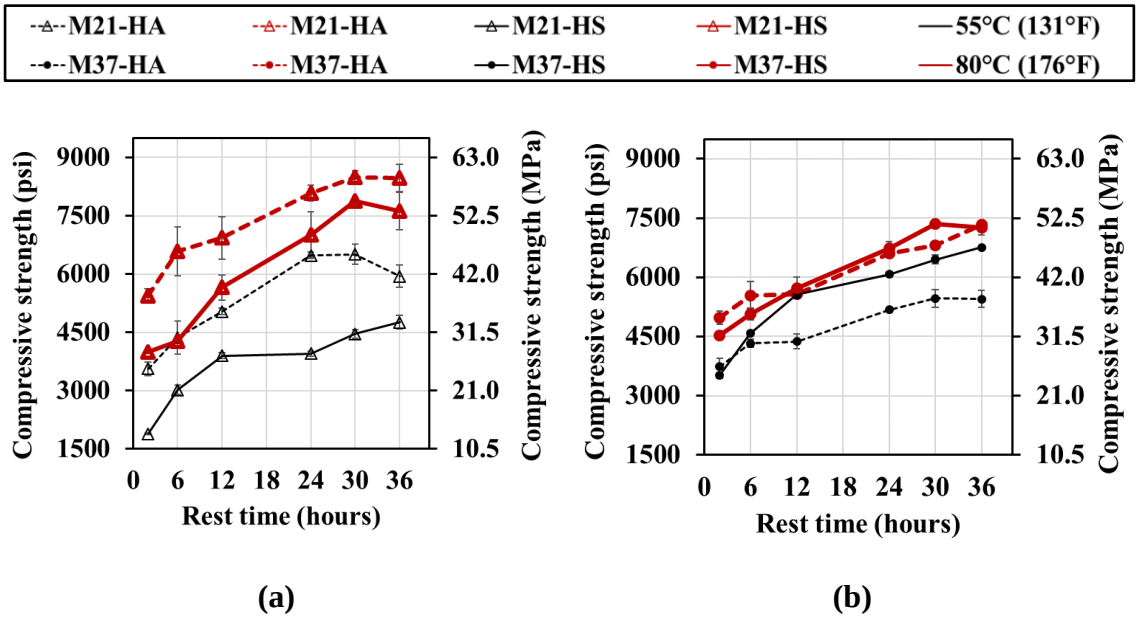

Figure 7. Effect of rest time on the compressive strength of oven-cured: a) M21, and b) M37.

This section of the study displayed that for mixtures, M21, synthesized using low calcium content, both curing regimes yielded very close strength. For mixtures, M37, synthesized using high calcium content, steam curing at 80°C (176°F) consistently yielded approximately 17% higher strength. Similarly, the 55°C (131°F) steam-cured M37-HA displayed 27% higher strength than the corresponding oven-cured mixture. However, the 55°C (131°F) steam-cured M37-HS displayed 17% lower strength than the corresponding oven-cured mixture. Furthermore, in no case a rest time of 12 hours resulted in a reduction in the compressive strength. Most mixtures reached 72% to 100% of their peak strengths when had a rest time of 12 hours. Considering also practicality, 12 hours was selected as an optimum rest time for all mixtures used in the remaining of this study.

Table 3. Summary of short-term compressive strength development

Mix	est time	Compressive Strength									
	(hrs)	Ambient		Oven-55°C		Oven-80°C		Steam-55°C		Steam-80°C	
		psi	MPa	psi	MPa	psi	MPa	psi	MPa	psi	MPa
M21-HA	2	-	-	3570	24.6	5440	37.5	4044	27.9	4555	31.4
	6	-	-	4371	30.1	6591	45.4	5400	37.2	6869	47.4
	12	106.0	0.70	5038	34.7	6929	47.8	6006	41.4	7620	52.5
	24	630.0	4.30	6482	44.7	8090	55.8	5846	40.3	7855	54.2
	30	951.0	6.60	6511	44.9	8493	58.6	5816	40.1	9048	62.4
	36	1350	9.30	5945	41.0	8470	58.4	5814	40.1	9221	63.6
M21-HS	2	-	-	1888	13.0	4002	27.6	2660	18.3	3058	21.1
	6	-	-	3024	20.8	4266	29.4	2732	18.8	3509	24.2
	12	51.00	0.30	3899	26.9	5652	39.0	3744	25.8	5710	39.4
	24	86.00	0.60	3953	27.3	7014	48.4	4303	29.7	6753	46.6
	30	110.0	0.80	4464	30.8	7887	54.4	4741	32.7	7201	49.7
	36	155.0	1.10	4763	32.8	7630	52.6	5163	35.6	7120	49.1
M37-HA	2	-	-	3732	25.7	4977	34.3	4115	28.4	6521	45.0
	6	-	-	4327	29.8	5533	38.1	5425	37.4	7166	49.4
	12	1567	10.8	4375	30.2	5566	38.4	6073	41.9	8341	57.5
	24	3539	24.4	5173	35.7	6602	45.5	6416	44.2	8584	59.2
	30	4582	31.6	5462	37.7	6803	46.9	6735	46.4	7969	54.9
	36	4642	32.0	5446	37.5	7329	50.5	6988	48.2	8179	56.4
M37-HS	2	-	-	3522	24.3	4524	31.2	3797	26.2	5520	38.1
	6	-	-	4578	31.6	5064	34.9	4828	33.3	7031	48.5
	12	1282	8.80	5555	38.3	5727	39.5	5914	40.8	8477	58.4
	24	3785	26.1	6078	41.9	6743	46.5	5832	40.2	8648	59.6
	30	3831	26.4	6452	44.5	7347	50.7	5726	39.5	7546	52.0
	36	3959	27.3	6759	46.6	7253	50.0	5557	38.3	7234	49.9

4.3. LONG TERM STRENGTH DEVELOPMENT OF AACFA MORTARS

4.3.1. Ambient-cured Specimens. The strength of ambient-cured specimens increased with time (Table 4 and Figure 8), due to the nucleation and growth of different formed products at different rates, with M37 mixes displayed strengths approximately

187% of that of M21 in average. The strengths at the different ages were normalized by the corresponding strength at 28 days, f'_m, (Figure 8b). The compressive strengths of M37 mixes reached 0.51 f'_m at one day of curing where f'_m was 49.3 MPa (7150 psi). The strength gain continued up to a period of 56 days, beyond that no more significant strength development occurred. Both M37 mixtures developed strengths at the same rate as both mixtures had Ca-rich products and hence hydration was the governing reaction. The availability of Ca ions in the solution, determined the amount of CSH products formed which governed the strength development process, and thus the presence of extra silica and sodium species in the mix had little impact on the compressive strength of these mortar specimens. Therefore, the strength of mixes M37 grew fast at ambient conditions up to 28 days. As formed product grew, they increased in volume, occupying the majority of particles dissolution sight and thus considerably hindered further reaction to happen [26], which explains the small strength evolution at later ages. The mixes reached an average 118% f'_m at 90 days.

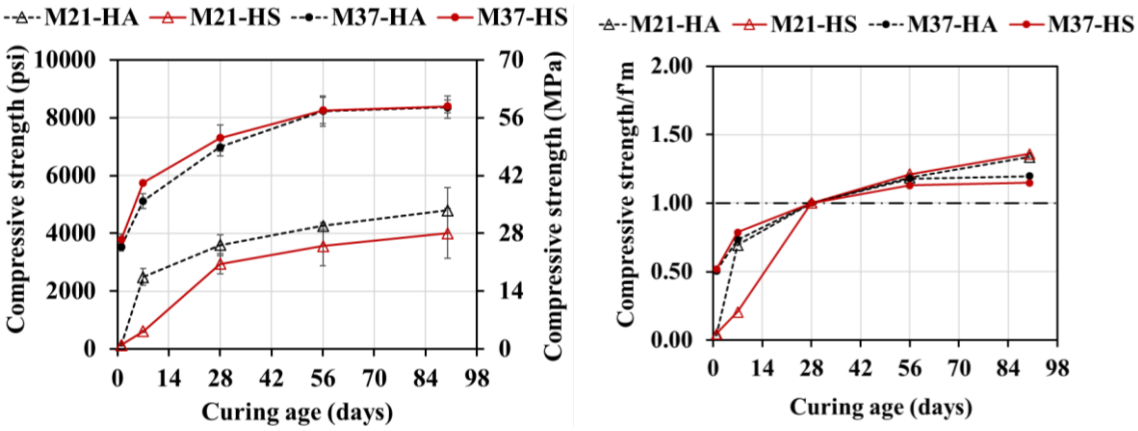

(a) (b)

Figure 8. Ambient compressive strength development of AACFA mortars: (a) absolute value, and (b) normalized f'_m.

Mixes M21 demonstrated very low compressive strengths at the age of one day, but later a significant increase evolved with time. The precursor FA C21 had relatively a low calcium content and hence the main products formed during the hardening process were essentially geopolymeric gels such as calcium-aluminosilicate-hydrate (CASH), sodium-aluminosilicate-hydrate (NASH), and/or calcium-sodium-aluminosilicate-hydrate (CNASH), yet these formed products do require high temperature for a rapid strength development. The formation of each of these products depends on the amount and the form in which each of the Ca, Si, Al, and Na is available in the precursor and activator materials. For mix M21-HA, a relatively rapid strength development was observed within one week of curing reaching 69% f'_m where f'_m was 24.8 MPa (3590 psi) and then reached 134% f'_m at 90 days.

Mix M21-HS demonstrated a low strength development during the first two weeks of curing but progressively increased over time reaching f'_m of 20.3 MPa (2950 psi). This was followed by a rate of increase similar to that of mix M21-HA for the remaining curing time attaining 136% f'_m at 90 days. The lower strength development of mix M21-HS compared to mix M21-HA at early ages was due to the effect of the concentration of the silica in the activator. In the case of M21-HS which had high silica content, polysialate-disioloxo are the main formed oligomers from the hydrolysis of dissolved ions in the solution of the mix M21-HS, which had a slower polycondensation rate than polysialate and polysialate-siloxo that were formed in the case of M21-HA with low silica content.

4.3.2. Thermally-cured Specimens. Elevated temperatures had a significant influence on the geopolymerization process, since the reaction kinetics requires a certain

amount of heat in order to be accelerated. However, the reaction did not stop at the end of the thermal-curing process (Figures 9 and 10).

4.3.2.1. Oven-cured strength development. The 55˚C (131˚F) oven-cured one-day compressive strengths for mixes M21 and M37 were 30.8 and 34.3 MPa (4470 and 4968 psi), respectively, which increased to 43.3 and 39.0 MPa (6270 , and 5790 psi) when the curing temperature was increased to 80˚C (176˚F) corresponding to strength increases of 42% and 15%, respectively (Figure 9). Increasing the curing temperature increased the initial rate of reaction leading to accelerated formation and growing of geopolymer products and hence relatively higher strength.

The strength increased linearly with time and with higher rate of increase for the 55˚C (131˚F) oven-cured specimens. The 90-day compressive strength values of the 55˚C (131˚F) and 80˚C (176˚F) increased by 45% - 70% and 10 – 25% compared to those of one-day compressive strengths reaching values of 40.1 - 57.2 MPa (5820 - 8300 psi), and 46.6 MPa - 58 MPa (6760 psi to 8410 psi) respectively.

The lower rate of increase in the case of 80˚C (176˚F) occurred since the reacted products formed during the hardening process would cover the surface of the fly ash particles when samples were cured at higher temperature of 80˚C (176˚F). Therefore, more dissolution sights of fly ash particles would be blocked, and less dissolution from fly ash particles occurred and no significant increase in the formed geopolymer product would happen leading to a limited increase in compressive strength. While samples cured at 55˚C (131˚F) would have less formed products, thus more uncovered surface and more dissolution sights. In this case, as time passes more dissolved species from FA particles

would condense the available to form new products producing strong and stable gel structure, and thus higher strength [8][12].

Table 4. Summary of Long-Term compressive strength development.

Mix	Age	Measured Compressive Strength: psi (MPa)									
	days	Ambient		Oven-55°C		Oven-80°C		Steam-55°C		Steam-80°C	
		psi	MPa	psi	MPa	psi	MPa	psi	MPa	psi	MPa
M21-HA	1	125	0.9	5038	34.7	6929	47.8	6006	41.4	6912	47.7
	7	2492	17.2	5227	36.0	7036	48.5	6101	42.1	6600	45.5
	28	3591	24.8	6118	42.2	7490	51.6	6555	45.2	6468	44.6
	56	4255	29.3	6750	46.5	7916	54.6	7457	51.4	6322	43.6
	90	4799	33.1	7679	52.9	8411	58.0	7807	53.8	6251	43.1
M21-HS	1	139	1.0	3899	26.9	5612	38.7	3744	25.8	6342	43.7
	7	609	4.2	4011	27.7	6086	42.0	3989	27.5	5521	38.1
	28	2946	20.3	4293	29.6	6159	42.5	4391	30.3	5177	35.7
	56	3567	24.6	4994	34.4	6360	43.9	4641	32.0	5111	35.2
	90	4008	27.6	5818	40.1	6504	44.8	5158	35.6	4869	33.6
M37-HA	1	3539	24.4	4375	30.2	5973	41.2	5857	40.4	7734	53.3
	7	5119	35.3	4523	31.2	6108	42.1	6676	46.0	7720	53.2
	28	6985	48.2	5850	40.3	6263	43.2	6833	47.1	7460	51.4
	56	8237	56.8	6563	45.3	6729	46.4	6653	45.9	7390	51.0
	90	8367	57.7	7455	51.4	6755	46.6	7120	49.1	6630	45.7
M37-HS	1	3785	26.1	5727	39.5	5611	38.7	5914	40.8	7072	48.8
	7	5747	39.6	6135	42.3	5617	38.7	6814	47.0	7014	48.4
	28	7305	50.4	6424	44.3	5652	39.0	6835	47.1	6942	47.9
	56	8254	56.9	7161	49.4	6544	45.1	7194	49.6	6847	47.2
	90	8393	57.9	7186	49.5	6999	48.3	7480	51.6	6734	46.4

4.3.2.2. Steam-cured strength development. The strength increased linearly with time and with higher rate of increase for the 55℃ (131℉) steam-cured specimens. The 90-day compressive strength values of the 55℃ (131℉) increased by 21% - 38% compared to those of one-day compressive strengths reaching values of 35.6 - 53.8 MPa (5160 – 7810 psi) (Figure 10). However, for the 80℃ (176℉) steam-cured specimens, the strength

decreased by 5% - 23% compared to those of one-day strengths reaching 33.6 MPa - 46.4 MPa (4870 psi - 6730 psi) (Figure 10b). As explained in the case of 80℃ (176℉) oven-curing, the rate of reaction is high, therefore polycondensation between oligomers occurred so fast and as a consequence, the formed geopolymeric gel grew so fast surrounding most of the unreacted fly ash particles and thus considerably reducing the dissolution sights and potentially blocked all dissolution sights and thus the reaction process stopped. Furthermore, during the curing process, the relative humidity in the steam chamber was very high (95%), but after curing, sample were stored in ambient condition with a lesser relative humidity which resulted in mortar specimens losing moisture progressively creating voids at the same time. In the case of samples cured at 55℃ (131℉), since dissolution continued, voids are progressively filled with newly formed products growing and resulted in an increase in strength. But in the case of samples cured at 80℃ (176℉) no more products are formed, and voids remained unfilled; these voids weaken the structure of the geopolymeric gel resulting in strength regression.

4.3.3. Strength of Ambient vs. Thermally-cured Specimens. Figures 11-12 summarizes the effect of all three curing regimes on the different mixes. Oven and steam-curing at either 55℃ or 80℃ (131 or 176℉) of M21 mixes developed one-day compressive strengths higher than those of the ambient-cured specimens (Figures. 9-10).

Furthermore, both steam and oven curing developed approximately the same one-day compressive strength. Furthermore, the 90-day compressive strength of the oven-cured and steam-cured ranged from 30% to 63% and 60% to 75% greater than those of the ambient cured specimens, respectively. That was due to the nature of formed reacted products and the precursor which is rich in alumina and silicate; therefore, the

geopolymerization process was accelerated in the presence of heat while it was quite slow at ambient temperature. Furthermore, both specimens oven-cured or steam-cured at 55℃ (131℉) displayed approximately the same strength. For higher curing temperature of 80℃ (176℉), oven-cured specimens displayed a 32% to 35% higher compressive strengths compared to those steam-cured. This occurred as the steam-cured specimens lost strength with time as explained earlier. The one-day strength of oven-cured M37 mixtures demonstrated also similar strength development as M21 mixes. That was because the leaching properties of calcium is hindered at elevated temperatures and thus the formed products in this case would be rich in Al and Si species as well as Ca content, in contrast to the case where they were cured in ambient conditions as explained earlier.

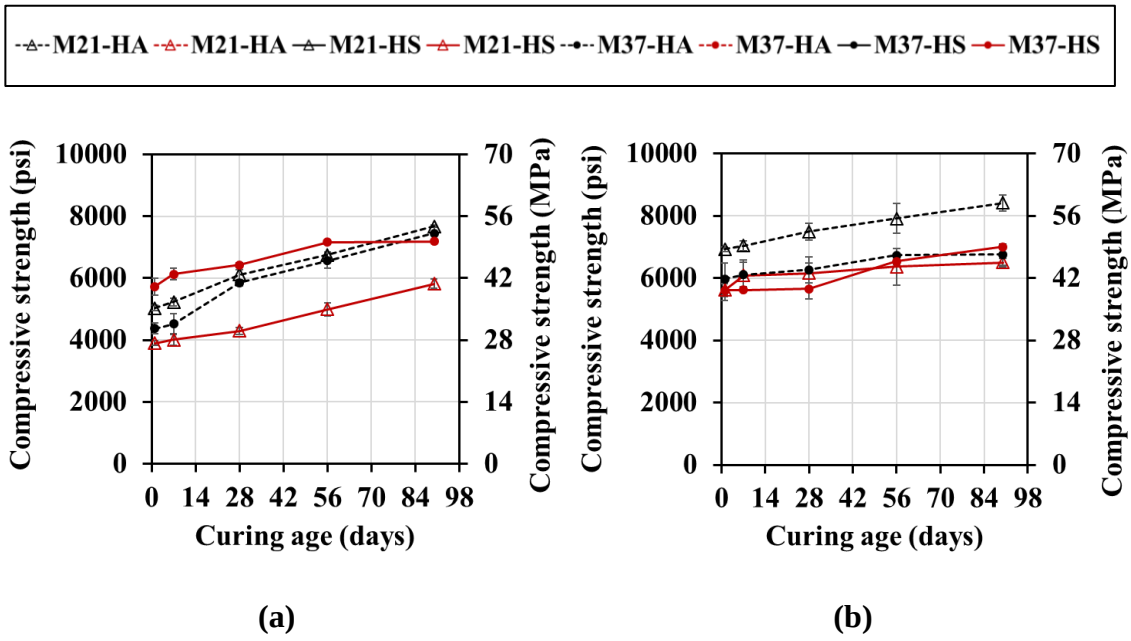

Figure 9. Compressive strength evolution of oven-cured specimens cured at: a) 55℃ (131℉), and b) 80℃ (176℉).

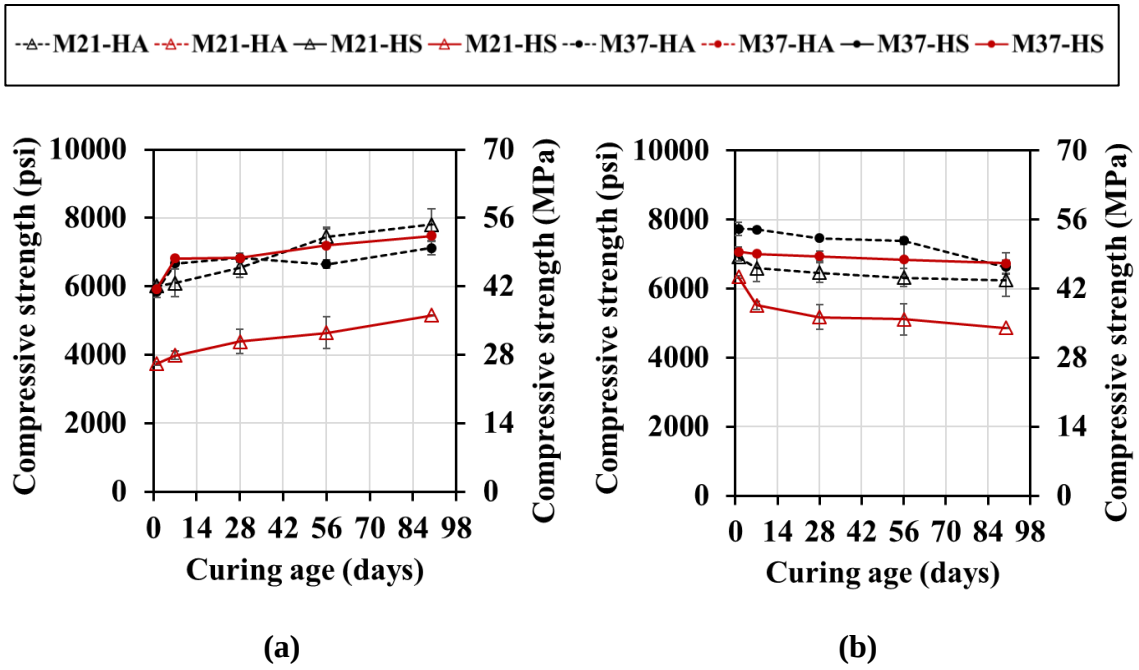

Figure 10. Compressive strength evolution of steam cured specimens cured at: a) 55℃ (131℉), and b) 80℃ (176℉).

For M37 mixes, since it is expected for the reacted products to be essentially rich in Ca; therefore, the moisture provided by the steam curing was beneficial for the reaction. Which explained the higher strength reported right at the end of the curing regime. And due to this favorable reaction environment created by the steam regime and the moisture room, much of the reaction happened during the 9 hours of steam curing followed by 6 days of curing in the moisture room, and thus less far strength increased occurred over time. However, the 90-day compressive strength of oven or steam-cured M37 mixes were approximately the same and were 10% to 15% lower than those of the ambient cured specimens. This is related to the type of the formed products as explained earlier.

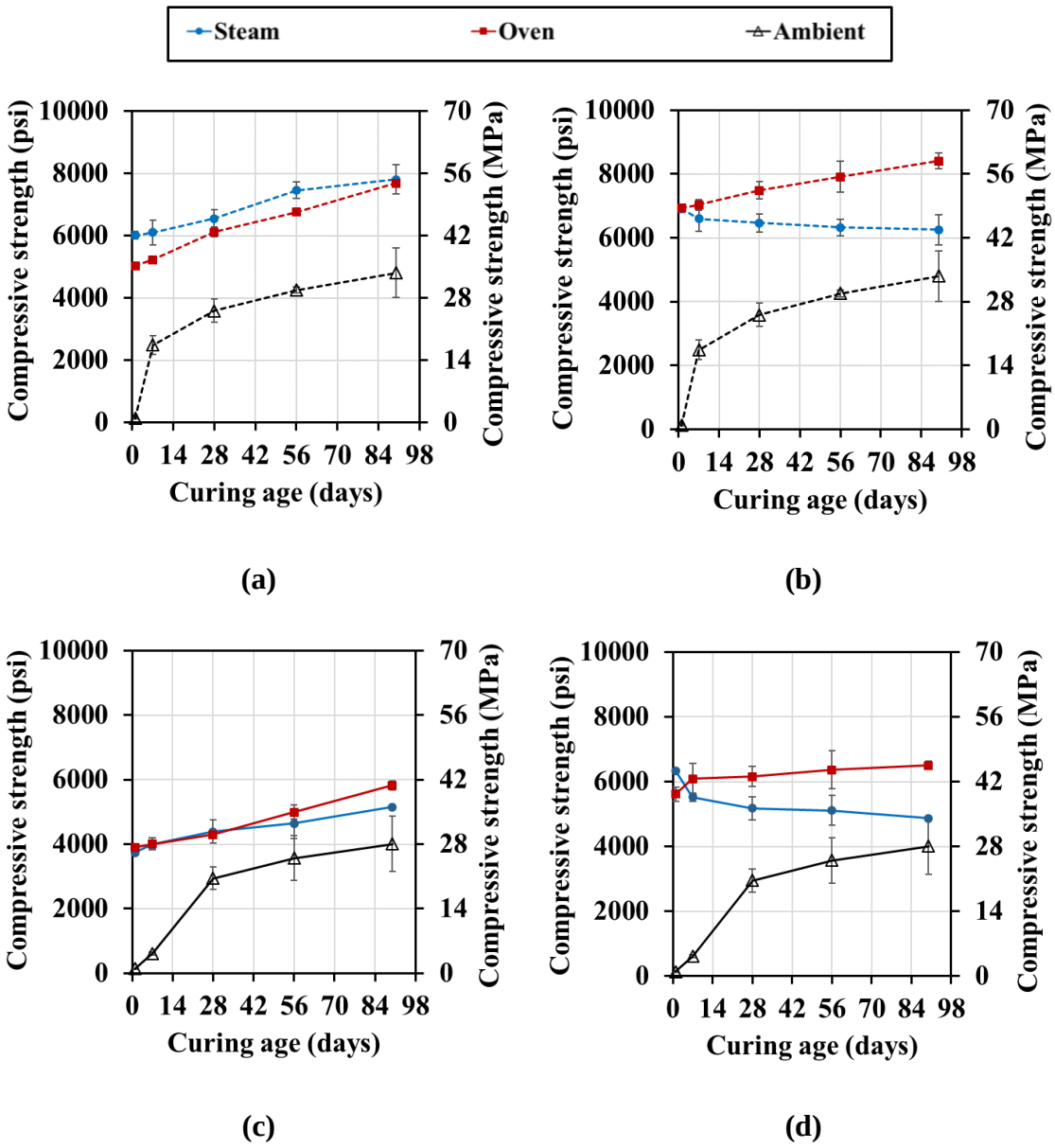

Figure 11. Comparison between ambient curing, oven, and steam curing for: a) M21-HA at 55ºC (131ºF), b) M21-HA at 80ºC (176ºF), c) M21-HS at 55ºC (131ºF), and d) M21-HS at 80ºC (176ºF).

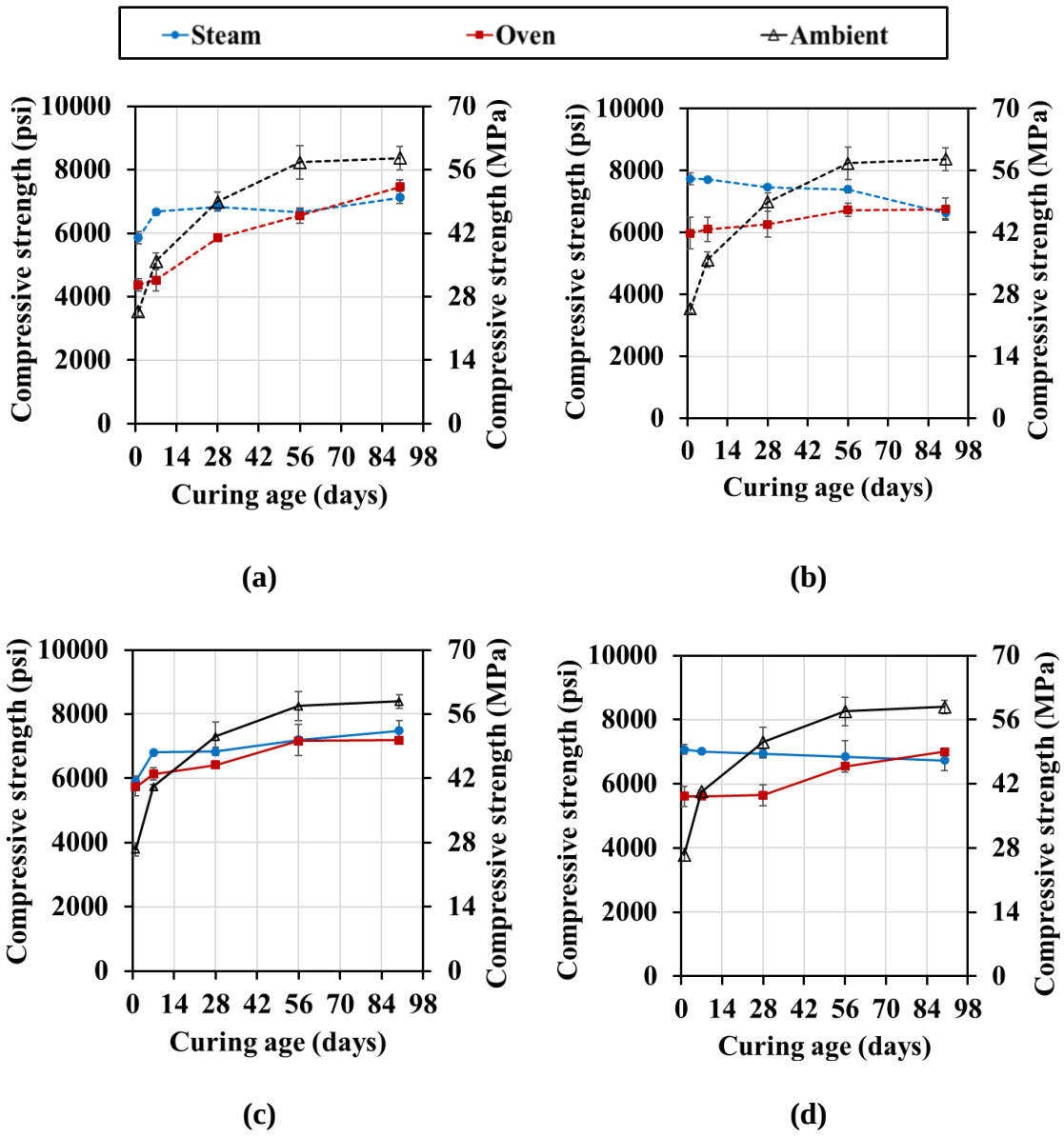

Figure 12. Comparison between ambient curing, oven, and steam curing for: a) M37-HA at 55ºC (131ºF), b) M37-HA at 80ºC (176ºF), c) M37-HS at 55ºC (131ºF), and d) M37-HS at 80ºC (176ºF).

4.4. MICROSTRUCTURE AND NANOSTRUCTURE ANALYSIS

4.4.1. X-Ray Diffraction Analysis. Figure 13 shows results of XRD measurement conducted on raw FAs and paste powder from each mix cured in ambient condition. The main crystal phases present in the FA C37-2.65 were: Anatase (hereinafter A),

Periclase (hereinafter P), Quartz (hereinafter Q), Gehlenite (hereinafter G), and Hatrurite (hereinafter H) while those in the FA C21-2.20 were A, Q, G, and P. The presence of A crystals were due to its addition as an internal for crystal phases quantification purposes (Table 5). The XRD patterns of M21 mixes (Figure 13a) did not show significant change compared to the raw FA which confirmed the low early ambient compressive strengths.

The one-day compressive strength of the steam-cured M37 mixes demonstrated 56% to 126% and 3% to 34% higher strengths than those of the ambient-cured and oven-cured specimens, respectively.

The XRD patterns of M37 (Figure 13b) showed a reduction in peak intensities of Q, G, and H indicating dissolution of these species. The XRD patterns displayed new small sharp peaks corresponding to the formation of calcium-silicate-hydrate CSH (hereinafter C) and Katoite (hereinafter K) which is mainly calcium-aluminosilicate-hydrate products (CASH) responsible for the early age high strength of M37 mixes cured under ambient conditions (Figure 8). The reduction of Q and H was higher in the case of M37-HS compared to the M37-HA indicating more geopolymerization and hydration reactions took place. However, there were more dissolution of G and higher peak of C for M37-HA compared to the M37-HS. These changes in Q, G, H, and C balanced each other and can explain the small difference in compressive strength between M37-HA and M37-HS.

The XRD patterns of oven-cured mixes are shown in Figure 14. In the case of mixes M21, there was a reduction in the peak intensity of G indicating a dissolution of Ca, Al, and Si species. The reduction in the peak was more significant in the case of M21-HA which contributed to the higher strength of M21-HA compared to M21-HS. There was also a noticeable broad hump forming at 28º - 30º, and 41º which indicated a formation of an

amorphous product from the geopolymeric reaction. In addition, a wider hump was noticed in the XRD patterns of mixes cured at 80ºC (176ºF) than for those cured at 55ºC (131ºF) since more product formed at higher temperature as explained earlier. A much broader hump implies a much dense gel structure, and hence higher strength, which explain the difference in strength of mixes cured at these two temperatures (Figure 9).

The crystalline content decreased from 13% in FA C21 to 4% – 7% in mixes M21 indicating that more amorphous products were formed (Table 5). However, no new peaks were formed indicating that there were no new crystalline compounds formed.

For oven cured mixes M37 (Figure 14b), a formation of small peaks at 17º and 28º indicated the presence of CASH products. The reaming peaks in M37 corresponded to the crystals phases present in the raw FA C37. Therefore, strength development of oven-cured M37 as observed in Figure 9, mainly depended on the growth of CASH products. The absence of any CSH formation in the XRD occurred since elevated temperatures hindered the leaching of calcium in FA [18].

The XRD patterns of steam-cured M21 mixes (Figure 15) were similar to those of the oven-cured mixes but with wider humps observed at 28º - 30 º and 41º for steam-cured specimens which explained the slightly high strength of steam-cured mixes compared to the oven-cured ones. Since the wide hump represented the formation of a denser amorphous gel as explained earlier.

In the case of mixes M37, in addition to the broad hump occurring at 2Ɵ of 28º - 30 º, there were formation of new peaks at 38ºwhich were K crystals forming (CASH) (Figure 15b). Sharper peaks of K crystals high intensities and broader humps indicating amorphous compounds with were observed in mixes cured at 80ºC (176ºF) rather than

those cured at 55ºC (131ºF) which explained the higher compressive strength of these mixes compared to those cured at a lower temperature.

Table 5. Measured crystalline content (%)

Mix	Days	Ambient	Oven-55°C	Oven-80°C	Steam-55°C	Steam-80°C
C21-2.20				12.9		
M21-HA	1	7.6	7.1	6.1	5.8	5.4
	7	6.1	7.5	8.4	6.7	6.6
	90	4.1	5.7	5.4	4.1	5.3
M21-HS	1	7.3	6.0	5.7	6.3	6.7
	7	8.8	6.4	7.1	7.3	7.9
	90	6.2	7.3	7.8	5.6	7.3
C37-2.65				15.9		
M37-HA	1	6.9	8.0	8.2	7.2	7.2
	7	6.8	8.7	6.2	9.7	8.2
	56	6.4	6.8	7.8	6.1	7.0
M37-HS	1	6.1	5.8	5.2	5.9	6.2
	7	5.2	7.8	8.4	7.6	6.2
	56	7.6	7.2	5.4	6.1	6.3

When looking at the temporal development of crystalline phase's formation in XRD patterns of ambient-cured paste mixes as shown in Figure 16, it was observed that over time, a decrease in intensity of crystal phases originally present in the unreacted FAs happened especially in those G and H crystals , which indicated a continuous dissolution taking place.

However, an increase in the peak intensity of newly formed crystalline phases was observed, this indicated a continuous growth of formed products over time, resulting in the observed increase in the ambient compressive strength over the 90 days of curing (Figure 8). In the case of M37 mixes, it was essentially due to the growth of CSH and CASH (Figure 16b) with a faster growth rate, while for M21 mixes, it was essentially due to the

formation of an amorphous geopolymeric gel with a relatively slow growth rate, as indicated by the broad hump at 2Θ of 28 - 30° widening with time.

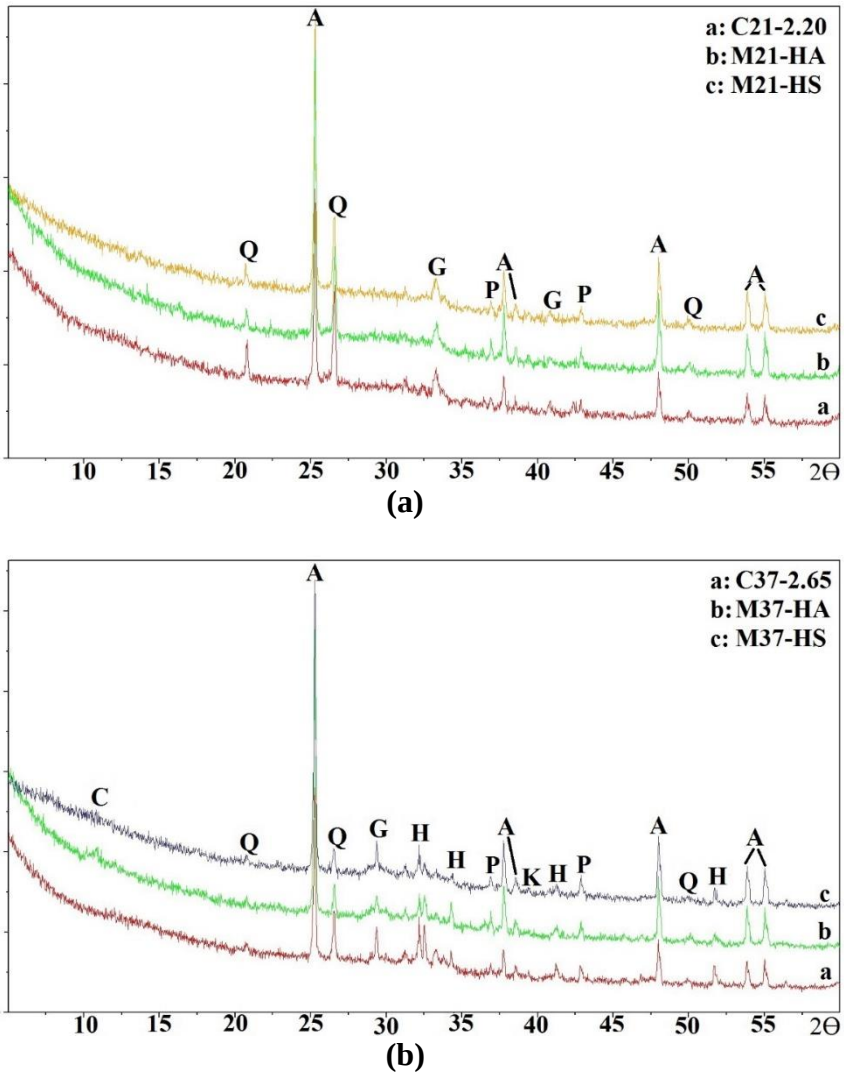

Figure 13. XRD patterns of unreacted FAs and AACFA pastes ambient-cured for one day: a) M21 mixes, and b) M37 mixes.

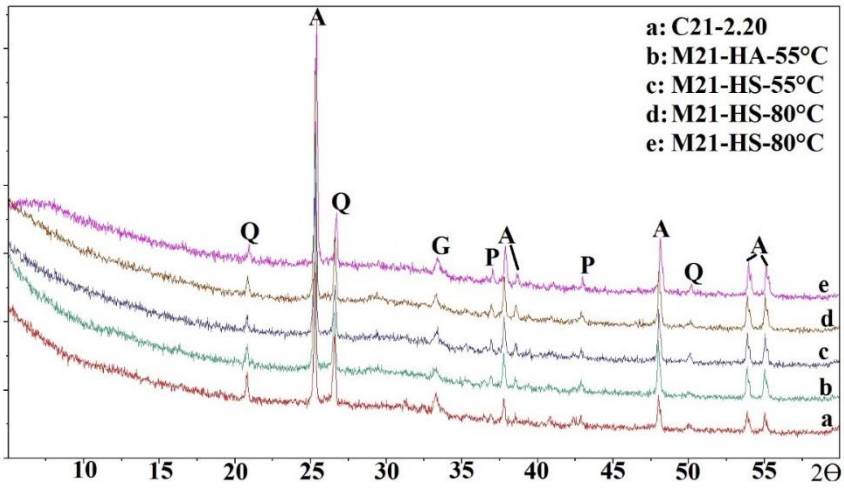

(a)

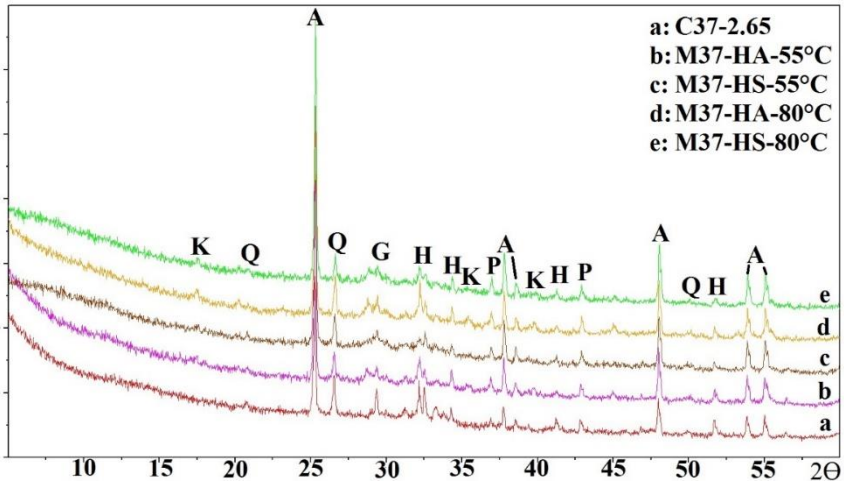

(b)

Figure 14. XRD patterns of unreacted FAs and AACFA pastes oven-cured at 55ºC or 80ºC for: a) M21 mixes, and b) M37 mixes.

4.4.2. SEM and EDS Analysis. Figure 17 shows SEM images of both FA C21 and P21 pastes steam-cured at 80ºC (176ºF). The unreacted FA particles had spherical shapes that varied in sizes (Figure 17a). The EDS results showed that the main elements in the unreacted FA C21 particles were O, Si, Al, and Ca with the presence of Na, Mg and Fe in small quantities (Figure 18a).

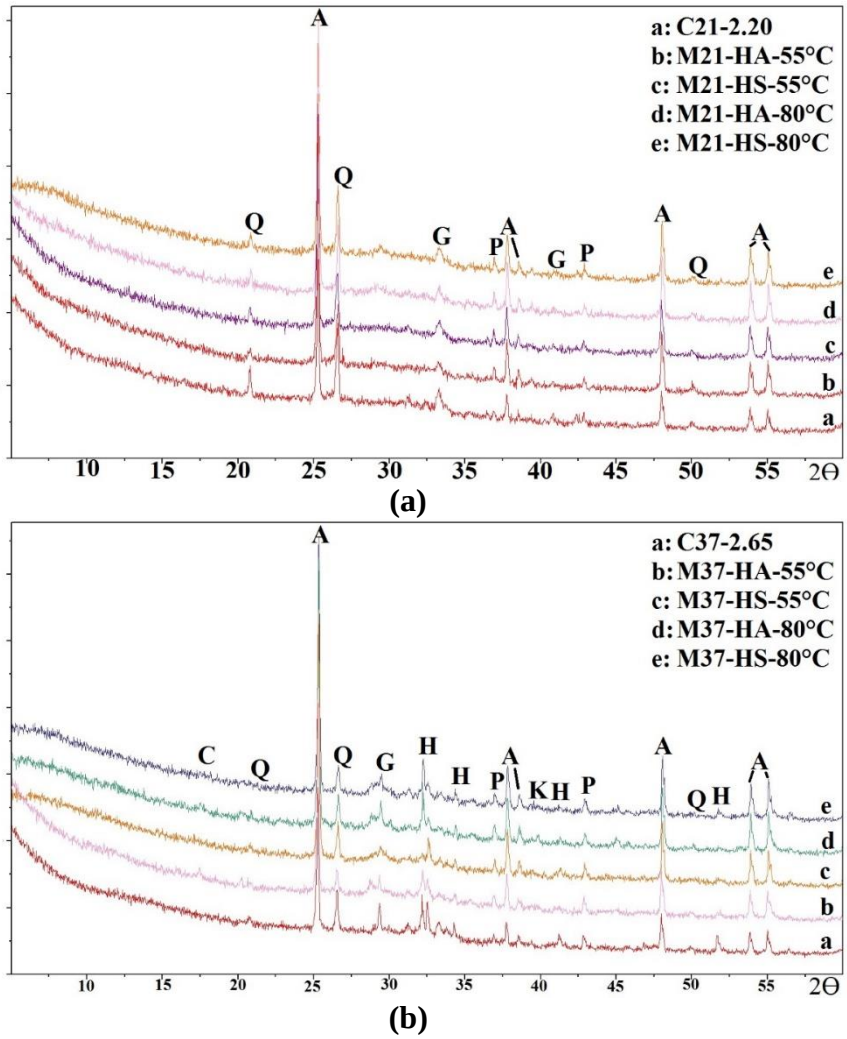

Figure 15. XRD patterns of unreacted FAs and AACFA pastes steam-cured at 55ºC or 80ºC for 9 hours. a) M21 mixes. b) M37 mixes.

After the FA getting in contact with water and liquid activators, dissolved species from these FA particles reacted with available dissolved ions from the activators and led to the formation of a gel that linked all separate FA particles together (Figure 17b). There was formation of a light layer around each fly ash particles representing the resulting products formed during the geopolymer reaction. The observed amorphous structure of the formed product gel explained why they could not be detected by X-Rays during the XRD

test, and thus resulted in a much broad hump rather than sharp peaks, specifically in XRD results of FA C21 as no peaks corresponding to formed products were spotted.

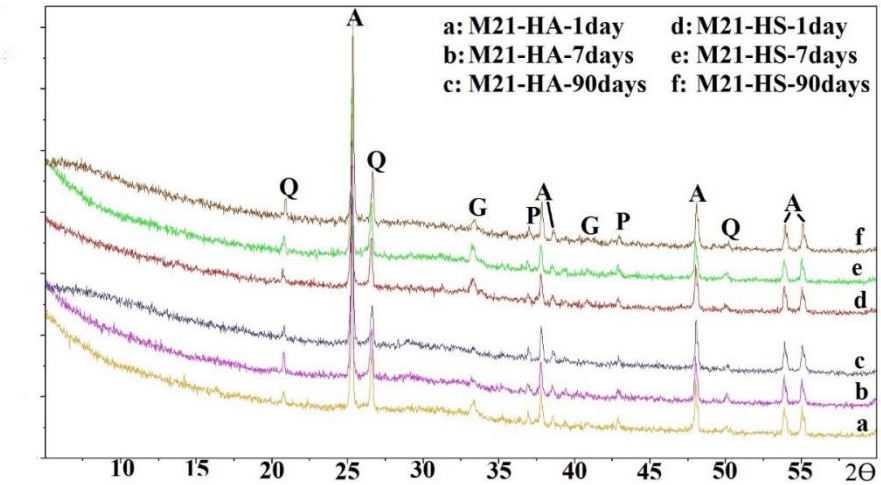

(a)

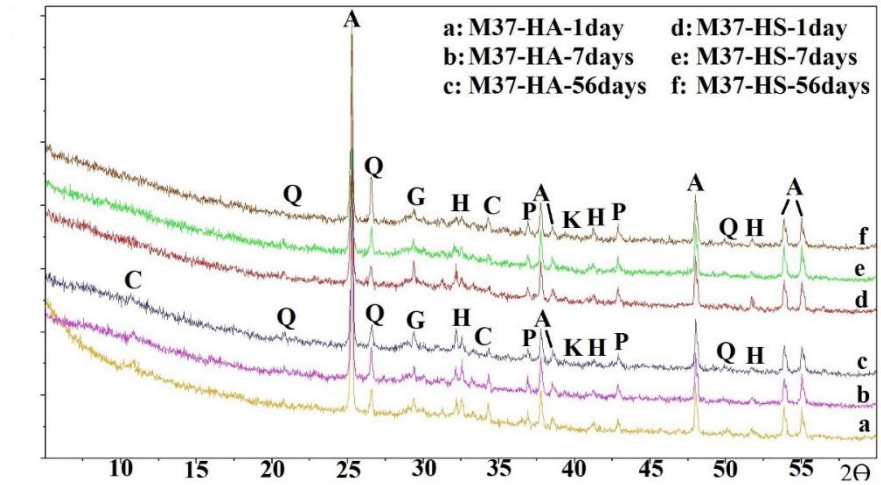

(b)

Figure 16. XRD patterns of AACFA pastes ambient-cured, stored and tested after 1, 7, 56, and 90 days. a) M21 mixes. b) M37 mixes.

Two different areas, A and B, were spotted and analyzed using EDS where A represented the area of an existing FA particle in the paste as it remained in a circular shape, and B the area of a formed reacted product (Figure 18b). The EDS at area A

showed a very low intensity of Ca relative to the intensities of Si, Al and O (Figure 18b). (Figure 18a) indicating that more Ca species leached from the partially dissolved FA particle than Al and Si species.

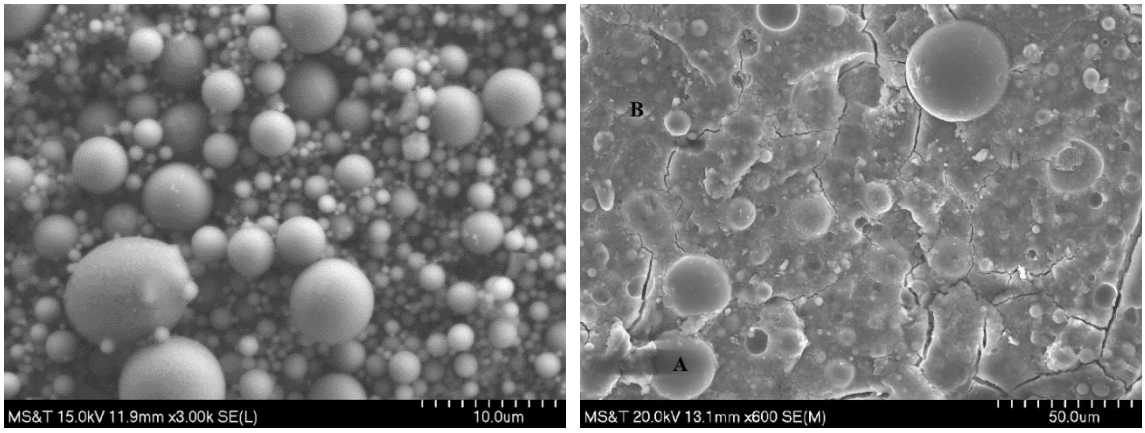

(a) **(b)**

Figure 17. SEM images of FA and geopolymer pastes: a) Unreacted FA C21-2.20, and b) P21 paste.

This explained the reduction of peak intensity of Ghelenite crystals as shown earlier in the XRD results of M21 mixes. Furthermore, the predominant elements present in area "B", the formed product gel area, was Ca, Na, Si, Al, and O (CNASH) which correspond to the geopolymer gel (Figure 18c). CNASH yields a fast strength development if cured at high temperature. However, if cured at ambient temperature, the strength development happens in at a very slow rate. This explained why the strength development of M21 mixes was very slow under ambient curing regime (Figure 9) but had a fast strength development under heat curing regimes (Figures 9-10). In addition, the presence of many partially reacted FA particles fully surrounded with the formed geopolymer gel was due to the faster

growth of formed products since this paste sample was originally steam-cured at 80ºC (176ºF).

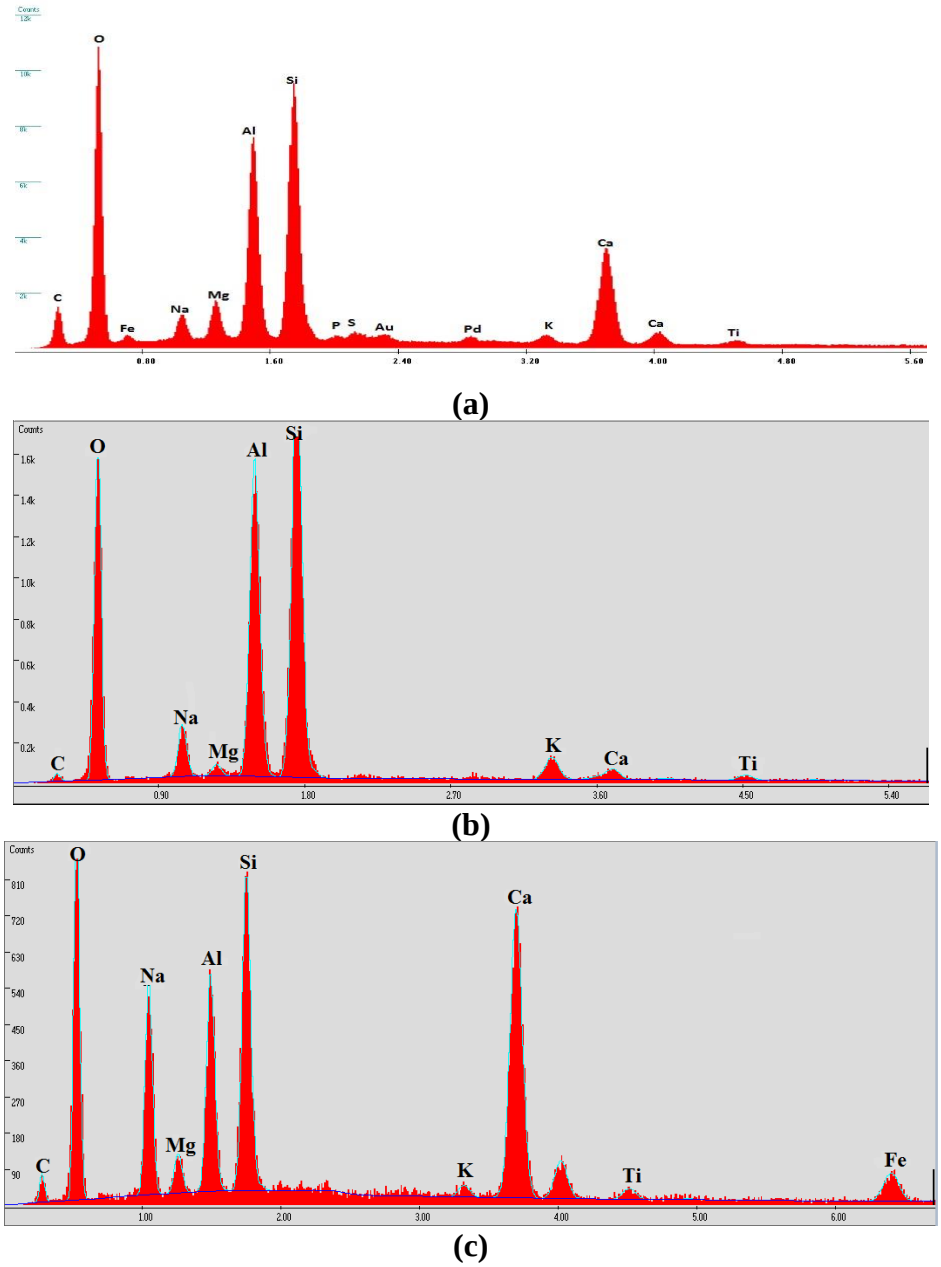

Figure 18. EDS results of FA C21.20 and geopolymer pastes. a) Unreacted FA C21-2.20. b) Reacted M21 FA particle "A" and c) Reacted M21 FA particle "B"

It is evident that further dissolution of elements would be hindered and thus as a consequence low or no strength development would occur over time. As it was the case for all mortar mixes steam-cured at 80ºC (176ºF).

5. CONCLUSIONS

Four alkali-activated mortar mixes with varying mix proportions were synthesized using two different types of class C FA, (C37 and C21). These mortar mixes were subjected to different rest times prior to being ambient, oven, or steam-cured. The steam and oven-curing were at either 55ºC (131ºF) or 80ºC (176ºF). From the obtained results, it was concluded that:

- Each mixture had a different optimum rest time ranged from 12 hours to 30 hours. Increasing the rest time beyond that optimum value resulted in a reduction in the strength. It was found that a rest time of 12 hours beneficial for all mixture resulting in an average of 46% increase in the compressive strength compared to the more common two-hours rest time.
- The chemical composition of the FA played an important role in the strength development of AACFA. Ambient-cured M37 mixes, with relatively higher calcium content, reached higher strength of approximately 49.3 MPa (7100 psi) at 28 days. The specimens reached 50% of their 28 days compressive strength at one-day. Beyond 28 days, the strength increased by about 10% by the age of 56 days and no more significant strength increased beyond that. Ambient-cured M21 mixes, with lower calcium and higher alumina and silica contents, demonstrated very low compressive strengths at

early ages but a significant increase evolved with time reaching 24.8 MPa (3590 psi) at 28 days. At 90 days, the mixes developed approximately 35% higher strengths than their 28 days compressive strength.

- The initial strength development of 80ºC (176ºF) oven and steam-cured specimens was very rapid resulting in compressive strength of approximately 45 MPa (6530 psi) after only 9 hours of curing. But after the thermal curing process, a different scenario was observed in their long-term strength development. For oven-cured mixes, an increase up to 20% was measured between 1 day and 90 days. For steam-cured mixes, a reduction up to 23% was measured between 1 day and 90 days due self-desiccation of specimens.
- For 55ºC (131ºF) oven and steam-cured specimens, slow strength developed at one-day reaching 41.4 MPa (6010 psi), but a considerable strength increase happened at late ages, reaching 75% increase in the compressive strength at 90 days with no significant difference between steam and oven curing.
- Ambient-cured M37 mixes displayed strength that exceeded both oven and steam-cured strengths at 28 days; at 90 days, M37 mixtures displayed strengths up to 26% higher than thermally-cured this was attributed to the presence of C-S-H products as revealed by XRD results. For M21 mixes, ambient curing resulted in the lowest strength, compared to thermal curing, up to 90 days and the microstructure analysis of pastes mixes revealed the predominance of geopolomeric gel (CNASH) which requires heat for high strength development.

REFERENCES

[1] J. Davidovits, “Geopolymer chemistry and properties,” in *Geopolymer*, 1988, vol. 88, pp. 25–48.

[2] J. L. Provis and S. A. Bernal, “Geopolymers and related alkali-activated materials,” *Annu. Rev. Mater. Res.*, vol. 44, pp. 299–327, 2014.

[3] P. De Silva, K. Sagoe-Crenstil, and V. Sirivivatnanon, “Kinetics of geopolymerization: role of Al2O3 and SiO2,” *Cem. Concr. Res.*, vol. 37, pp. 512–518, 2007.

[4] A. Palomo, M. W. Grutzeck, and M. T. Blanco, “Alkali-activated fly ashes: a cement for the future,” *Cem. Concr. Res.*, vol. 29, pp. 1323–1329, 1999.

[5] D. Hardjito, S. E. Wallah, D. M. J. Sumajouw, and B. V. Rangan, “On the Development of Fly Ash-based Geopolymer Concrete_Djwantoro Hardjito dkk,” no. 101, pp. 467–472, 2005.

[6] D. Hardjito and B. V Rangan, “LOW-CALCIUM FLY ASH-BASED By,” *Concrete*, pp. 1–103, 2005.

[7] P. Chindaprasirt, T. Chareerat, and V. Sirivivatnanon, “Workability and strength of coarse high calcium fly ash geopolymer,” *Cem. Concr. Compos.*, vol. 29, no. 3, pp. 224–229, 2007.

[8] T. Bakharev, “Geopolymeric materials prepared using Class F fly ash and elevated temperature curing,” *Cem. Concr. Res.*, vol. 35, pp. 1224–1232, 2005.

[9] Y. Hou, D. Wang, W. Zhou, H. Lu, and L. Wang, “Effect of activator and curing mode on fly ash-based geopolymers,” *J. Wuhan Univ. Technol. Mater. Sci. Ed.*, vol. 24, no. 5, pp. 711–715, 2009.

[10] C. Gunasekara, D. W. Law, and S. Setunge, “Long Term Engineering Properties of Fly Ash Geopolymer Concrete,” *4th Int. Conf. Sustain. Constr. Mater. Technol.*, no. September, p. 2019, 2016.

[11] D. L. Y. Kong and J. G. Sanjayan, “Effect of elevated temperatures on geopolymer paste, mortar and concrete,” *Cem. Concr. Res.*, vol. 40, no. 2, pp. 334–339, 2010.

[12] A. Wardhono, C. Gunasekara, D. W. Law, and S. Setunge, “Comparison of long term performance between alkali activated slag and fly ash geopolymer concretes,” *Constr. Build. Mater.*, vol. 143, pp. 272–279, 2017.

[13] P. Duxson, A. Fernández-Jiménez, J. L. Provis, G. C. Lukey, A. Palomo, and J. S. J. van Deventer, “Geopolymer technology: the current state of the art,” *J. Mater. Sci.*, vol. 42, pp. 2917–2933, 2007.

[14] T. Phoo-Ngernkham, C. Phiangphimai, N. Damrongwiriyanupap, S. Hanjitsuwan, J. Thumrongvut, and P. Chindaprasirt, “A Mix Design Procedure for Alkali-Activated High-Calcium Fly Ash Concrete Cured at Ambient Temperature,” *Adv. Mater. Sci. Eng.*, vol. 2018, 2018.

[15] E. Gomaa, S. Sargon, C. Kashosi, and M. ElGawady, “Fresh properties and compressive strength of high calcium alkali activated fly ash mortar,” *J. King Saud Univ. - Eng. Sci.*, vol. 29, no. 4, 2017.

[16] M. M. Abdulazeez, B. Shrestha, E. Gomaa, and A. Ramadan, “BOND BEHAVIOR OF STEEL H-PILE BRIDGE COLUMNS ENCASED IN CONCRETE,” no. November, 2018.

[17] E. Gomaa, S. Sargon, C. Kashosi, and A. Gheni, “Effect of Different Class C Fly Ash Compositions on the Properties of the Alkali-Activated Concrete,” no. Icpic, pp. 3–9, 2018.

[18] X. Guo, H. Shi, and W. A. Dick, “Compressive strength and microstructural characteristics of class C fly ash geopolymer,” *Cem. Concr. Compos.*, vol. 32, pp. 142–147, 2010.

[19] T. K. Erdem, L. Turanli, and T. Y. Erdogan, “Setting time: an important criterion to determine the length of the delay period before steam curing of concrete,” *Cem. Concr. Res.*, vol. 33, pp. 741–745, 2003.

[20] S. P. Sargon, E. Y. Gomaa, C. Kashosi, A. A. Gheni, and F. Ash, “Effect of Curing Temperatures on Zero-Cement Alkali-Activated Mortars,” no. Icpic, 2018.

[21] A. Fernández-Jiménez, A. Palomo, and M. Criado, “Microstructure development of alkali-activated fly ash cement: A descriptive model,” *Cem. Concr. Res.*, vol. 35, no. 6, pp. 1204–1209, 2005.

[22] P. Chindaprasirt and W. Chalee, “Effect of sodium hydroxide concentration on chloride penetration and steel corrosion of fly ash-based geopolymer concrete under marine site,” *Constr. Build. Mater.*, vol. 63, pp. 303–310, 2014.

[23] ASTM, “Standard Test Method for Slump of Hydraulic-Cement Concrete,” *Astm C143/C143M*, no. 1, pp. 1–4, 2015.

[24] T. Textiles, “Standard Test Method for,” *Annu. B. ASTM Stand.*, vol. i, pp. 2–5, 2005.

[25] S. A. Mironov, “Some generalizations in theory and technology of acceleration of concrete hardening,” *Highw. Res. Board Spec. Rep.*, 1966.

[26] B. Lothenbach, F. Winnefeld, C. Alder, E. Wieland, and P. Lunk, “Effect of temperature on the pore solution, microstructure and hydration products of Portland cement pastes,” *Cem. Concr. Res.*, vol. 37, no. 4, pp. 483–491, 2007.

II. A COMPARISON BETWEEN ONE-PART AND TWO-PART MIXING OF CLASS C FLY ASH-BASED ALKALI-ACTIVATED MORTARS

Cedric Chani Kashosi[1], and Mohamed A. ElGawady[2]

[1]Graduate Research Assistant; Civil, Architectural and Environmental Engineering, Missouri University of Science and Technology.

[2]Professor and Benavides Faculty Scholar; Civil, Architectural and Environmental Engineering, Missouri University of Science and Technology, senior author.

EMPHASIZE

- One-part AACFA mixed mortar were synthesized using the same mix design from two-part mixed mortars.
- Nine one-part mortar mixtures were synthesized using three different mix design and three different FAs. Nine corresponding two-part mixtures were synthesized as well using the same mix design and FAs.
- The setting time and workability properties, compressive strength and microstructure development of one-part mortar mixtures were compared to those for corresponding two-part mixtures.

ABSTRACT

For the past few decades, promising results of researches on zero-cement binders to progressively increase their use in the construction industry as a replacement for Portland cement (OPC) for concrete production has emerged. However due to the high corrosiveness of liquid materials used to produce these binders, requiring extreme handling precautions, developing a one-part mixing system is needed for replacement of the used conventional two-part system. This paper establishes a parallelism between one-part and two-part mixing system of alkali-activated mortars. One-part mortars produced using only solid particles, were made out of the same mixing proportions used to produce the conventional two-part alkali-activated mortars, which normally made using solid precursor and liquid activators. Both one-part and two-part mortar specimens were mixed, cured and tested under the same conditions. The fresh and hardened properties as well as the microstructure development were compared for both one-part and two-mortar mixes. Setting time results demonstrated that one-part mortars set faster than corresponding two-part mortar mixes; while the workability were relatively the same. In terms of strength development, at early ages of eight hours, the compressive strength of one-part mortar mixes were equivalent to only 3% of corresponding two-part mixes. However, it increased up to 50% of that in two-part mortars specimens after 24 hours of oven curing. Micro structure analysis demonstrated presence of hydrogarnet crystal phases in one-part mortar mixes which was responsible for the faster setting properties of these mortars. But also factors such as low pH, lack of solubility of solid activator played a significant role in lowering the strength of alkali-activated mortars at different ages compared to conventional two-part mixes.

1. INTRODUCTION

The use of concrete in the construction industry has increased so much to a level of making it the most used man-made material, and second used material on earth after water. When associating this high usability rate of concrete to the manufacturing process of ordinary Portland concrete (OPC), which emits a high quantity of carbon dioxide to the atmosphere, it result in a negative environmental footprint that keeps on increasing and needs to be taken care of [1]. The use of by-product materials such as ground granulated blast furnace slag (GGBFS) and coal fly ash (FA) in a full substitution for OPC as the main binder for concrete, in response to its negative environmental impact, is a plausible solution that is still being investigated by many authors. These binders are commonly called geopolymers or alkali-activated (AA) binders.

AA binder results from a reaction between an aluminosilicate source material and an alkaline activator. These binders exhibit good properties such as high early compressive strength, and better durability such as acid resistance and fire resistance [2,3]. AA binders normally are produced using a two-part mix [4–7] where a solid source material is mixed with a high alkalinity liquid activator and extra water may be added mostly for rheology purposes. However, its applicability is still restricted to laboratory and pre-cast industries with facilities required to accommodate for storage, and handling of the liquid activators which are very corrosive materials. In addition, producing this type of binders needs well-trained personnel, which put extra limit on using it. In order to overcome these restrictions, the development of a much simpler, safer and user-friendly version of AA binder using one-part mixing with all solid components is essential.

Over the years, different combinations of materials have been proposed by researchers to develop one-part AA binder. Most of these authors proposed complex mixes such as the case with Heitzmann et al. [8] who came up with a mix of metakaolin, amorphous silica, slag, potassium hydroxide, potassium silicate combined with either fly ash or calcined clay. Same thing with Davidovits [9] when he proposed a one part mix composed of metakaolin, slag, sodium/potassium disilicate. With intensions of developing a much more commercial one-part zero-cement binder, Duxson [10] did suggest to mix coal and feldspar rich in calcium, melted separately, cooled and grinded together to produce powdered one-part zero-cement precursor. All of the above proposed one-part binders used very complex materials or combination of materials, were not cost effective, and still needed well-trained personnel to handle; which made them hard to be implemented.

In terms of using fly ash, more recent researches have been conducted using much simpler combination of materials. Hajimohammadi et al. [11] used only class F fly ash combined with solid sodium hydroxide and sodium silicates. In his experiments, fly ash was mixed to solid sodium silicate before adding water and at last, solid sodium hydroxide were added to the wet mix. Results from his experiment reported compressive strength of 65 MPa after 3 weeks of continuous heat curing at 40º C, this long duration of the curing process made it hard to be implemented. Yang and Song [12], developed one-part zero-cement using fly ash as well with the same combination of solid sodium hydroxide and sodium silicate but cured all specimens at ambient temperature, reporting a 28 days compressive strength of 9.45 MPa, yet while repeating the same experience by substituting fly ash with slag, the strength increased up to 50 MPa after 28 days of ambient curing. However, in term of cost of evaluation, the use of slag is very expensive compared to fly

ash. Askarian [13] included OPC into in various proportions to form a hybrid OPC-class F fly ash geopolymer concrete, and reported that it did had a significant effect on the compressive strength at early ages and at ultimate strength because of the rapid reaction between OPC and the used alkali activators. The compressive strength of concrete specimens increased from 11.4MPa to 33.4Mpa after 28 days of ambient curing, but a decrease in the workability and setting time occurred as a result of the addition of OPC into zero-cement mixes.

Since the majority of the produced fly ash in the united states are class C fly ash with a relatively high calcium content, it is important to develop a one-part zero-cement mix that utilize this fly ash as the precursor. According to the best knowledge of the authors, there is no published research that addressed this point. In this study, class C fly ash was used in attempting to produce one-part zero-cement mortars.

As an initial trial, the same mix proportions used to produce two-part AAM in previous studies [14], were used to generate one-part AAM in this study. All activator solutions were replaced by solid materials, while keeping the ratio between different elements constant. Both one-part and two-part AAM mixes were made, and a comparison between one-part and two-part mixing were conducted to evaluate the difference in terms of fresh properties, and compressive strength development during early ages. A microstructure analysis of these binders was investigated as well in order to determine the difference of phase compositions occurring in each of the two type of AA binder.

2. MATERIALS PROPERTIES

2.1. FLY ASH

Three class C fly ashes with different characteristics were used as precursor (Table 1). The calcium content of the FAs varied from 21% to 37%, the alumina content from 14% to 20 %, and the silica content from 37% to 44%. The nomenclature of the FAs started with the letter C followed by the percentage of calcium oxide present in that FA. The fineness of FA particles was measured by evaluating the surface area using a Nova 2000e surface area analyzer according to the Brunauer-Emmett-Teller (BET) theory (Table1).

Table 1. Characteristics of Fly ashes

Composition	**Fly Ash (FA) Name**		
Oxides (%)	C21	C29	C37
CaO	21.2	28.8	36.9
Al_2O_3	20.1	17.4	13.9
SiO_2	43.9	37.9	36.9
Na_2O	2.87	1.85	1.62
MgO	4.29	8.00	4.80
Fe_2O_3	4.96	3.67	3.52
K_2O	0.70	0.39	0.62
P_2O_5	0.51	0.71	0.70
TiO_2	1.36	1.17	0.87
MnO	0.05	0.04	0.03
LOI	0.40	0.82	0.50
Si/Al ratio	2.20	2.20	2.65
Surface area (m^2/Kg)	2560	2921	3925

2.2. ACTIVATORS

Both liquid and solid activators were used in this study. The solid activators consisted of sodium hydroxide pellets (SH) and solid sodium silicate (SS). The liquid sodium silicate was a type D solution with ingredient composition of 56% water and 44% sodium silicate. The liquid sodium hydroxide was a 10M solution prepared in the laboratory by dissolving solid sodium hydroxide pellets into distilled water. These two liquid solutions, SS and SH, were mixed together half an hour prior to mortar mixing and the resulting mix were used as the activator medium for the mortar preparation.

2.3. SAND

The sand used in this study was obtained from the Missouri river, with a specific gravity of 2.6, and met the ASTM C30 requirement in terms of gradation. It was made surface saturated dry (SSD) and sieved to remove all larger particles retained on #8 sieve size prior to use it in the mortar.

3. EXPERIMENTAL PROCEDURE

3.1. MIX DESIGN

Three different mixtures including low alkaline (LA), high alkaline (HA), and high silicates (HS) were prepared out of each fly ash using two different mixing procedures, i.e., one-part and two-part mixing, i.e., 18 mixtures were investigated during this research. Both LA and HA mixtures are considered also low silicate (Table 2). For comparison purposes, both the one-part and two-part mixing were designed to have the same amount of water

and solid activator, i.e., SS and SH. Therefore, despite the difference between the ratio of liquid activator to FA (LA/FA) used for two-part mixing, and the ratio of solid activator to FA (SA/FA) used for one-part mixing, the total ratio of activator to FA (AC/FA) is the same in both one-part and two-part mixing (Tables 2 and 3).

Table 2. Mix design ratio

Mix design	Mixing	LA/FA	SA/FA	AC/FA	W*/FA	SS/SH
LA	Two-Part	0.275	--	0.105	0.380	1.000
	One-Part	--	0.105	0.105	0.380	1.375
HA	Two-Part	0.301	--	0.114	0.380	1.000
	One-Part	--	0.114	0.114	0.380	1.385
HS	Two-Part	0.275	--	0.108	0.400	2.000
	One-Part	--	0.108	0.108	0.400	3.143

LA: Liquid activator, SA: solid activator, AC/FA: Activator/Fly ash ratio
*Considering the water presented in both SS and SH solutions were considered

The selection of these three mix designs was based on a previous study conducted using the same FAs where a wide range of mix proportions were investigated and optimized [14]. The nomenclature of the mortar mixtures consisted of a letter "M" standing for mortar, followed by percent of the calcium content in the precursor, a short dash, and either LA, HA or HS for alkaline solution. For example, mix M21-HA represented a mortar mix made from FA C21, using the "HA" mix design.

3.2. MIXING PROCEDURE

A Hobart mixer and a mixing time of 13 minutes were used for all mixtures following Gomaa et al. (2019). In the case of one-part, the SS and SH were mixed together with the fly ash for two minutes; then, sand was added to the mixture and mixed for another

minute at speed of 130 rpm to allow a homogenous mix. Water was then added gradually over two minutes and then the mix was stopped for 0.5 minutes in order to remove stuck particles at the bottom and on the walls of the mixing bowl. Finally, the mix was restarted at speed of 300 rpm for six minutes.

Table 3. Unit quantities of mix design

Mixing system	**One Part Mixing**			**Two-Part Mixing**		
Mix Name	LA	HA	HS	LA	HA	HS
Unit quantities	Kg/m^3 (lb/ft^3)					
Liquid SS	-- --	-- --	-- --	75 (4.68)	82 (5.12)	98 (6.12)
Solid SS	33 (2.06)	36 (2.25)	44 (2.75)	-- --	-- --	-- --
Liquid SH	-- --	-- --	-- --	75 (4.68)	82 (5.12)	49 (3.06)
Solid SH	24 (1.49)	26 (1.62)	14 (0.87)	-- --	-- --	-- --
Water	207 (12.9)	208 (13.0)	214 (13.4)	121 (7.55)	113 (7.05)	132 (8.24)
Sand	1500 (93.6)	1500 (93.6)	1470 (91.7)	1500 (93.6)	1500 (93.6)	1470 (91.7)
Fly ash	545 (34.0)	545 (34.0)	535 (33.4)	545 (34.0)	545 (34.0)	535 (33.4)

In the two-part mixing, sand and fly ash were mixed together for one minute at a speed of 130 rpm, followed by gradually adding water to the mixture over one minute. Then, the mix was stopped and scrapped for 0.5 minutes to remove stuck particles, restarted and the activator solution were added to the mixture into a 5 equivalent proportions over five minutes. The mix was stopped for a second time and scrapped for 0.5 minutes and restarted at a speed of 300 rpm for 5 more minutes.

3.3. CURING PROCESS

After mixing, mortar was placed into a 50 mm cube brass molds and compacted per ASTM C109-16a. Then, the specimens were sealed into plastic oven bags, in order to avoid moisture loss, and oven cured at different temperatures and durations as follows. One group of the specimens were cured at 30º C, simulating ambient temperature during a summer season in the Midwest of the US [15], for 24 hours or 168 hours (7-days). The other group of specimens were cured at either 55º C or 70º C for either 8, 16, or 24 hours.

3.4. FRESH AND HARDENED PROPERTIES TESTS

The workability and setting time of all mortar mixtures were measured per ASTM C143/C 143M and ASTM C807, respectively. The workability was measured by compacting two equivalent layers of mortar mixtures into a standard cone with a known base diameter of 100 mm (4 in) resting on a circular base plate, safely remove the cone, rising and dropping the base plate 25 times within 15 seconds, and finally record the expansion of the mortar over the plate (flow). The setting time was measured by means of a Vicaat needle, recording the penetration of the needle into the mortar over time (Figure 1). At the end of the curing process, all mortar specimens were removed from the oven and demolded. The compressive strengths of three replicate cubes per mixture were measured using a Tinius Olsen compression machine per ASTM C109-16a and the average strength per mixture was determined.

(a) **(b)**

Figure 1. Tests on fresh properties of zero-cement mortars. a) Flow test. b) Setting time test.

3.5. MICRO STRUCTURE ANALYSIS

The formation of chemical components during the hardening process under each curing condition was investigated using X-Ray Diffraction technics (XRD) on both one-part and two-part AA paste. Paste was selected rather than mortar to avoid including diffraction patterns of quartz crystals present in sand grains, and thus obtaining more accurate results. Paste mixtures corresponding to the different mortar mixtures were prepared and cured using the same characteristics as the corresponding mortar mixes. The pastes were then crushed into very fine particles using a mortar and pestle. Approximately 1 gram of the resulting powder for each paste sample was placed into a sample holder and XRD measurements were performed using a PANalytical Multipurpose Diffractometer utilizing a Cu source and a PIXcel detector. Diffraction patterns of the present crystalline phases in each sample reflected in the form of sharp peaks appearing at different 2Ɵ locations were determined and analyzed. A comparison between XRD patterns of one-part

and the corresponding two-part paste samples was evaluated in order to determine the difference in phase composition of the two AA mixes.

4. RESULTS AND DISCUSSION

The fresh and hardened properties of all mixtures are discussed in this section. The section also includes discussion of the microstructure of the paste mixtures.

4.1. FRESH PROPERTIES

The one-part mixtures set two to ten times faster than the corresponding two-part mixtures, depending on the variation of Si/Al ratio and the surface area of FA. The final setting time values of the one-part AAM mixtures ranged from 30 to 85 min for M29, 45 to 165 min for M21, and 120 to 190 min for M37 (Figure 2). While in the case of two-part mixing, the setting times ranged from 300 to 320 min, 290 to 330 min, and 210 to 245 min for M29, M21, and M37, respectively.

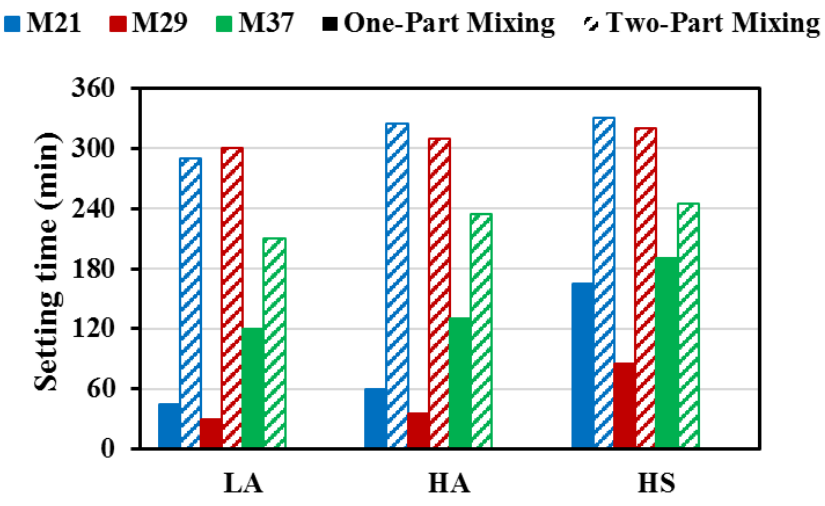

Figure 2. Setting time results of AAM.

For all mixtures, the setting time decreased with decreasing the Si/Al content in the mixture solution (Figure 3). In the case of the two-part mixtures, the availability of dissolved silica species in the liquid sodium silicate activator before the dissolution of the FA particles led to a high Si/Al ratio in the mixture solution which resulted in longer setting time.

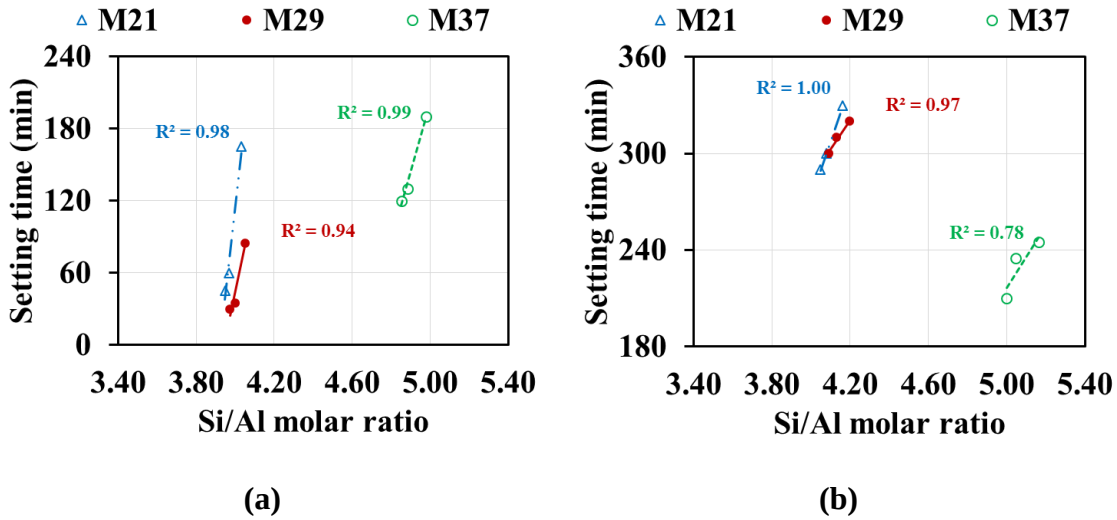

Figure 3. Correlation between Si/Al and setting time of AAM: a) One-part mortar mixtures. b) Two-part mortar mixtures.

However, in the case of the one-part mixtures, all constituents, i.e., FA and solid activators dissolute, the faster dissolution of calcium and alumina species in water compared to silica led to formation of calcium-aluminum-hydrates components such as Hydrogarnet (CaO)3.(Al2O3).(H2O)6 which triggers flash setting of cementitious materials [16]. This phenomenon explains the rapid setting time of all one-part mixtures compared to the corresponding two-part mixtures. As a result, both mixes LA and HA with low silica content had lower setting time values compared to mixes HS. The alkalinity had insignificant effect on the setting time with LA had slightly shorter setting time. In addition,

M29 mortar mixes had the shortest setting times among all the mixes due to the highest surface area FA C29 (Table 1), a faster reaction rate is expected to occur as compared to the two other FA batches. M37 mixes took long time to set since they had the smallest surface area and thus slower reaction rate.

Workability results were expressed in percentage increase (%), with 0 representing zero flow, and 150 the maximum flow that can be recorded (Figure 4). The trend of the workability was similar to that of the setting time results. The one-part AAM mixes had less workability compared to their corresponding two-part AAM mixes. The workability values of the one-part mixtures ranged from 5% to 65 %, 50% to 70 %, and 65% to 95 % for mixes M29, M21, and M37, respectively, while those of the corresponding two-part mixtures ranged from 85% to 125%, 85% to 110% , and 85 to 105 %, respectively. The poor workability of one-part mixes compared to two-part mixes was essentially due to their faster setting properties for the reason mentioned earlier.

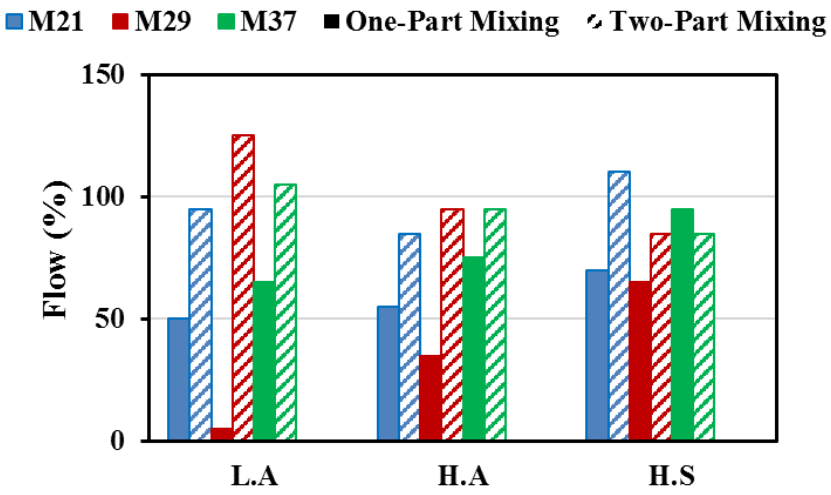

Figure 4. Workability of AAM.

4.2. COMPRESSIVE STRENGTH DEVELOPMENT OF ZERO-CEMENT MORTAR

In this section, the compressive strength development of both one-part and two-part zero-cement mortar cured under ambient and oven curing regimes are discussed.

4.2.1. Compressive Strength of Zero-cement Mortars Cured at Ambient Temperatures.

M37 had the highest compressive strength values for specimens cured at 30° C (86° F), followed by M29, and M21 with two-part mixes displayed higher compressive strengths than the corresponding one-part mixes. The compressive strength of the one-part mixtures cured at 30° C (86° F) for 24 hours ranged from 17.4 to 25.4 MPa (2520 to 3680 psi) for M29, from 0.84 to 10.5 MPa (120 to 1520 psi), for M21, and 11.5 to 15.7 MPa (1670 to 2280 psi) for M37 (Figure 5). These values represented approximately 94% to 99% of the compressive strength of their corresponding two-part M29, 5% to 42% for M21, and 38% to 52% for M37.

The compressive strength of the one-part and two-part mixture increased with increasing the curing time to 7 days. The compressive strength values increased by approximately 37%, 15%, and 44% for mixes LA, HA, and HS mixes of M29; approximately 120% and 290 % for LA and HA mixes of M21, while in the case of mix HS, the 7-day compressive strength was 10 times greater than the 1-day strength. For M37 mixes, a 76%, 89%, and 75% strength increase were observed between the 1-day and 7-day strength of mixes LA, HA, and HS, respectively. The tremendous difference in the compressive strengths of one-part and two-part AAM mixes was due to the physical properties of the mix (i.e. workability), the pH, and the solubility product of the materials. As stated earlier, in the case of one-part mixing system the dissolutions of all materials in

water started simultaneously. Contrary to the two-part mixing system, using liquid activator solutions created a favorable environment for the geopolymer reaction by improving the dissolution and hydrolysis mechanisms [17,18] which affected the compressive strength development of the mixes.

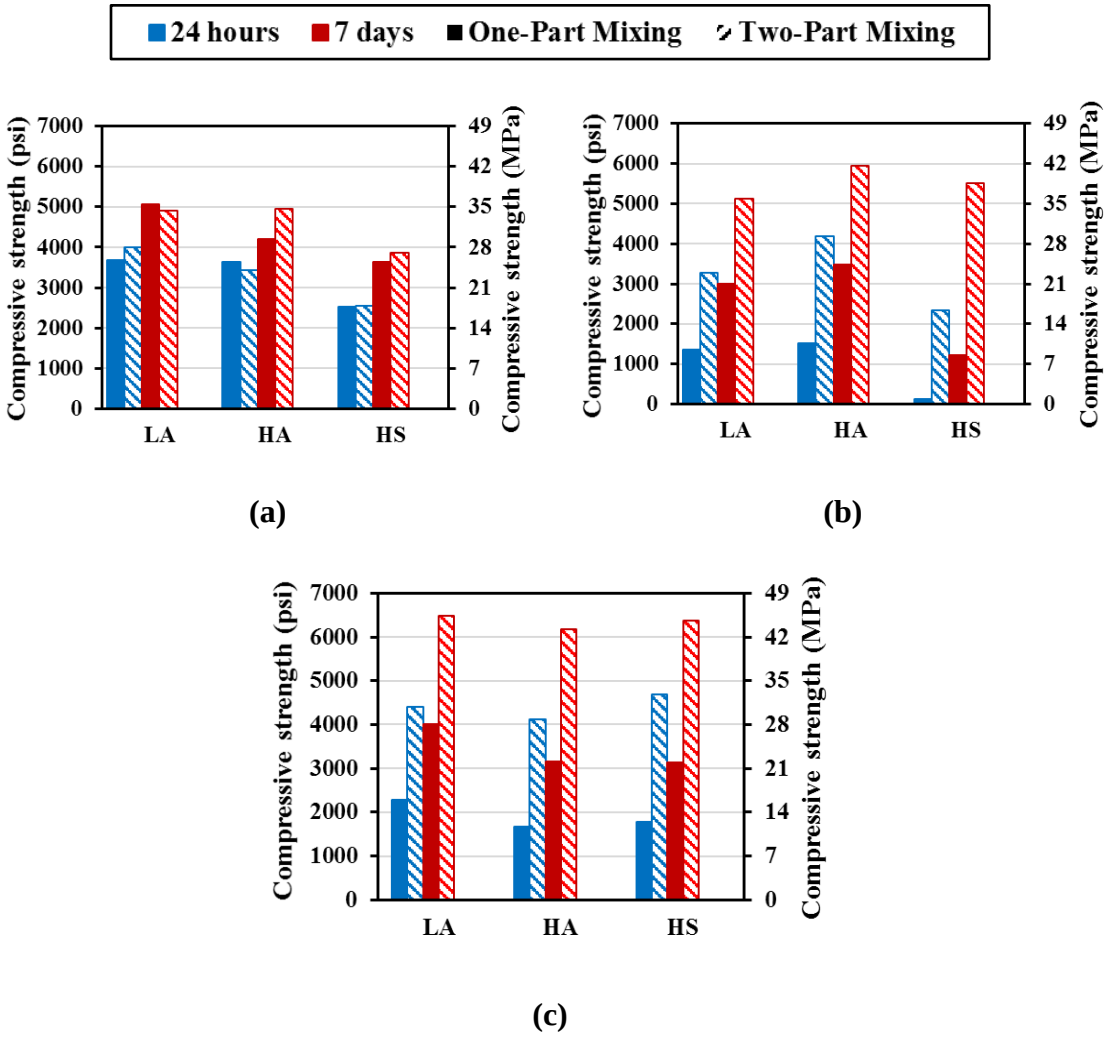

Figure 5. Compressive strength of AAM cured at 30° C for 24 hours and 7 days: a) M29 mixtures. b) M21 mixtures. c) M37 mixtures.

The geopolymer reaction is influenced by the Si/Al and calcium content of the precursor as well as the alkalinity and constituent of the activators. The silica availability

controls the strength development while the alumina content controls the setting properties [12]. In the case of two-part mixes, the high availability of dissolved silica in addition to the presence of dissolved calcium led to formation of products such calcium-silicate-hydrate (CSH) which influence the high strength development of cementitious materials at ambient temperature. For one-part mixes, the faster dissolution of alumina compared to silica, leads to a high concentration of dissolved alumina in the solution which reduces the dissolution capacity of Si in water [19]. In addition, the dissolution of calcium species and hydroxyl ions in the mix, would lead to having a solution saturated essentially with calcium, alumina and hydroxyl ions, and thus precipitation of products such as calcium hydroxide (CaOH) and calcium-aluminate-hydrates which hinders the strength development of the mixes [20].

The variation of compressive strength of AAM mixes with respect to their source material (FA), was mainly due to the difference in the chemical composition of their respective source materials (i.e. FA). FA C37 having the highest calcium content, had the higher ability for its mixes to develop relatively higher strength at 30° C (86° F). FA C21 with the lowest calcium content and higher Al and Si content, required much elevated temperature for fast strength development.

However due to the high surface area of FA C29 (Table 1) compared to the remaining FAs, both the dissolution and the reaction rate of M29 mixes happened faster, which influenced the strength development of these mixes at early ages, allowing the 1-day strength of one-part mixes to be similar to those of two-part mixes (Figure 5a).

4.2.2. Compressive Strength of Zero-Cement Mortars Cured at Elevated Temperatures.

The compressive strength results of the one-part M29-HS cured at 55° C (131° F) reached a maximum of 1.5 MPa (220 psi) after 24 h of curing (Figure 6). However, those of mixes M29-LA and M29-HA increased from 7.89 to 11.7 MPa (1150 to 1690 psi), and from 14.2 to 19.3 MPa (2070 to 2800 psi), respectively, when the curing duration was increased from eight hours to 24 hours. These increases are corresponding to an average strength increase of about 36 - 48%. The two-part mortar mixes displayed compressive strengths of 20 – 23.4 MPa (2900 - 3400 psi) for all M29 mixes, after eight hours of curing; which increased to 27.6 to 32.4 MPa (4000 to 4700 psi) after 24h of curing. These values represent approximately 175% of that of the corresponding one-part M29-LA and M29-HA mixes.

Increasing the curing temperature to 70° C (158° F), improved the strength of one-part M29-LA and M29-HA cured for eight hours by approximately 12%. However, when these mixes were subjected to extended curing time of 16 and 24 hours at 70° C (158° F), they displayed either slightly improved or unchanged strength. Furthermore, higher curing temperature and extending curing time was quite effective for the one-part M29-HS reaching 17.8 MPa (2580 psi) at 24 hours curing time being 11 times greater than the corresponding mixture cured at 55° C (131° F).

In the case of two-part mixing and with increasing the curing temperature, the compressive strengths of mixes M29-HS and M29-HA were approximately the same at eight hours curing and then increased from about 27.6 to 31.0 MPa (4000 to 4500 psi) as the curing duration was increased to 24 hours, respectively; and the strength of mix M29-LA increased from 19.3 to 24.8 MPa (2800 to 3600 psi). Furthermore, increasing the curing

temperature from 55°C (131°F) to 70° C (158° F) increased the compressive strength by an average of 6% for mixes HA and HS, and 24% for mix LA . At short curing duration of eight hours, the strength of the two-part mix M29-HS was 13 times greater than its one-part counterpart. However, by 24 hours of curing, the one-part mixing strength considerably increased and the average strength of all one-part M29 mixes reached 50% - 80% of the corresponding two-part mixes.

The relatively higher compressive strength of the two-part mixes when compared to the corresponding one-part mixes were related to the favorable reaction environment created by the liquid activators used in two-part as mentioned earlier. The lower strength development of mix M29-HS compared to mixes M29-LA and M29-HA for both one-part and two-part mixes cured at 55° C (131° F) was related to the proportion configuration of these mixes. As shown in Table 2, mix HS had a SS/SH ratio of 2, while mixes LA and HA had a SS/SH ratio of 1, therefore the lower availability of hydroxyl ions in mix HS as compared to mixes LA and HA implied a lower pH, and thus a relatively slower dissolution rate of the element in this mix (HS). But when the curing temperature was increased to 70° C (158° F), a considerable increase in strength of this mix occurred especially for the one-part mixing, since with increasing the temperature more silica dissolved and contributed to the strength development of mixes leading to formation of compounds rich in silica, calcium and alumina (CASH).

The compressive strengths of the one-part mix M21-HS cured at 55° C (131° F) reached a maximum of 0.34 MPa (50 psi) after 24 h of curing (Figure 7). However, those of mixes M21-LA and M21-HA significantly increased by 395% to 670%, i.e. from

approximately 4 MPa (600 psi) to 18.5 and 26.7 (2680 and 3900 psi), respectively, when the curing duration was increased to 24 hours.

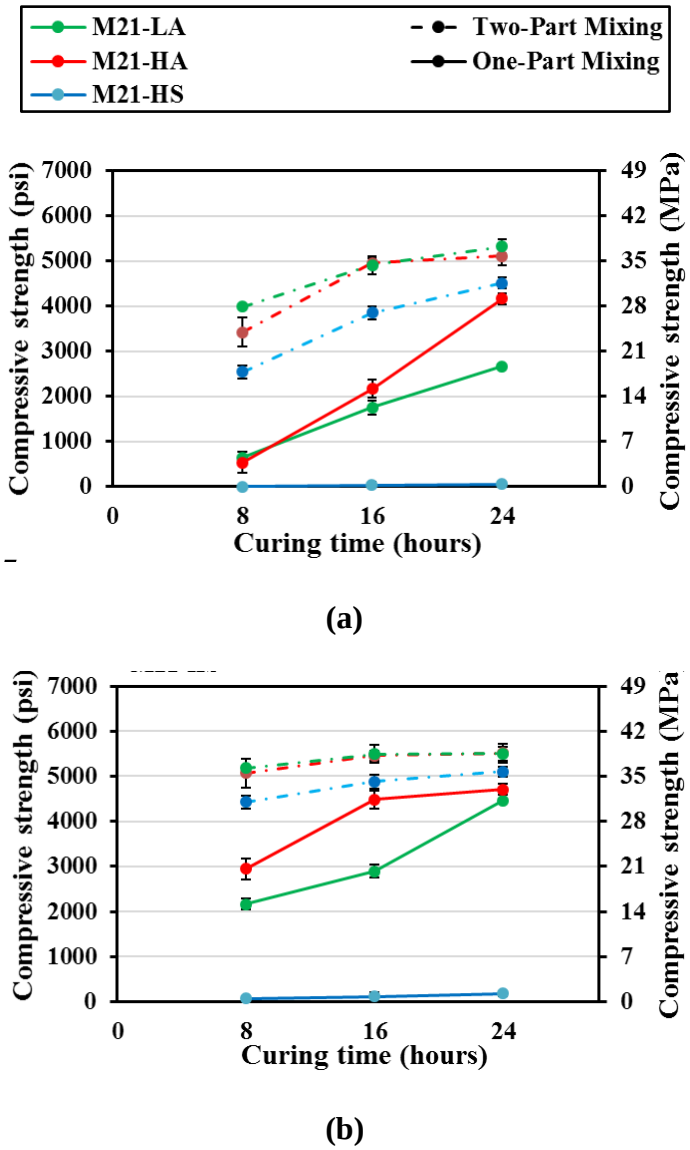

Figure 6. Compressive strength of M21 mortar specimen's oven cured at: a) 55° C (131° F), b) 70° C (158° F)

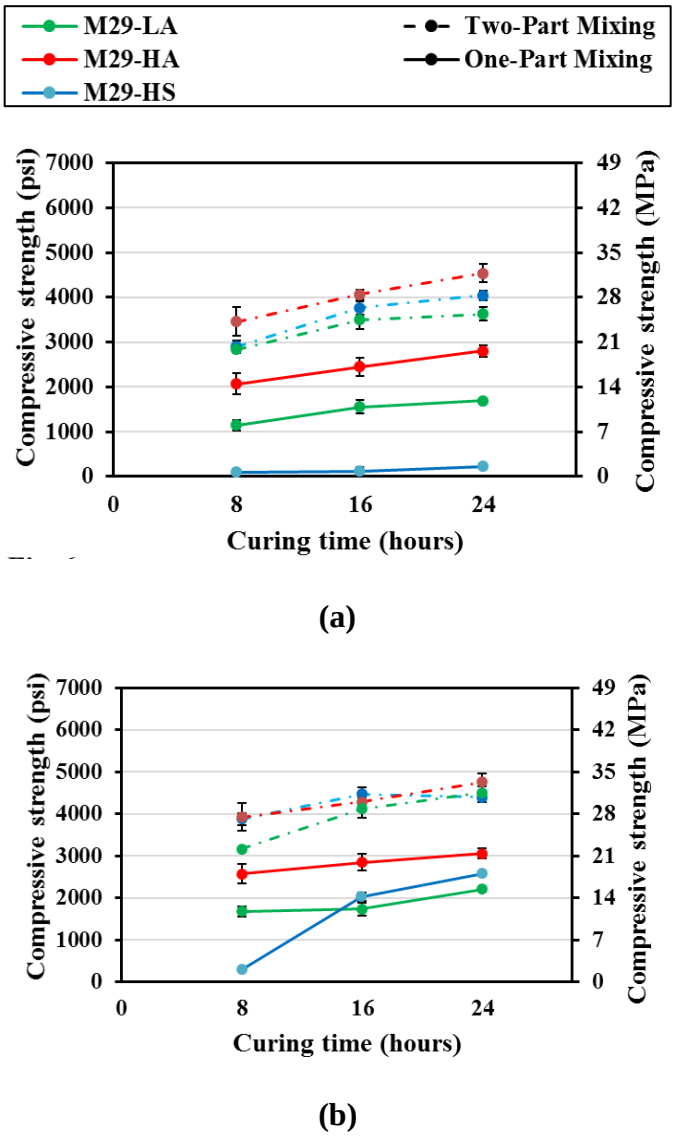

Figure 7. Compressive strength of M29 mortar specimen's oven cured at: a) 55° C (131° F), or b) 70° C (158° F).

The two-part mortar mixes displayed compressive strengths of 17.2 MPa to 27.5 MPa (2500 to 3990 psi) for all M21 mixes, after eight hours of curing; which increased to 31 to 36.7 MPa (4500 to 5320 psi) after 24 hours of curing. These strengths of the two-part M21-LA and M21-HA mixes cured for 24 hours represented approximately

125% to 200% of the corresponding one-part mixtures. For the case of two-part M21-HS mix, the strength was multiple folds higher than that of the corresponding one-part mix at all curing times since the one-part developed very low strength.

Increasing the curing temperature to 70° C (158° F), improved the strength of one-part M21-LA and M21-HA cured for eight hours by approximately 300% and 445% compared to curing at 55° C (131° F). The specimens continued to gain strength as the curing time increased to 16 hours and 24 hours for M21-HA and M21-LA, respectively.

However, neither the higher curing temperature nor the extending curing time was effective for the one-part M21-HS reaching 0.7 MPa (100 psi) at 24 hours curing time.
In the case of two-part mixing and with increasing the curing temperature to 70° C (158° F), the compressive strengths of all mixes at eight hours curing increased by 30% to 74% compared to those cured at 55° C (131° F) and then slightly increased reaching 35.2 to 37.9 MPa (5100 to 5500 psi) as the curing duration was increased to 24 hours. At short curing duration of eight hours, the average strengths of the two-part mix M21-LA and M21-HA was approximately 140 - 170% of its counterpart one-part. However, by 24 hours of curing, the one-part mixing strength considerably increased, and the average strength of two-part mixes reached 17% -23% of the corresponding one-part mixes.

The poor strength development observed in the case of mix M21-HS as compared to mixes M21-LA and M21-HA for both one- and two-part AAM was related the less amount of sodium hydroxide in the activator as mentioned earlier. In addition, due to the lower calcium content of FA C21 as shown with Table 1, formed products in this case would essentially be rich in silica and alumina, which requires high temperature for faster strength development as it is related to the activation energy theory whereby higher kinetic

energy is needed to intrigue the geopolymerization action [21]. The kinetic energy increased by either increasing the temperature or prolonging the duration of curing. This explained the high rise in strength of all mixes as the temperature was increased from 55° C to 70° C (from 131° F to 158° F), or when the duration of curing went from eight hours to 24 hours.

The compressive strength of M37 mortar mixes is summarized in Figure. 8. At 55° C (131° F) of oven curing, for one-part mixing, the compressive strength of mix M37-HS was less than 0.55 MPa (80 psi) after the first eight hours of curing, then consistently increased to reach up to 17.2 MPa (~2500 psi) after 24 hours of curing; while strengths of mixes M37-LA and M37-HA only increased from 13.8 – 14.5 MPa (2000 - 2100 psi) to 17.2 – 20.7 MPa (2500 and 3000 psi) as the duration of curing went from eight to 16 hours, respectively. This represented about 200% strength increase in the case of mix M37-HS; 45% and 25% for mixes M37-LA and M37-HA, respectively.

In the case of corresponding two-part mixing, mix M37-HS demonstrated a high strength from early ages equal to 26.9 MPa (3900 psi) after only eight hours of curing; mixes M37-LA and M37-HA had strengths equal to 23.4 and 22.8 MPa (3400 and 3300 psi), respectively. These strengths were 1.6, 1.7 times greater than the one-part mixing for mixes LA and HA; and 40 times greater for mix HS, respectively.

When the curing temperature was elevated to 70° C (158° F), the strength of one-part mixes increased considerably especially in the case of mix M37-HS which had a compressive strength of 11.7 MPa (1700 psi) after only eight hours of curing, and 25.5 MPa (3700 psi) after 24 hours; while the strength of mixes M37-LA and M37-HA went from 22.1 – 23.4 MPa (3200 – 3400 psi) to 27.6 – 28.2 MPa (4000 – 4100 psi) as the curing

duration increased from eight to 24 hours. This represented a rise in compressive strength on a scale of 1.5 for all three mixes when considering the final strength after 24 hours of curing, as the temperature went from 55 to 70° C (131 to 158° F).

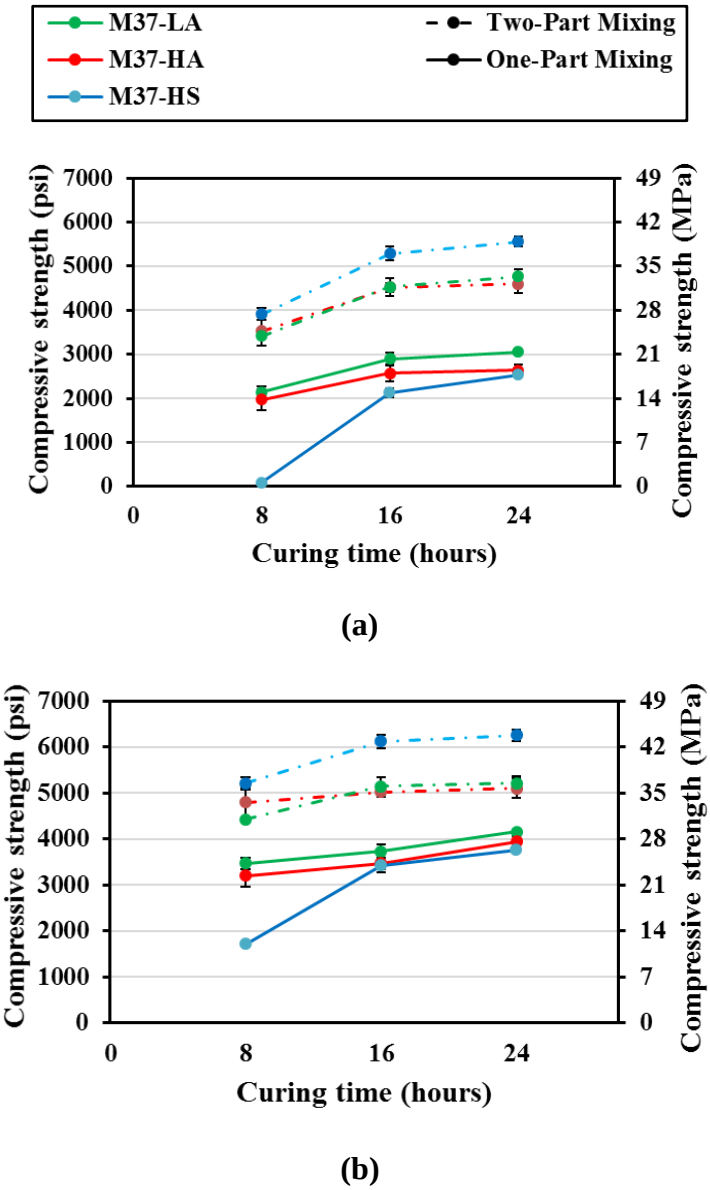

Figure 8. Compressive strength of M37 mortar specimens oven cured at: a) 55° C (131° F), b) 70° C (158° F)

For equivalent two-part mixes cured at the same temperature, all three mixes had high compressive strength from early ages, ranging between 31 MPa (4500 psi) for mix M37-LA and 35.2 MPa (5100 psi) for mix M37-HS after eight hours of curing. Then only a slight increase of about 20% happened as the duration of curing went from eight to 24 hours for these mixes. The final compressive strength of two-part mixes were 1.2 to 1.6 times greater than their corresponding one-part mixes.

FA C37 had the highest calcium content among all the three used FAs, therefore formed products of M37 mixes would essentially be rich in Ca species, which explained their higher ambient strength, as discussed earlier. But as the temperature increases, the leaching of Ca is known to be reduced [22]. This explained why there wasn't a major change in strength as the temperature increased from 55 to 70° C (131 to 158° F) in the case of two-part mixes. However, for one-part mixes, the rise in temperature increased the dissolution rate of elements and thus led to higher strength.

4.3. MICRO STRUCTURE ANALYSIS

The crystalline phases present in both unreacted FAs and AA paste mixtures were determined using X-Ray diffraction (XRD) analyses. The correlation between the crystalline phases and their effects on the setting time, workability and compressive strength properties. Crystalline phases such as Quartz (hereinafter Q), Periclase (hereinafter P), Hatrurite (hereinafter H), Lime (hereinafter L), Mullite (hereinafter M), and Gelhenite (hereinafter G) were the expected crystalline phases of the unreacted FA. For the AA paste mixtures, the presence of crystalline phases in the form of calcium-silicate-hydrates (CSH) generally improve the ambient strength of mixes, while the

presence of crystalline phases in the form of calcium-alumina-hydrates (CAH) were found to be responsible for the flash setting of mixes and thus negatively impact the setting time and workability properties as well as the compressive strength of mixes. The presence of calcium hydroxide (CH) was also found to hinder the strength development of mixes as well. The presence of crystalline phases in a form of sodium-aluminosilicate-hydrates, (NASH), calcium-aluminosilicate-hydrates (CASH), and/or calcium-sodium-aluminosilcate-hydrates (CNASH), and zeolites (Z) were spotted in geopolymer mixes cured at elevated temperatures as they do require heat for faster strength development. However, AA formed products are mostly in an amorphous phases rather than crystalline, and are usually spotted by a broad peak occurring at 2Θ locations of 28 - 30°.

The XRD results showed that there were differences in the formation of crystal phases depending on mixing type (one-part vs. two-part), mix proportions (LA, HA, and HS), and type of FAs used (C21, C29, and C37) (Figures 9 – 19). These differences in the crystal phases depended essentially on the chemical composition of FAs, nature of activator used, and curing temperature as describe in the next sub-sections.

4.3.1. XRD Results of M29 AA Paste Mixtures. The XRD of M29 mixes displayed peaks that corresponded to Q, P, G, and L crystalline phases which constituted the majority of unreacted components. In the case of newly formed components, for one-part M29 mixes cured at 30° C (86° F), the presence of peaks corresponding to hydrogarnet (hereinafter H*), were spotted at 2Θ of 18º - 20º, and calcium-aluminum-oxide-hydrate (hereinafter C*) at 2Θ of 30º - 32º in all three mixes (i.e. M29-LA, M29-HA, and M29-HS). In addition, the presence of CSH (hereinafter C) were spotted at 2Θ of 7º in M29-LA

and M29-HA, while kilchoanite (hereinafter K*) were spotted at 2Θ of 29° - 30° in mix M29-HS (Figure 9a).

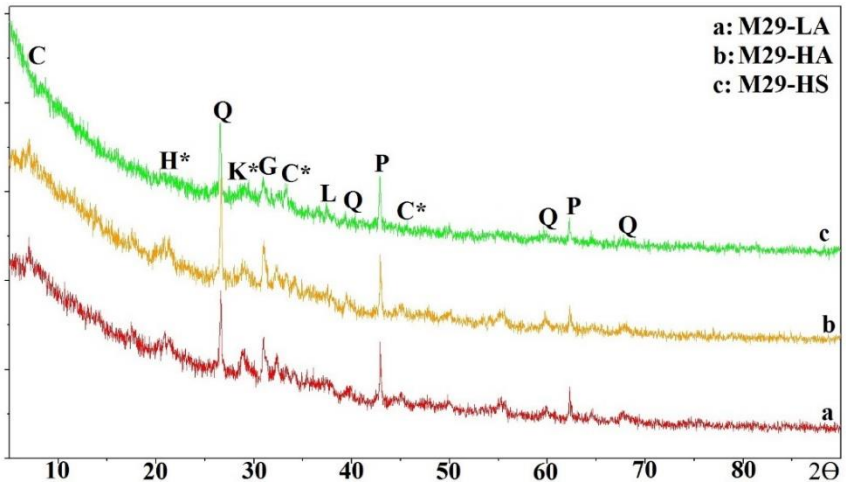

(a)

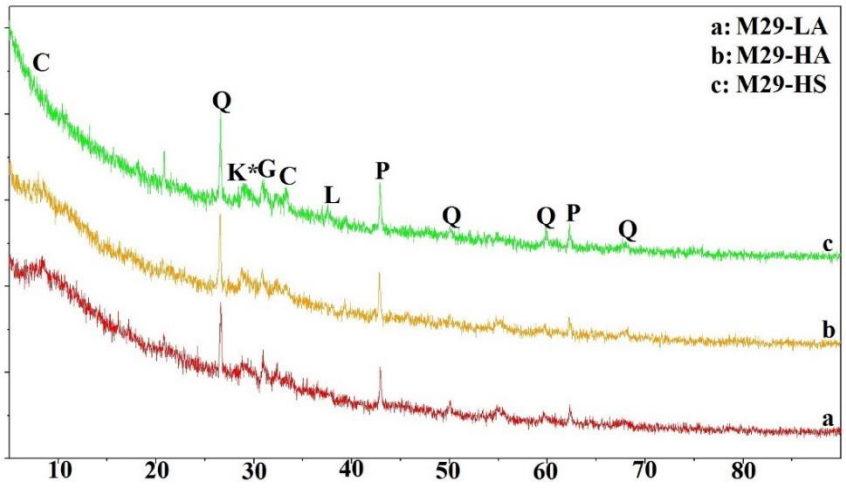

(b)

Figure 9. XRD Results of M29 mixes ambient-cured. a) One-part mixes. b) two-part mixes.

For two-part M29 mixes, the presence of CSH (C) peaks at 2Θ locations of 7º, 30° - 32° were more predominant in mixes M29-LA and M29-HA, while kilchoanite peaks were found in mix M29-HS (Figure 9b).

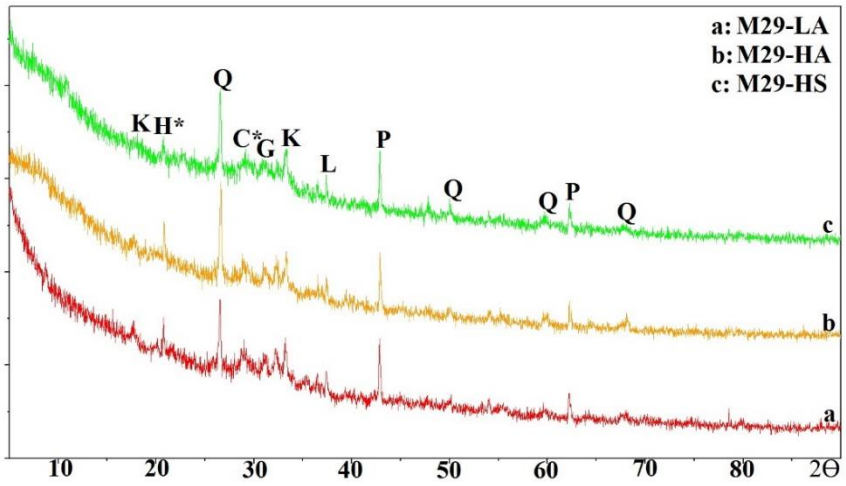

(a)

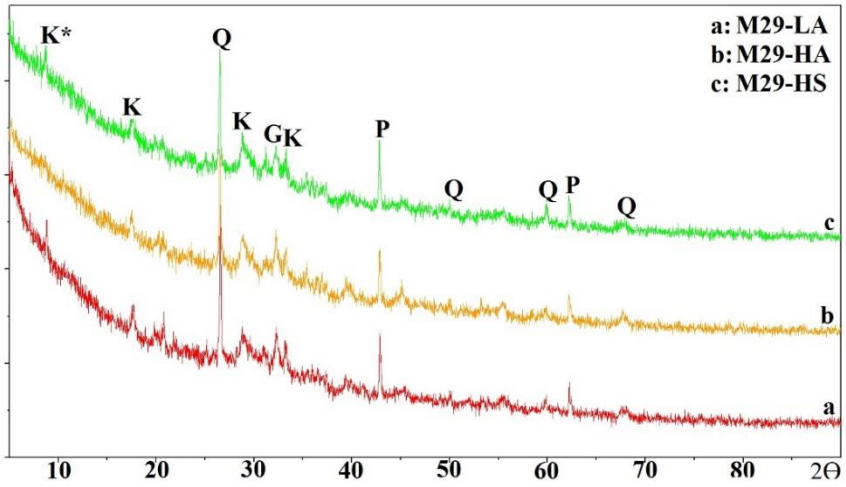

(b)

Figure 10. XRD Results of M29 mixes oven-cured at 55º C (131º F). a) One-part mixes. b) two-part mixes.

When M29 mixes cured at 55° C (131º F), XRD patterns of one-part M29 mixes were predominately composed of peaks corresponding to katoite (hereinafter K), hydrogarnet, and calcium-aluminum-oxide-hydrate (hereinafter C*) (Figure 10a). While for two-part M29 mixes, the presence of katoite was predominant in mixes M29-LA and M29-HS while kilchoanite was in M29-HS (Figure 10b).

At 70° C (158º F) of curing, XRD patterns of one-part M29 mixes were displayed peaks of katoite, hydrogarnet, and calcium-aluminum-oxide-hydrate, just like at 55° C (131º F) but with high peak intensity (Figure 11a). While in the case of two-part M29 katoite was the predominant peaks observed in all three mixes (Figure 11b).

The presence of crystal phases rich in aluminum (Al) and hydroxyl (OH) species in one-part M29 mixes cured at ambient temperature (i.e. 30° C or 86 º F) explained the faster setting properties of these mixes, as newly formed components were in form of CAH which are best known to trigger flash setting. However, the presence of CSH crystals were responsible the relatively high ambient compressive strength of these mixes (Figure 5a). In fact due to the high surface area of C29, the dissolution of FA elements happened at faster rate than in the case of C21, therefore some Si species could be dissolved and react with Ca to form CSH. At elevated temperatures, more Si could be dissolved and react with Ca and Al to form CASH products and thus results in high strength with increase in temperature (Figure 6a).

In the case of two-part M29 mixes, the presence of CSH and kilchoanite which are CSH products were responsible for the higher ambient compressive strength. When the curing temperature were elevated to 55° C (131º F) and later to 70° C (158º F), less Ca species were dissolved leading to a less concentration of Ca relative to Al and Si, thus

leading to formation of CASH products such as katoite which result in higher strength with increasing the curing temperature (Figure 6b).

4.3.2. XRD Results of M21 AA Paste Mixtures. At ambient temperature of 30° C (86º F), for one-part M21 mixes, XRD patterns did not reveal peaks corresponding to new formed products other than Hydrogarnet spotted at 2Ɵ of 30º - 32º, the remaining peaks corresponded to crystal phases of as Quartz, Periclase and Gelhenite for all three mixes M21-LA, M21-HA and M21-HS (Figure 12a). In the case of two-part mixes, the presence of a broad peak was observed by peaks located at 2Ɵ of 31° - 33° which corresponded to an amorphous product forming essentially a geopolymer gel (Figure 12b).

At 55° C (131° F), XRD patterns of one-part M21 mixes revealed the presence of Katoite at 2Ɵ of 26º – 28º mostly in mixes M21-LA and M21-HA, in addition to the unreacted components as mentioned earlier. In the case of two-part M21 mixes, a broad peak at 2Ɵ locations of 28° - 30° was observed while only peaks corresponded to unreacted components only were observed (Figure 13).

At 70° C (158° F), there were not a huge difference between the observed XRD patterns compared to those of M21 mixes cured at 55° C (131° F), expect the fact that the broad peak at 2Ɵ locations of 28° - 30° became more intense at 70° C (158° F) for two-part mixes, and the presence of zeolites p (hereinafter Z) in XRD patterns one-part M21-HS (Figure 14).

The presence of hydrogarnet in one-part M21 mixes, explained the faster setting properties of these mixes in comparison to their corresponding two-part mixes (Figures 2 – 4), since hydrogarnet is a CAH product known to cause flash setting and negatively affect the compressive strength of mixes as describe earlier.

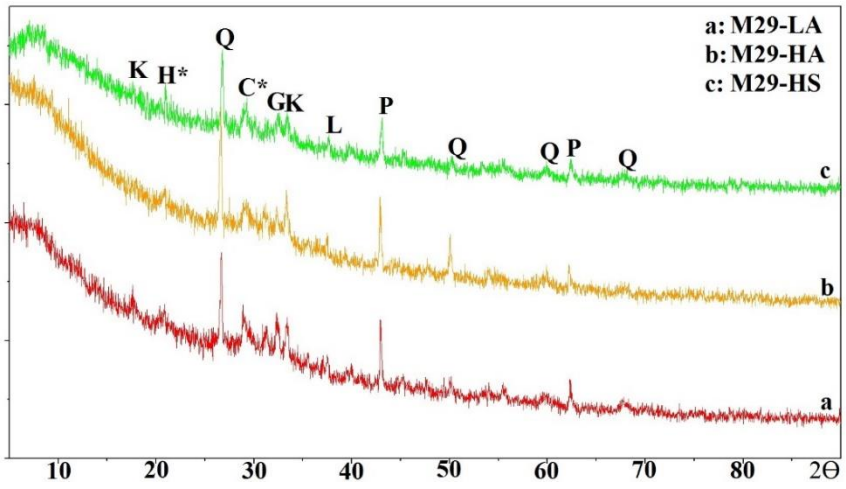

(a)

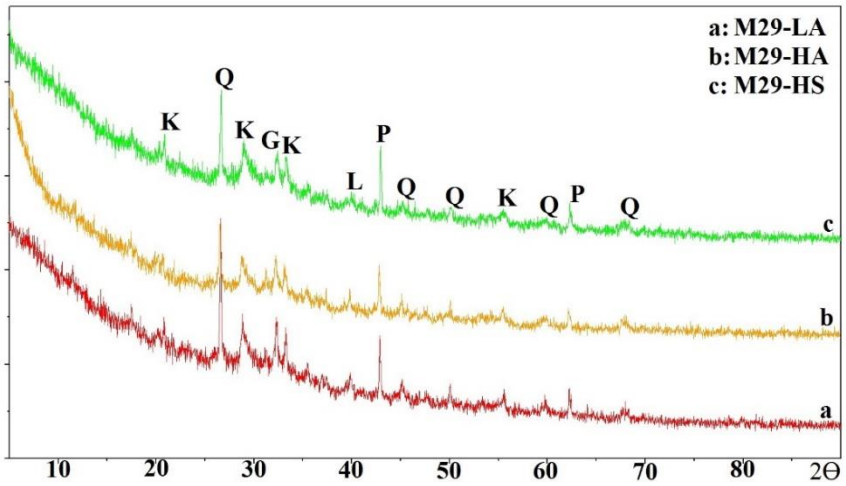

(b)

Figure 11. XRD Results of M29 mixes oven-cured at 55º C (131º F). a) One-part mixes. b) two-part mixes.

The presence of katoite in M21-LA and M21-HA mixes cured at elevated temperatures, explained the observed rise in compressive strength of these two mixes in comparison to mix M21-HS, as katoite is a CASH product which results in higher strength at elevated temperatures. Similarly, the presence of zeolite p in one-part M21-HS explained

the observed slight rise in compressive strength of this mix when cured at 70° C (158° F) (Figure 7b).

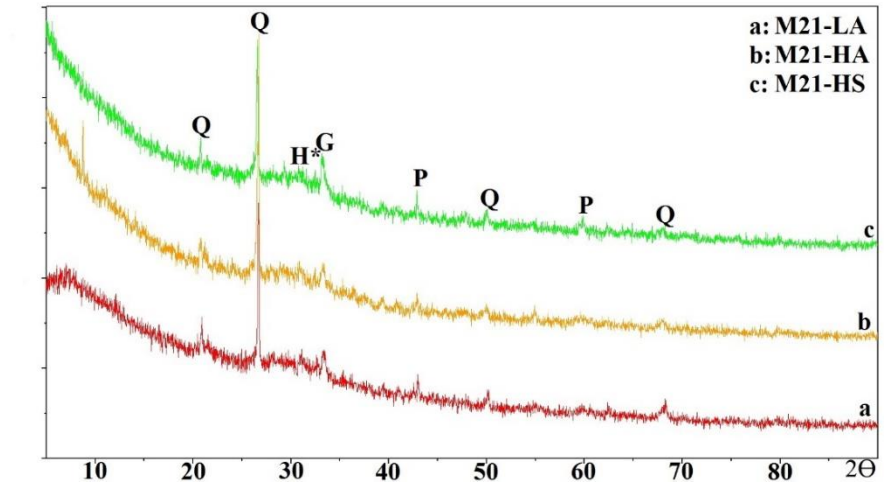

(a)

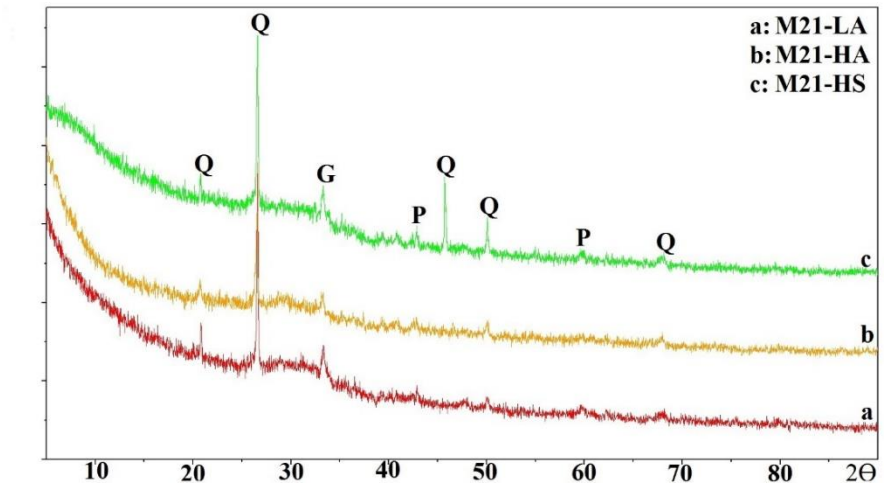

(b)

Figure 12. XRD Results of M21 mixes ambient-cured. a) One-part mixes. b) Two-part mixes.

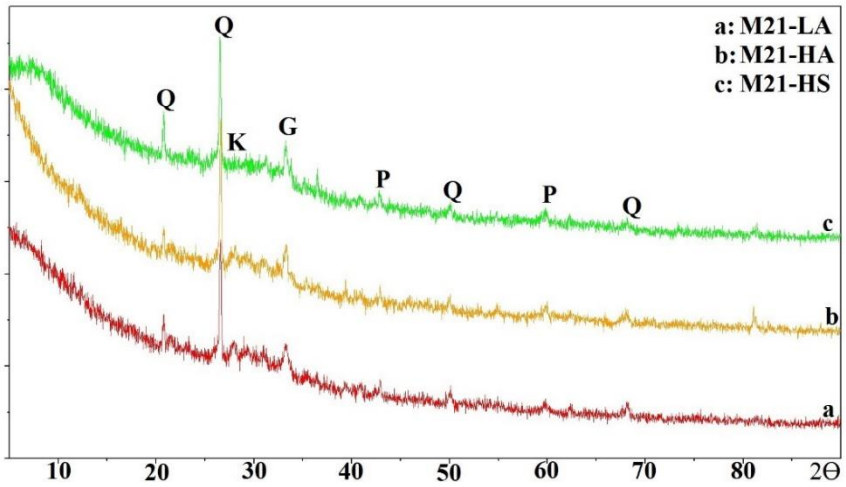

(a)

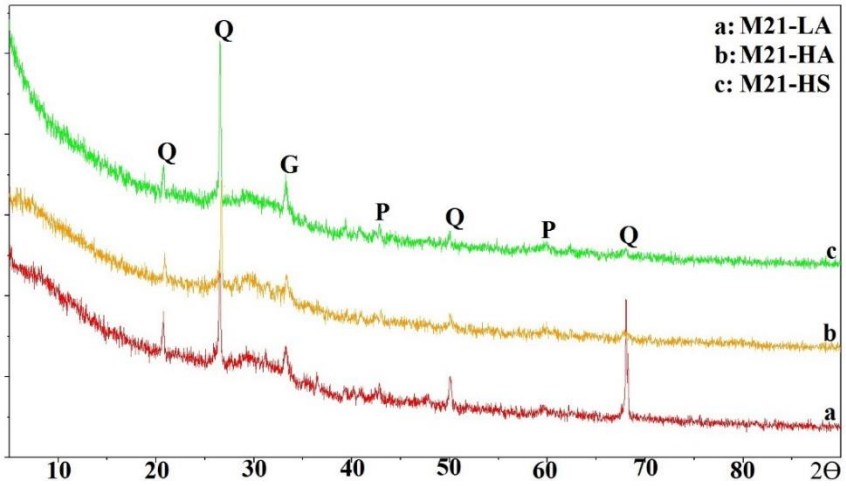

(b)

Figure 13. XRD Results of M21 mixes oven-cured at 55º C (131º F). a) One-part mixes. b) Two-part mixes.

The observed broad peak occurring at 2Θ locations of 28° - 30° in two-part M21 mixes, which is characteristic of the presence of an amorphous geopolymer gel that requires heat for faster strength development, explains the observed higher compressive strength of two-part M21 mixes. In addition, the observed high intensity of the broad peak in M21 mixes cured at 70° C (158° F) compared to those cured at 55° C (131° F)

represented the presence of more formed products, thus a much dense gel, which explained the higher compressive strength of M21 mixes cured at this temperature (i.e. 70° C or 158° F).

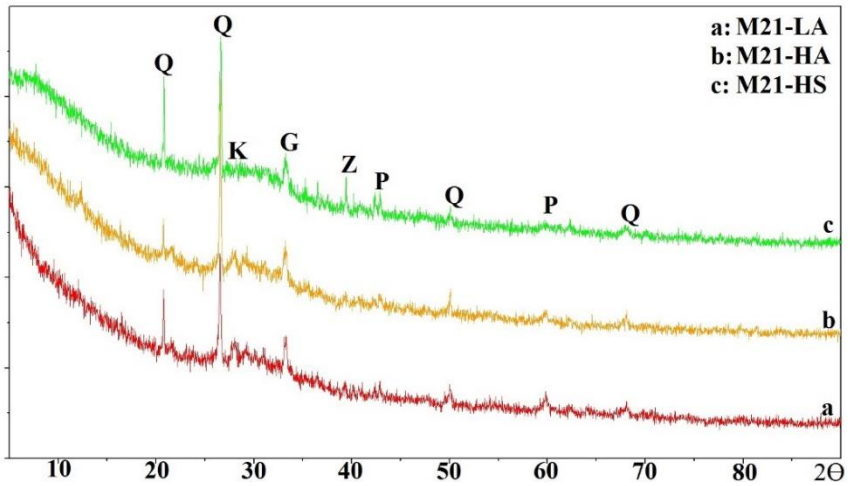

(a)

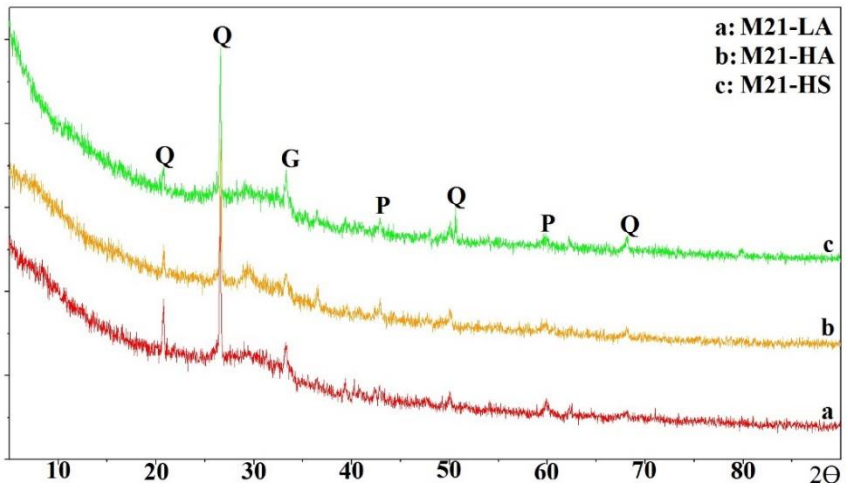

(b)

Figure 14. XRD Results of M21 mixes oven-cured at 70º C (158º F). a) One-part mixes. b) Two-part mixes.

4.3.3. XRD Results of M37 AA Paste Mixtures. XRD results of one-part and two-part M37 mixes are shown in Figures 15 – 17. The predominant unreacted components were Quartz, Periclase, and Hatrurite (hereinafter H). In the case of newly formed products,

for one-part M37 mixes cured at 30° C (131º F), the presence of peaks at 2Θ locations of 29° - 30°, and 50° corresponded to CSH for all three mixes M37-LA, M37-HA, and M37-HS, respectively (Figure 15a). For two-part M29 mixes, CSH peaks were spotted at 2Θ locations of 29° - 32° and 50° for mixes all three mixes (Figure 15b).

At 55° C (131º F) of curing temperature, in the case of one-part M37 mixes, a reduction in CSH peaks at 2Θ locations of 29° - 32° and 50° were observed, while the formation of new peak corresponding to Portlandite (hereinafter P*) were spotted at 2Θ locations of 18° - 20° in all three mixes (Figure 16a).

While in the case of corresponding two-part, the presence of katoite peaks was spotted at 2Θ of 30°, in addition to the CSH peaks at 2Θ locations of 28° and 50° (Figure 16b). At 70° C (158 º F) of curing temperature, XRD patterns of one-part M37 mixes were predominantly composed of katoite peaks at 2Θ of 30°, and Portlandite at 2Θ of 18°-20º with high intensity than peaks observed at 55° C (131º F) (Figure 17a). While in the case of two-part M37 mixes, calcium-aluminum-oxide-hydrate peaks were observed at 2Θ locations of 31° – 33°. (Figure 17b).

For both one-part and two-part M37 mixes, the observed higher ambient compressive strength in comparison to M29 and M21 mixes was due to the presence of CSH as explained earlier. However, the observed less effect of increasing temperature to the compressive strength of oven-cured mixes was due to the presence of Portlandite which was spotted to form as the temperature increased from 55° C (131º F) to 70° C (158 º F). In fact, as more Portlandite form, the pH of the solution decreases and thus the overall dissolution of Al and Si decreases as well, which reduces the resulting compressive strength.

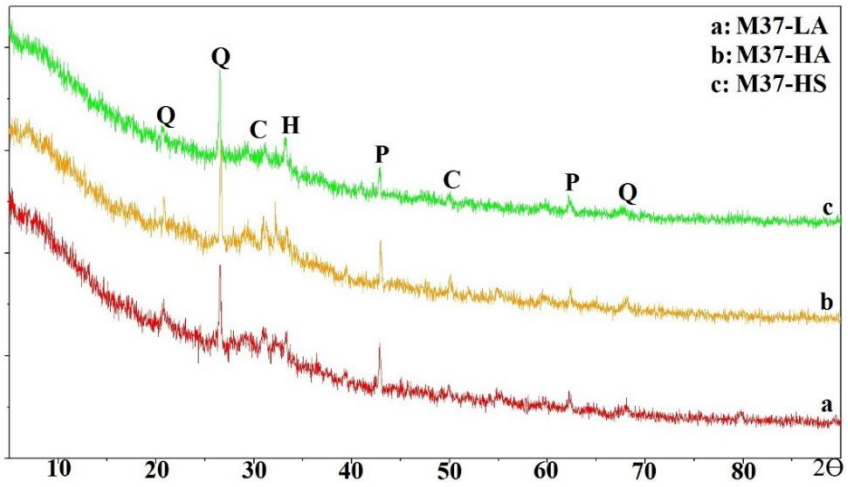

(a)

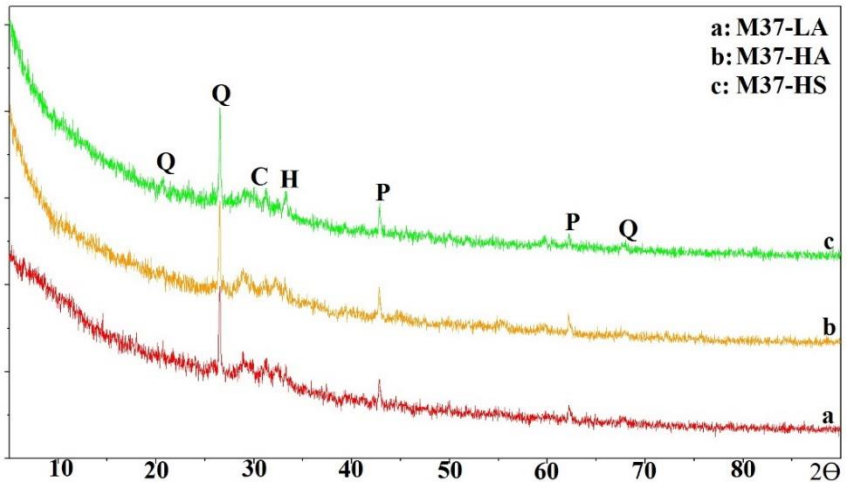

(b)

Figure 15. XRD Results of M37 mixes ambient-cured. a) One-part mixes. b) two-part mixes.

4.3.4. XRD Summary. The XRD results of AA mixes demonstrated that the presence of already available soluble Si and OH species in the activating solution of two-part mixes favorited the development of crystal phases rich in Si and Ca such as CSH or CASH, which were found to be beneficial for strength development of these mixes. While in the case of one-part mixes, with all species dissolving at the same time, the presence of

crystal phases such as CAOH, CH, and Hydrogarnet; rich in alumina or hydroxyl ions, which were found to impact negatively the setting properties and strength development of AA mixes.

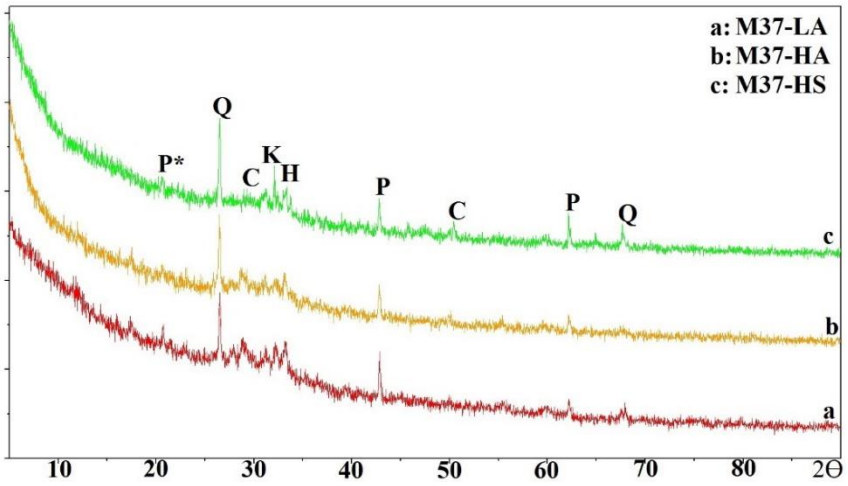

(a)

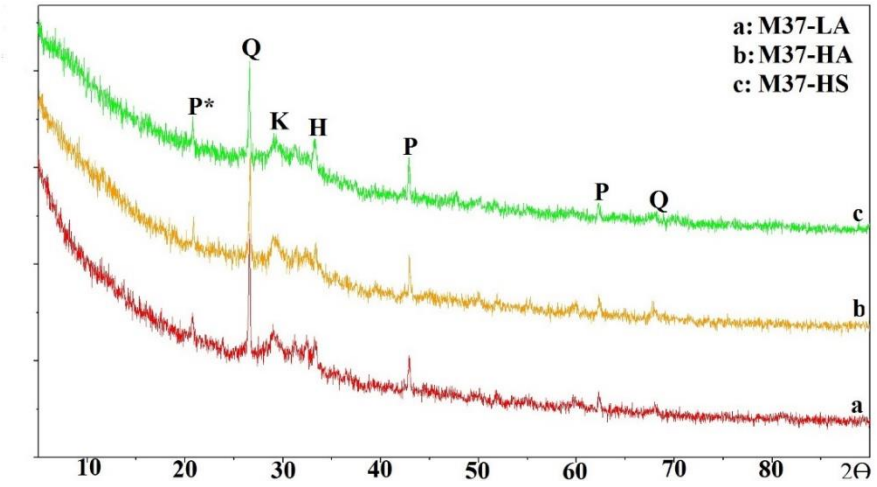

(b)

Figure 16. XRD Results of M37 mixes oven-cured at 55º C (131º F). a) One-part mixes. b) Two-part mixes.

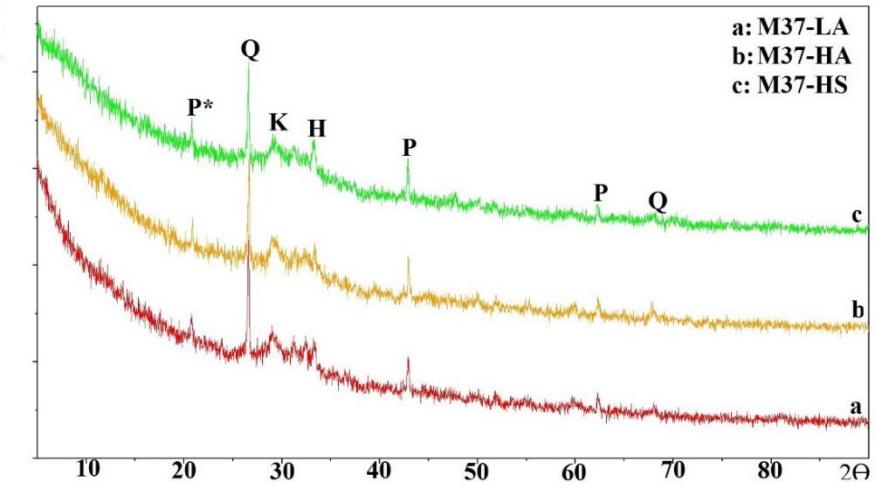

(a)

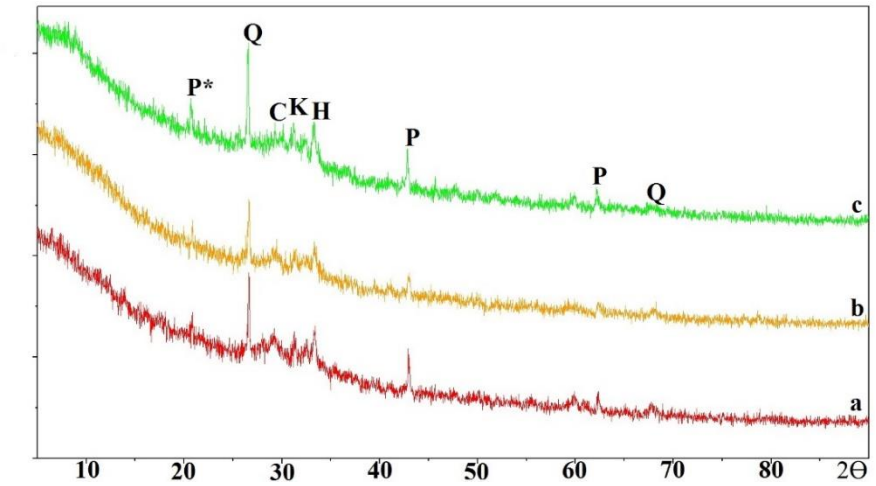

(b)

Figure 17. XRD Results of M37 mixes oven-cured at 70º C (158º F). a) One-part mixes. b) Two-part mixes.

5. CONCLUSIONS

AAM mixtures were made through one-part mixing by using only solid particles and two-part mixing using a combination of solid precursor and liquid activator solutions. Three different FAs were used (C21-2.20, C28-2.20, and C35-2.65) out of which three mix proportions (L.A, H.A, and H.S) were used to produce one-part and two-part mortar mixes.

Fresh properties and harden properties of mortars mixes were assessed and a comparison between results of one-part and two-part mixing were conducted which resulted in the following conclusions:

In terms of setting time properties, one-part mortar samples set faster than two-part mortars for all mixes made from each of the three FAs (i.e. C21-2.20, C29-2.20, and C37-2.65, respectively). This was mainly due to the Si/Al ratio and surface area of each FA. For one-part mixes, the flash setting of mixes was due to the presence of calcium-aluminum-hydrates such as hydroganet resulting from the fast dissolution of Ca and Al in water as compared to Si. The faster setting properties of one-part mixes influenced their workability.

In terms of strength development, the compressive strength of one-part mortar mixes cured at temperature were extremely lower than those of corresponding two-part mixes at early ages, equivalent to 3 – 10% of corresponding two-part mixes after 1 day of curing. But increased with time, reaching up to 35 – 50 % of corresponding two-part mixes compressive strength after only 7 days of curing. This was mainly due to the low rate of reaction of these mixes.

When cured at elevated temperatures, (i.e. 55° and 70° C), the compressive strength of one-part mortars increased with either an increasing in temperature (i.e. from 55 to 70° C) or a prolonged duration of curing (i.e. from 8h, to 16h and 24h respectively). This phenomenon was also noticed to happen in the case of two-part mortars, but the tremendous difference in the compressive strength depended on factors such as: pH, solubility of activator, and fresh properties of mixes.

In terms of microstructure analysis, the use of soluble species in the case of two-part mixes; resulted in formation of crystal phases such as calcium-silicate-hydrate (CSH), or even other forms of reacted calcium-silicate-oxides such as kilchoanite, these later being responsible for faster strength development. While on the other side, the simultaneous dissolution of all species in one-part mixes favorited formation of crystal phases such as hydrogranet, calcium hydroxide which inhibit compressive strength of mortar specimens. Special mix design and procedure need to be developed to fit one-part mix. In addition, more research is required to improve the fresh properties of one-part AAM. An investigation of an optimum resting time, curing duration and temperature is needed to be conducted.

REFERENCES

[1] E. Worrell, L. Price, N. Martin, C. Hendriks, and L. O. Meida, "CARBON DIOXIDE EMISSIONS FROM THE GLOBAL CEMENT INDUSTRY," *Annu. Rev. Energy Environ.*, vol. 26, no. 1, pp. 303–329, Nov. 2001.

[2] T. Bakharev, "Resistance of geopolymer materials to acid attack," *Cem. Concr. Res.*, vol. 35, pp. 658–670, 2005.

[3] P. K. Sarker and S. Mcbeath, "Fire endurance of steel reinforced fly ash geopolymer concrete elements," *Constr. Build. Mater.*, vol. 90, pp. 91–98, 2015.

[4] J. Davidovits, "Geopolymer chemistry and properties," in *Geopolymer*, 1988, vol. 88, pp. 25–48.

[5] A. Palomo, M. W. Grutzeck, and M. T. Blanco, "Alkali-activated fly ashes: a cement for the future," *Cem. Concr. Res.*, vol. 29, pp. 1323–1329, 1999.

[6] P. De Silva, K. Sagoe-Crenstil, and V. Sirivivatnanon, “Kinetics of geopolymerization: role of Al2O3 and SiO2,” *Cem. Concr. Res.*, vol. 37, pp. 512–518, 2007.

[7] J. L. Provis and S. A. Bernal, “Geopolymers and related alkali-activated materials,” *Annu. Rev. Mater. Res.*, vol. 44, pp. 299–327, 2014.

[8] R. F. Heitzmann, M. Fitzgerald, and J. L. Sawyer, “Mineral binder and compositions employing the same.” Google Patents, 1987.

[9] J. Davidovits, “Method for obtaining a geopolymeric binder allowing to stabilize, solidify and consolidate toxic or waste materials.” Google Patents, 1994.

[10] P. Duxson and J. L. Provis, “Designing precursors for geopolymer cements,” *J. Am. Ceram. Soc.*, vol. 91, pp. 3864–3869, 2008.

[11] A. Hajimohammadi and J. S. J. van Deventer, “Characterisation of one-part geopolymer binders made from fly ash,” *Waste and Biomass Valorization*, vol. 8, pp. 225–233, 2017.

[12] K.-H. Yang and J.-K. Song, “Workability loss and compressive strength development of cementless mortars activated by combination of sodium silicate and sodium hydroxide,” *J. Mater. Civ. Eng.*, vol. 21, pp. 119–127, 2009.

[13] M. Askarian, Z. Tao, G. Adam, and B. Samali, “Mechanical properties of ambient cured one-part hybrid OPC-geopolymer concrete,” *Constr. Build. Mater.*, vol. 186, pp. 330–337, 2018.

[14] E. Gomaa, S. Sargon, C. Kashosi, and M. ElGawady, “Fresh properties and compressive strength of high calcium alkali activated fly ash mortar,” *J. King Saud Univ. - Eng. Sci.*, vol. 29, no. 4, 2017.

[15] S. P. Sargon, E. Y. Gomaa, C. Kashosi, A. A. Gheni, and F. Ash, “Effect of Curing Temperatures on Zero-Cement Alkali-Activated Mortars,” no. Icpic, 2018.

[16] A.-K. Maier, L. Dezmirean, J. Will, and P. Greil, “Three-dimensional printing of flash-setting calcium aluminate cement,” *J. Mater. Sci.*, vol. 46, no. 9, pp. 2947–2954, May 2011.

[17] C. K. Yip and J. S. J. Van Deventer, “Microanalysis of calcium silicate hydrate gel formed within a geopolymeric binder,” *J. Mater. Sci.*, vol. 38, pp. 3851–3860, 2003.

[18] W. K. W. Lee and J. S. J. Van Deventer, “Structural reorganisation of class F fly ash in alkaline silicate solutions,” *Colloids Surfaces A Physicochem. Eng. Asp.*, vol. 211, pp. 49–66, 2002.

[19] R. K. Iler, “Effect of adsorbed alumina on the solubility of amorphous silica in water,” *J. Colloid Interface Sci.*, vol. 43, pp. 399–408, 1973.

[20] D. Panias, I. P. Giannopoulou, and T. Perraki, “Effect of synthesis parameters on the mechanical properties of fly ash-based geopolymers,” *Colloids Surfaces A Physicochem. Eng. Asp.*, vol. 301, pp. 246–254, 2007.

[21] J. L. Provis and J. S. J. Van Deventer, “Geopolymerisation kinetics. 2. Reaction kinetic modelling,” *Chem. Eng. Sci.*, vol. 62, pp. 2318–2329, 2007.

[22] X. Guo, H. Shi, and W. A. Dick, “Compressive strength and microstructural characteristics of class C fly ash geopolymer,” *Cem. Concr. Compos.*, vol. 32, no. 2, pp. 142–147, 2010.

SECTION

2. SUMMARY, CONCLUSIONS AND RECOMMENDATIONS

2.1. COMPREHENSIVE SUMMARY

AACFA mortars were synthesized using three different types of class C FA sourced from Jeffrey (C29-2.20), Sikeston (C21-2.20), and Labadie (C37-2.65) power plants located in Missouri, US. The chemical composition of each FA was determined using X-Ray Fluorescence. Three different mix design namely: low alkaline (LA), high alkaline (HA), and high silicates (HS) mixtures were prepared out of each FA using two different mixing procedures, i.e., one-part and two-part mixing.

In the case of two-part mixed AACFA, four mortar mixes was synthesized, and were subjected to six different rest times prior to being ambient, oven, or steam cured. The steam and oven curing was for 9 hours at either 55º C (131º F) or 80º C (176º F). The optimum rest time was determined. After curing, the specimens were then stored in the laboratory for 1, 7, 28, 56, or 90 days and were tested to determine their strength development with time. XRD, SEM and EDS analysis were conducted to investigate the phase formation of reacted products. For one-part mixed AACFA, nine mortar mixtures were synthesized; three for each mix design and FA, in addition to nine corresponding two-part mixtures. The microstructure, fresh and harden properties of mortar mixtures were assessed and a comparison between results of one-part and equivalent two-part mixtures were conducted.

2.2. CONCLUSIONS

From the two studies conducted on AACFA mortars, the following were concluded. In the case of two-part mixed AACFA mortars:

- An optimum rest time of 12 hours were found beneficial to be applied to AACFA mortar prior being subjected to steam and oven curing regimes, resulting in a 40% - 42% increase in the compressive strength of M21 mixes, and 50% - 54% increase in the case of M37 mixes on average.
- The chemical composition of the FA played an important role in the long-term compressive strength development of AACFA mortar as it influenced the type of curing regime and curing temperature to be used. At early ages, M21 mixes due to their lower calcium content and higher alumina and silica content, required elevated temperatures (55 ºC and 80 ºC) for faster strength development; while M37 mixes with a relatively higher calcium content had the ability of attaining higher strength when cured at ambient temperature (22º C).
- In overall, steam curing resulted in higher initial compressive strength, followed by oven curing and finally ambient curing at early ages (i.e. within the first day of curing). But over time, a change rapidly occurred. For M37 mixes, the ambient compressive strength exceed both oven and steam strengths after 28 days; this was attributed to the presence of C-S-H products as revealed by XRD results. For M21 mixes, ambient curing resulted in the lowest strength throughout the entire curing period and the microstructure analysis of pastes mixes revealed the predominance of geopolomeric gel (CNASH) which requires heat for high strength development.

- The initial strength development of all mortars specimens heat cured (oven and steam curing regimes) at 80 ºC (176º F) was very rapid, resulting in compressive strength ranging between 35 to 42 MPa (5000 – 6000 psi) after only 9 hours of curing. But after the heat curing process, a different scenario was observed in their long term strength development. For mixes cured in the oven, an improvement in a scale of up 20% strength increase was observed between 1 day and 90 days of age.
- Mortar specimens heat cured at 55º C (131º F), had slow strength development at early ages, but a considerable strength increase happened at late ages, reaching 70 to 80% increase in the compressive strength of specimens after 90 days.
- A noticeable change in the compressive strength of all specimens were observed to happen within the first 56 days of age, after this period, no much change were reported.

When comparing the performance of one-part mixed AACFA mortars to corresponding two-part mixed mortars, it was observed that:

- In terms of setting time properties, one-part mortar samples set faster than two-part mortars for all mixes made from each of the three FAs (i.e. C21-2.20, C28-2.20, and C35-2.65, respectively). This was mainly due to the Si/Al ratio and surface area of each FA. For one-part mixes, the flash setting of mixes were due to the presence of calcium-aluminum-hydrates such as hydroganet resulting from the fast dissolution of Ca and Al in water as compared to Si. The faster setting properties of one-part mixes influenced their workability.
- In terms of strength development, the compressive strength of one-part mortar mixes cured at temperature were extremely lower than those of corresponding two-

part mixes at early ages, equivalent to 3 – 10% of corresponding two-part mixes after 1 day of curing. But increased with time, reaching up to 35 – 50 % of corresponding two-part mixes compressive strength after only 7 days of curing. This was mainly due to the low rate of reaction of these mixes.

- When cured at elevated temperatures, (i.e. 55° and 70 °C), the compressive strength of one-part mortars increased with either an increasing in temperature (i.e. from 55 to 80°C) or a prolonged duration of curing (i.e. from 8h, to 16h and 24h respectively). This phenomenon was also noticed to happen in the case of two-part mortars, but the tremendous difference in the compressive strength depended on factors such as: pH, solubility of activator, and fresh properties of mixes.
- In terms of microstructure analysis, the use of soluble species in the case of two-part mixes; resulted in formation of crystal phases such as calcium-silicate-hydrate (CSH), or even other forms of reacted calcium-silicate-oxides such as kilchoanite, these later being responsible for faster strength development. While on the other side, the simultaneous dissolution of all species in one-part mixes favorited formation of crystal phases such as hydrogranet, calcium hydroxide which inhibit compressive strength of mortar specimens.

2.3. RECOMMENDATIONS

2.3.1. Recommendations for Current Study. For two-part mixed AACFA mortars:

- Use a rest time of 12 hours for high-calcium AACFA, and 24 hours for low-calcium AACFA mortar mixtures prior to oven and steam curing.

- For high early compressive strength of AACFA mortars, use ambient curing for high-calcium AACFA mixtures, and heat curing (oven and steam) for low-calcium AACFA mixtures.
- In the case of oven curing, for a high early compressive strength, cure specimens at elevated temperatures (i.e. 80°C) while for a higher strength development at late ages, cure specimens at relatively less elevated temperatures (i.e. 55°C).
- In the case steam curing, avoid using higher curing temperatures (80°C), since it negatively affects the long-term strength development of AACFA mortar despite the higher short-term strength it can provide.

2.3.2. Recommendations for Future Work. For two-part mixed AACFA mortars:

- Investigate the long-term durability of AACFA mortar cured under various curing regimes.

For one-part mixed AACFA mortars:

- Develop a special mix design to result in higher compressive strength of one-part mixed AACFA.
- Use additives such as superplasticizer to improve the setting time and workability properties of one-part AACFA mortars.
- Investigate the effect of rest time on short-term and long-term development of one-part AACFA mortars.
- Investigate the effect of different curing regimes of the strength development of one-part AACFA mortars.
- Investigate the durability properties of one-part AACFA mortars.

BIBLIOGRAPHY

[1] Z. Sun and A. Vollpracht, "Isothermal calorimetry and in-situ XRD study of the NaOH activated fly ash, metakaolin and slag," *Cem. Concr. Res.*, vol. 103, pp. 110–122, 2018.

[2] J.-K. Kim, Y.-H. Moon, and S.-H. Eo, "Compressive strength development of concrete with different curing time and temperature," *Cem. Concr. Res.*, vol. 28, pp. 1761–1773, 1998.

[3] D. C. Adriano, A. L. Page, A. A. Elseewi, A. C. Chang, and I. Straughan, "Utilization and Disposal of Fly Ash and Other Coal Residues in Terrestrial Ecosystems: A Review 1," *J. Environ. Qual.*, vol. 9, pp. 333–344, 1980.

[4] Z. T. Yao *et al.*, "A comprehensive review on the applications of coal fly ash," *Earth-Science Rev.*, vol. 141, pp. 105–121, 2015.

[5] B. C. McLellan, R. P. Williams, J. Lay, A. Van Riessen, and G. D. Corder, "Costs and carbon emissions for geopolymer pastes in comparison to ordinary portland cement," *J. Clean. Prod.*, vol. 19, pp. 1080–1090, 2011.

[6] J. Davidovits, "Geopolymer chemistry and properties," in *Geopolymer*, 1988, vol. 88, pp. 25–48.

[7] C. K. Yip, G. C. Lukey, J. L. Provis, and J. S. J. van Deventer, "Effect of calcium silicate sources on geopolymerisation," *Cem. Concr. Res.*, vol. 38, no. 4, pp. 554–564, 2008.

[8] D. M. Roy, "Alkali-activated cements opportunities and challenges," *Cem. Concr. Res.*, vol. 29, pp. 249–254, 1999.

[9] A. Palomo, M. W. Grutzeck, and M. T. Blanco, "Alkali-activated fly ashes: a cement for the future," *Cem. Concr. Res.*, vol. 29, pp. 1323–1329, 1999.

[10] J. L. Provis and S. A. Bernal, "Geopolymers and related alkali-activated materials," *Annu. Rev. Mater. Res.*, vol. 44, pp. 299–327, 2014.

[11] P. De Silva, K. Sagoe-Crenstil, and V. Sirivivatnanon, "Kinetics of geopolymerization: role of Al2O3 and SiO2," *Cem. Concr. Res.*, vol. 37, pp. 512–518, 2007.

[12] ASTM, "Standard Specification for Coal Fly Ash and Raw or Calcined Natural Pozzolan for Use in Concrete," *Annu. B. ASTM Stand.*, pp. 3–6, 2010.

[13] R. F. Heitzmann, M. Fitzgerald, and J. L. Sawyer, “Mineral binder and compositions employing the same.” Google Patents, 1987.

[14] J. Davidovits, “Method for obtaining a geopolymeric binder allowing to stabilize, solidify and consolidate toxic or waste materials.” Google Patents, 1994.

[15] A. Hajimohammadi and J. S. J. van Deventer, “Characterisation of one-part geopolymer binders made from fly ash,” *Waste and Biomass Valorization*, vol. 8, pp. 225–233, 2017.

[16] M. Askarian, Z. Tao, G. Adam, and B. Samali, “Mechanical properties of ambient cured one-part hybrid OPC-geopolymer concrete,” *Constr. Build. Mater.*, vol. 186, pp. 330–337, 2018.

[17] D. Hardjito, S. E. Wallah, D. M. J. Sumajouw, and B. V. Rangan, “On the Development of Fly Ash-based Geopolymer Concrete_Djwantoro Hardjito dkk,” no. 101, pp. 467–472, 2005.

[18] D. Hardjito and B. V Rangan, “LOW-CALCIUM FLY ASH-BASED By,” *Concrete*, pp. 1–103, 2005.

[19] C. Gunasekara, D. W. Law, and S. Setunge, “Long Term Engineering Properties of Fly Ash Geopolymer Concrete,” *4th Int. Conf. Sustain. Constr. Mater. Technol.*, no. September, p. 2019, 2016.

[20] D. W. Law, A. A. Adam, T. K. Molyneaux, I. Patnaikuni, and A. Wardhono, “Long term durability properties of class F fly ash geopolymer concrete,” *Mater. Struct. Constr.*, vol. 48, no. 3, pp. 721–731, 2014.

[21] A. M. Fernández-jiménez, A. Palomo, and C. López-hombrados, “Engineering Properties of Alkali-Activated Fly Ash Concrete,” *ACI Mater. J.*, vol. 103, no. 2, pp. 15–17, 2006.

[22] G. S. Ryu, Y. B. Lee, K. T. Koh, and Y. S. Chung, “The mechanical properties of fly ash-based geopolymer concrete with alkaline activators,” *Constr. Build. Mater.*, vol. 47, pp. 409–418, 2013.

[23] D. L. Y. Kong and J. G. Sanjayan, “Effect of elevated temperatures on geopolymer paste, mortar and concrete,” *Cem. Concr. Res.*, vol. 40, no. 2, pp. 334–339, 2010.

[24] A. Wardhono, C. Gunasekara, D. W. Law, and S. Setunge, “Comparison of long term performance between alkali activated slag and fly ash geopolymer concretes,” *Constr. Build. Mater.*, vol. 143, pp. 272–279, 2017.

[25] I. Soroka, C. H. Jaegermann, and A. Bentur, “Short-term steam-curing and concrete later-age strength,” *Matériaux Constr.*, vol. 11, pp. 93–96, 1978.

[26] J. J. Shideler and W. H. Chamberlin, “Early strength of concrete as affected by steam curing temperatures,” in *Journal Proceedings*, 1949, vol. 46, pp. 273–283.

[27] T. Bakharev, “Geopolymeric materials prepared using Class F fly ash and elevated temperature curing,” *Cem. Concr. Res.*, vol. 35, pp. 1224–1232, 2005.

[28] Y. Hou, D. Wang, W. Zhou, H. Lu, and L. Wang, “Effect of activator and curing mode on fly ash-based geopolymers,” *J. Wuhan Univ. Technol. Mater. Sci. Ed.*, vol. 24, no. 5, pp. 711–715, 2009.

[29] K.-H. Yang and J.-K. Song, “Workability Loss and Compressive Strength Development of Cementless Mortars Activated by Combination of Sodium Silicate and Sodium Hydroxide,” *J. Mater. Civ. Eng.*, vol. 21, no. 3, pp. 119–127, Mar. 2009.

[30] P. Duxson, A. Fernández-Jiménez, J. L. Provis, G. C. Lukey, A. Palomo, and J. S. J. van Deventer, “Geopolymer technology: the current state of the art,” *J. Mater. Sci.*, vol. 42, pp. 2917–2933, 2007.

[31] T. Phoo-Ngernkham, C. Phiangphimai, N. Damrongwiriyanupap, S. Hanjitsuwan, J. Thumrongvut, and P. Chindaprasirt, “A Mix Design Procedure for Alkali-Activated High-Calcium Fly Ash Concrete Cured at Ambient Temperature,” *Adv. Mater. Sci. Eng.*, vol. 2018, 2018.

[32] K. Chaimoon, S. Pantura, S. Homwuttiwong, A. Wongkvanklom, and P. Chindaprasirt, “Factors affecting the workability and strength of alkali-activated high calcium fly ash concrete,” *Environ. Eng. Manag. J.*, vol. 11, no. 8, pp. 1425–1432, 2012.

[33] X. Guo, H. Shi, and W. A. Dick, “Compressive strength and microstructural characteristics of class C fly ash geopolymer,” *Cem. Concr. Compos.*, vol. 32, pp. 142–147, 2010.

[34] O. G. Rivera *et al.*, “Effect of elevated temperature on alkali-activated geopolymeric binders compared to portland cement-based binders,” *Cem. Concr. Res.*, vol. 90, pp. 43–51, 2016.

[35] E. Gomaa, S. Sargon, C. Kashosi, and M. ElGawady, “Fresh properties and compressive strength of high calcium alkali activated fly ash mortar,” *J. King Saud Univ. - Eng. Sci.*, vol. 29, no. 4, 2017.

[36] T. K. Erdem, L. Turanli, and T. Y. Erdogan, “Setting time: an important criterion to determine the length of the delay period before steam curing of concrete,” *Cem. Concr. Res.*, vol. 33, pp. 741–745, 2003.

[37] S. P. Sargon, E. Y. Gomaa, C. Kashosi, A. A. Gheni, and F. Ash, “Effect of Curing Temperatures on Zero-Cement Alkali-Activated Mortars,” no. Icpic, 2018.

[38] A. Fernández-Jiménez, A. Palomo, and M. Criado, “Microstructure development of alkali-activated fly ash cement: A descriptive model,” *Cem. Concr. Res.*, vol. 35, no. 6, pp. 1204–1209, 2005.

[39] P. Chindaprasirt and W. Chalee, “Effect of sodium hydroxide concentration on chloride penetration and steel corrosion of fly ash-based geopolymer concrete under marine site,” *Constr. Build. Mater.*, vol. 63, pp. 303–310, 2014.

[40] ASTM, “Standard Test Method for Slump of Hydraulic-Cement Concrete,” *Astm C143/C143M*, no. 1, pp. 1–4, 2015.

[41] T. Textiles, “Standard Test Method for,” *Annu. B. ASTM Stand.*, vol. i, pp. 2–5, 2005.

[42] B. Lothenbach, F. Winnefeld, C. Alder, E. Wieland, and P. Lunk, “Effect of temperature on the pore solution, microstructure and hydration products of Portland cement pastes,” *Cem. Concr. Res.*, vol. 37, no. 4, pp. 483–491, 2007.

[43] E. Worrell, L. Price, N. Martin, C. Hendriks, and L. O. Meida, “CARBON DIOXIDE EMISSIONS FROM THE GLOBAL CEMENT INDUSTRY,” *Annu. Rev. Energy Environ.*, vol. 26, no. 1, pp. 303–329, Nov. 2001.

[44] T. Bakharev, “Resistance of geopolymer materials to acid attack,” *Cem. Concr. Res.*, vol. 35, pp. 658–670, 2005.

[45] P. K. Sarker and S. Mcbeath, “Fire endurance of steel reinforced fly ash geopolymer concrete elements,” *Constr. Build. Mater.*, vol. 90, pp. 91–98, 2015.

[46] P. Duxson and J. L. Provis, “Designing precursors for geopolymer cements,” *J. Am. Ceram. Soc.*, vol. 91, pp. 3864–3869, 2008.

[47] K.-H. Yang and J.-K. Song, “Workability loss and compressive strength development of cementless mortars activated by combination of sodium silicate and sodium hydroxide,” *J. Mater. Civ. Eng.*, vol. 21, pp. 119–127, 2009.

[48] A.-K. Maier, L. Dezmirean, J. Will, and P. Greil, “Three-dimensional printing of flash-setting calcium aluminate cement,” *J. Mater. Sci.*, vol. 46, no. 9, pp. 2947–2954, May 2011.

[49] C. K. Yip and J. S. J. Van Deventer, “Microanalysis of calcium silicate hydrate gel formed within a geopolymeric binder,” *J. Mater. Sci.*, vol. 38, pp. 3851–3860, 2003.

[50] W. K. W. Lee and J. S. J. Van Deventer, “Structural reorganisation of class F fly ash in alkaline silicate solutions,” *Colloids Surfaces A Physicochem. Eng. Asp.*, vol. 211, pp. 49–66, 2002.

[51] R. K. Iler, “Effect of adsorbed alumina on the solubility of amorphous silica in water,” *J. Colloid Interface Sci.*, vol. 43, pp. 399–408, 1973.

[52] D. Panias, I. P. Giannopoulou, and T. Perraki, “Effect of synthesis parameters on the mechanical properties of fly ash-based geopolymers,” *Colloids Surfaces A Physicochem. Eng. Asp.*, vol. 301, pp. 246–254, 2007.

[53] J. L. Provis and J. S. J. Van Deventer, “Geopolymerisation kinetics. 2. Reaction kinetic modelling,” *Chem. Eng. Sci.*, vol. 62, pp. 2318–2329, 2007.

[54] X. Guo, H. Shi, and W. A. Dick, “Compressive strength and microstructural characteristics of class C fly ash geopolymer,” *Cem. Concr. Compos.*, vol. 32, no. 2, pp. 142–147, 2010.

VITA

Cedric Chani Kashosi was born in Kinshasa, Democratic Republic of the Congo. He graduated from College Alfajiri High School in 2009 where he was enrolled in the Math-Physics option. He did his undergraduate studies at Kampala International University in Kampala, Uganda where he graduated with a Bachelor of Science in Civil Engineering (BSCE) degree in December 2013.

In spring 2017, he began his Master program in Civil Engineering at Missouri University of Science and Technology in Rolla, United States. He worked as Graduate Research Assistant from January 2017 to December 2018. He received his Master's degree in Civil Engineering from Missouri University of Science and Technology in May 2019.